ABSTRACT

Title of Thesis:	CHARACTERIZATION AND EXPRESSION OF RUB1 CONJUGASE AND CULLIN1-LIKE GENES IN POPLAR ASSOCIATED WITH VEGETATIVE BUD DEVELOPMENT AND DORMANCY
Name of Degree Candidate	Banu Saritas-Yildirim
Degree and Year	Master of Science, 2006
Thesis Directed By:	Gary D. Coleman, Associate Professor, Department of Natural Resource Sciences and Landscape Architecture

Dormancy is an adaptive trait that ensures survival of plants in adverse growth conditions. By using phylogenetical, expression and protein analysis, RUB1 conjugase and Cullin1 were characterized in poplar dormancy. RUB1 conjugase and Cullin1 were annotated using sequence homology approach. RUB1 conjugase was expressed in apical buds during dormancy but not detected in those of *etr1-1* expressing poplars. Its transcript abundance was reduced in axillary buds, leaves and bark of *etr1-1* expressing poplars compared to wild types. RUB1 conjugase expression was not affected by AVG but reduced by 50μM ACC in apical buds of *etr1-1* expressing poplars. Cullin1 and EBF expression did not display significant difference in most tissues except for the Cullin1 expression in middle and bottom leaves during short-day treatments in wild types. Two novel RUB1-conjugated

proteins were detected during low temperature treatments. This study has built a foundation for further analysis of targeted protein degradation in dormancy.

CHARACTERIZATION AND EXPRESSION OF RUB1 CONJUGASE AND CULLIN1-LIKE GENES IN POPLAR ASSOCIATED WITH VEGETATIVE BUD DEVELOPMENT AND DORMANCY

By

Banu Saritas-Yildirim

Thesis submitted to the Faculty of the Graduate School of the
University of Maryland, College Park, in partial fulfillment
of the requirements for the degree of
Master of Science
2006

Advisory Committee:
Dr. Gary D. Coleman, Thesis Director/Chairman
Dr. Harry Swartz
Dr. Joseph Sullivan

ACKNOWLEDGEMENTS

I am thankful to Dr. Gary Coleman for giving me the opportunity to work with him and for being a great advisor to me. He always had time to discuss my project and give constructive criticisms.

I thank to Dr. Harry Swartz for helping me increase my knowledge and experience in tissue culture. It was amazing to learn how to dissect an embryo out from a seed.

I am thankful to Dr. Michael Cummings for guiding me in phylogenetical analysis.

TABLE OF CONTENTS

LIST OF TABLES

LIST OF FIGURES

INTRODUCTION

1. Dormancy

1.1. Dormancy: Terms and Definitions

Several terms have been used to describe plant dormancy including rest, quiescent, summer dormancy, and winter dormancy. These terms have to be criticized because they fail to describe the physiology of dormancy. Lang (1987) proposed a terminology and classification that considered growth, development, and physiology. From this Lang (1987) defined dormancy as the temporary suspension of visible growth of any plant structure containing a meristem. Three types of dormancy, endodormancy, paradormancy, and ecodormancy, were also defined based on the nature of the controlling signals (Lang, 1987).

Endodormancy is when the physiological factors triggering dormancy are within the dormant structure. Bud dormancy in trees is an example of endodormancy, where the terminal bud itself is capable of going dormant. Paradormancy is when the physiological factors are within the plant but outside the dormant structure. Apical dominance is an example of paradormancy. Ecodormancy occurs when environmental factors control dormancy. Numerous environmental factors including temperature, water, nutrients, and oxygen influence dormancy responses in plants. With inputs of environmental and endogenous signals, endo-, para-, and ecodormancy, either individually or cumulatively, act on dormant structures to initiate and/or maintain dormancy.

1.2. Growth Cycle and Dormancy in Trees

Temperate trees alternate between active growth and dormancy every year. Dormancy is an important adaptive trait in trees that assures survival of the tree during adverse growth conditions. Several tissues can go dormant including roots, vascular cambium, lateral buds, roots, seeds, and apical buds. Two types of buds are present: the apical buds (also called terminal buds) and the axillary buds. The structure, development and dormancy of terminal bud will be covered in further detail.

Terminal buds are the structures that play a major role in woody plant dormancy. Buds are short axis bearing a densely packed series of leaf primordia that are produced by the shoot apical meristem (definition from Rohde *et. al*., 2000). A bud consists of a shoot meristem, embryonic leaves and stipules surrounded by bud scales (Rohde *et. al*., 2000). Although the principal structure can vary between species, ages, and physiological states, a typical woody plant apical meristem has three distinguished zones: a central zone, peripheral zone and a rib zone (Brown, 1971). The cells in the central zone provide a pool of indeterminate cells. The peripheral zone is the zone of cell division that gives rise to new cells in the apical meristem and of primordia.

In spring, the primordia formed through organogenesis at the apical meristem expand into leaves, which is followed by elongation of internodes, activation of cambium and initiation of axillary buds (Owens and Molder, 1976; Crabbe and Barnola, 1996; reviewed by Rohde *et. al*., 2000) (**Figure 1**). These processes stop in an organized way during formation of bud development and induction of dormancy.

Internode elongation stops and leaf primordia develop into to bud scales (Rohde *et. al*., 2000). In early fall, bud formation continues through organogenesis. At this point, the primordia are still physiologically active. In late fall, the primordia becomes inactive and bud scales form a tight structure around the apex and bud dormancy occurs (Rohde *et. al*., 2000).

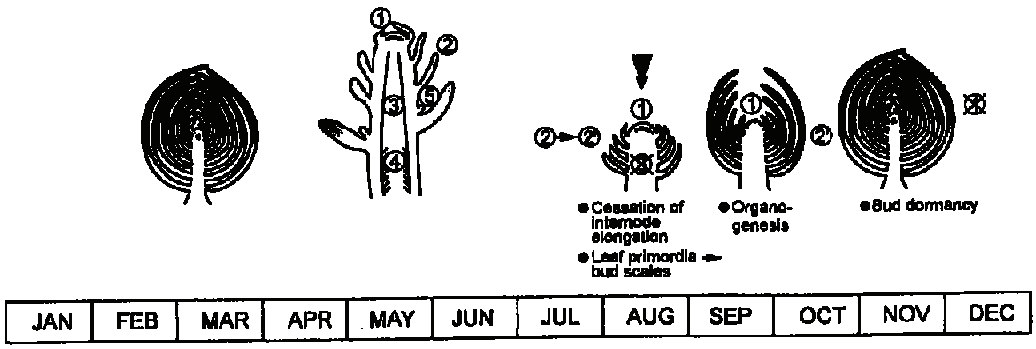

Figure 1. Formation of the dormant bud in *Populus* on a time table. In a growing apex; (1) formation of the primordia, (2) expansion into leaves, (3) elongation of the internodes, (4) activation of the cambium, (5) initiation of the axillary buds, (2') formation of bud scales (Owens and Molder, 1976; Crabbe and Barnola, 1996; Figure from Rohde *et al*., 2000)

1.3. Factors Affecting Vegetative Bud Development and Dormancy

Dormancy and vegetative bud development are affected by several endogenous and exogenous factors. Exogenous factors are environmental inputs that modify and influence bud development and dormancy. While favorable environmental conditions promote bud break and growth burst, unfavorable conditions can facilitate and/or maintain bud dormancy. These factors include the effects of temperature, day light length, and water availability. Endogenous factors, on the other hand, are internal inputs that are produced by the plant itself. These factors are plant hormones such as auxin, cytokinins, gibberellin, abscisic acid, and ethylene.

1.3.1. The Effects of Temperature on Dormancy

Temperature affects cellular and physiological processes of organisms. The rate of reactions in processes involving enzyme activity and membrane transportation are dependent on temperature (Mathews and van Holde, 1995). In case of enzymatic reactions, a certain temperature should be maintained for proper function. The fluctuations in temperature can reduce the rate of reactions, make enzymes unavailable to reaction machinery and promote onset of a different set of cellular events.

Some animals can keep their body temperature constant, which minimizes the effects of ambient temperature on cellular and physiological processes. However, plants can not maintain a constant internal temperature and are vulnerable to changes

in external temperature. Ultimately, temperature has a major influence on plant cellular and physiological processes including dormancy.

A dormant bud requires exposure to low temperatures in order to regain growth and development (Noodèn and Weber, 1978). The requirement of low temperature (i.e. chilling requirement) is genetically determined (Samish, 1954). Low temperatures also have varying effects depending on the developmental stage of dormancy. For example, chilling temperatures (0-10^{o}C) result in increased dormancy during bud development and decreased dormancy after bud maturation (Lavarenne *et al*., 1975; Mauget, 1981). The chilling requirement studies on horticultural plants such as blueberries and peaches have shown involvement of specific proteins. The changes in these bud specific proteins were associated with dehardening and dormancy in blueberries (Arora *et al*., 1997). These proteins are dehydrins, a subgroup of late embryogenesis abundant (LEA) proteins (Close, 1997). The study with sibling peach system suggested involvement of bark-storage protein in dormancy induction and release (Arora *et al*., 1996).

1.3.2. The Effects of Photoperiod on Dormancy

Plants are dependent upon light for survival. Light provides energy for photosynthesis and signals information about the surroundings of the plant. Plants use these signals for timing of their developmental stages. Photoreceptors are responsible light perception. Three types of photoreceptors are present in plants; Red/Far-red (R/FR) absorbing phytochromes, Blue/UV-A absorbing cryptochromes and phototropins.

Among the three, probably the most studied photoreceptors are phytochromes. Phytochromes can exist in two interconvertible forms: R-absorbing form (Pr) or FR-absorbing-form (Pfr) (Sharrock, 1994). R form absorbs maximum light at 660nm while it is 730nm for FR form. The Pr form of phytochromes is considered to be the inactive form and it is synthesized in dark. Upon red-light treatment, it is immediately converted to active form (Pfr) (Sharrock, 1994). The Pfr form is the active form that initiates biological responses. Pfr can also spontaneously revert to the Pr form in the dark over time, which is called dark reversion (Nagy and Schäfer, 2002). *Arabidopsis* has five phytochrome genes (*PHYA, PHYB, PYHC, PYHD*, and *PHYE*) (Clack *et al*., 1994). PHYA functions in dark and is repressed in light. It was shown that dark-grown seedlings are abundant in PHYA (Nagy and Schäfer, 2002). During dark treatment PHYB stays at low levels, which is reversed immediately after light treatment. Light enhances degradation of PHYA while increasing expression of PHYB (Quail *et. al.,* 1995).

In addition to photosynthesis, light takes a role in photomorphogenesis (e.g. leaf development, chloroplast development, and stem elongation), seed germination, regulation of flowering, and dormancy (Carabelli *et al*., 1996; Delvin *et al*., 1996; Howe et al., 1995). Phytochromes send a signal from leaves towards the actual target, the shoot apex, which responds to this signal by going dormant (Vince-Prue, 1994). In order to initiate and maintain dormancy, woody plants perceive the length of the photoperiod (Hauser et al., 1998; Vince-Prue, 1994). Long days (16 hours light) sustain shoot elongation, while short days (8-10 hours of light) induce growth cessation and formation of terminal buds (Olsen *et al*., 1997b and references therein).

The involvement of phytochromes in dormancy has been shown by studies where the photoperiod was disrupted by a night break. Since the length of dark period is important for regulation of dormancy (Vince-Prue, 1984), interruption of the dark period would result in altered dormancy. In fact, the *Populus* that were applied a night break failed to induce dormancy (Vince-Prue, 1975). Studies at the molecular level also tried to establish a link between phytochromes and dormancy. For example, overexpression of the oat phytochrome A gene in hybrid aspen trees was proposed to change the critical day length (the longest photoperiod that induces growth cessation) and to prevent cold acclimatization (Olsen *et al.,* 1997b). In another molecular level study, a QTL (Quantitative Trait Loci) analysis using *Populus* has shown that PHYB2 maps to linkage groups J_T and J_P, both of which contain a bud flush QTL in the same marker interval (Frewen *et al*., 2000).

1.3.3. The Effects of Plant Hormones on Dormancy

Phytohormones play important roles in plant growth including bud development and dormancy. Bud development and dormancy are subject to endogenous hormonal regulation. All five main plant hormones, namely abscisic acid (ABA), gibberellins (GAs), cytokinins, auxin, and ethylene, have been shown to influence dormancy and bud development.

Biosynthesis and regulation of ABA biosynthesis have been deciphered using ABA-deficient mutants especially from *Arabidopsis thaliana* (Schwartz *et al*., 2003). It was shown that ABA is synthesized through cleavage of a C_{40} carotenoid precursor. This cleavage is followed by a two-step conversion of the intermediate xanthoxin to ABA (Taylor *et al*., 2000; Finkelstein and Rock, 2002; Seo and Koshiba, 2002;

Schwartz *et al*., 2003). ABA plays a role in many cellular processes including seed development, germination, vegetative growth, and environmental stress responses (Finkelstein and Rock, 2002; Xiong and Zhu, 2003).

ABA coordinates growth and development with responses to the environment. Under non-stress conditions, endogenous levels of ABA are at low levels. ABA levels increase in response to environmental stresses and during seed maturation (Finkelstein and Rock, 2002). The results from ABA-deficient and ABA-insensitive plants have shown that ABA is the most important factor in seed dormancy (Bewley, 1997). Although ABA has significant roles in seed dormancy, its involvement in bud dormancy is not well understood. However, studies have provided insights on ABA and its possible role in bud dormancy. In apples, differing chilling requirements were used to establish a relationship between ABA and low temperatures. In this study, ABA content declined in buds during winter months, however, warm controls were not included in the study (Powell and Maybee, 1984). It is not certain how low temperatures contribute to decline in ABA levels.

Gibberellins (GAs) are a large family of diterpeniod compounds, important in plant developmental processes including seed germination, stem elongation, leaf expansion, trichome development, and flower and fruit development (Davies, 1995). Environmental stimuli such as light and temperature have been shown to affect GA-involved processes by changing GA-concentration or its responsiveness (Davis, 1995; Kamiya and Garcia-Martinez, 1999). In woody plants, cessation of stem elongation occurs with short day treatments. Since stem elongation is controlled by GAs, it can be deduced that GAs might as well be involved in shot-day induced growth cessation.

The relationship between GAs and short-days has been extensively studied. It has been shown that changes in GA metabolism occur during short-day-induced growth cessation (Juntilla, 1990; Juntilla and Jensen 1988). Poplars overexpressing phytochrome PHYA were impaired in perception of short days and also unable to down regulate GAs in response to short days (Olsen *et al*., 1997a).

Cytokinins and auxins are also very important plant hormones whose roles in dormancy have been implicated. Auxins have been associated with paradormancy. Terminal buds, where auxins are produced, exert apical dominance over axillary buds and maintain them under dormancy (Cline, 1994 and 1996). Transgenic poplars expressing IAA biosynthesis genes under shoot specific promoters have shown elevated levels of IAA (Tuominen *et al.,* 1995). Moreover, axillary buds failed to outgrow after decapitation of these transgenic plants (Tuominen *et al.,* 1995). Although auxins are responsible for apical dominance in many trees, cytokinins are the hormones that provide apical dominance in conifers (Bollmark *et al*., 1995). It was shown that cytokinins may influence apical control mostly during bud development in late summer and early spring (Bollmark *et al*., 1995).

The role of ethylene in dormancy has been established in potato. Endogenous ethylene is essential for full expression of potato microtuber endodormancy (Suttle *et al*., 1998). Ethylene also is likely to have an important role in woody plant dormancy. It was shown that overexpression of a mutant allele of *Arabidopsis* ethylene receptor gene (*etr1-1*) in *Populus* created altered bud development and dormancy (Coleman *et al.,* unpublished data). The *etr1-1* expressing poplars formed loose buds compared to wild type poplars. Moreover, they failed to enter endodormancy. Transgenic

ethylene-insensitive birches (*Betula pendula*), which express the dominant *etr1-1* mutation, ceased elongation compared to wild type under short days. The formation of terminal buds was abolished and endodormancy was delayed in the plants expressing *etr1-1* mutant allele (Ruonala *et al*., 2006). These suggest that ethylene plays an important role in bud development and dormancy.

2. Ubiquitin/ 26S Proteasome Pathway

2.1. Ubiquitin and 26S Proteasome Pathway

Plants, like animals and fungi, use a variety of polypeptides as tags to alter the function, location and turnover of intracellular proteins. In plants, several polypeptide tags have been identified, including Ubiquitin, RUB (Related-to-Ubiquitin), SUMO (Small ubiquitin-like modifiers), and APG12 (Autophagy-defective-12) that play important roles in post-translational modification of protein function (Loeb and Haas, 1992; Vierstra, 1996; del Pozo and Estelle, 1999a)

Ubiquitin was the first protein modifier identified. It is a 76 amino acid protein that is ubiquitously present in all eukaryotes. Ubiquitin is one of the most phylogenetically conserved proteins in eukaryotes, but has not been found in prokaryotes (reviewed by Hochstrasser, 1996; Varshavsky, 1997). Ubiquitin amino acid sequence of higher plants differs from that of yeast by only two amino acids (reviewed by Hochstrasser, 1996). The highly conserved sequence of Ubiquitin would suggest important cellular and physiological functions. Ubiquitin is involved in targeted protein degradation, which is important in an organism's development, and a key component of the Ubiquitin/26S proteasome pathway. The Ubiquitin/26S proteasome pathway performs a house-keeping function through the proteolytic degradation of both abnormal proteins (i.e. damaged, improperly folded proteins) and normal proteins (reviewed by Esser *et al*., 2004). The proteolytic degradation of proteins is an important regulatory step in signal transduction pathways. In both cases, the target proteins are tagged with single or multiple Ubiquitin proteins before they are destined for proteolytic degradation.

Proteolytic degradation of proteins requires the involvement of several enzymes. Free Ubiquitins (Ubs) are attached to target proteins by an adenosine triphosphate (ATP)-dependent conjugation (Simpson, 1953). The conjugation consists of E1 (Ub activating enzymes), E2 (Ub conjugating enzymes) and E3 (Ub ligases), and begins with Ubs and ATP. An acyl phosphoanhydride bond is formed between the adenosine monophosphate (AMP) of ATP and C-terminal glycine carboxy group of Ub (Haas *et al*., 1982; Haas and Rose, 1982). Ub is, then, transferred to E1 via a thiol-ester linkage (Haas *et al*., 1982; Haas and Rose, 1982). This activated Ub is transferred to E2 enzyme by transesterification (Haas and Siepmann, 1997). Finally, Ub is delivered to an E3. As an end product, an Ub-protein is conjugated to the target protein (Haas and Siepmann, 1997). This pathway is repeated several times resulting in attachment of multiple Ubs to the target protein. Once the target is polyubiquitinated, then it is targeted to the 26S proteasome complex where it is degraded proteolytically to its amino acids (Gregori *et al*., 1990; Chau *et al*., 1989). The schematic presentation of Ubiqutin/26S proteasome pathway is shown in **Figure 2**.

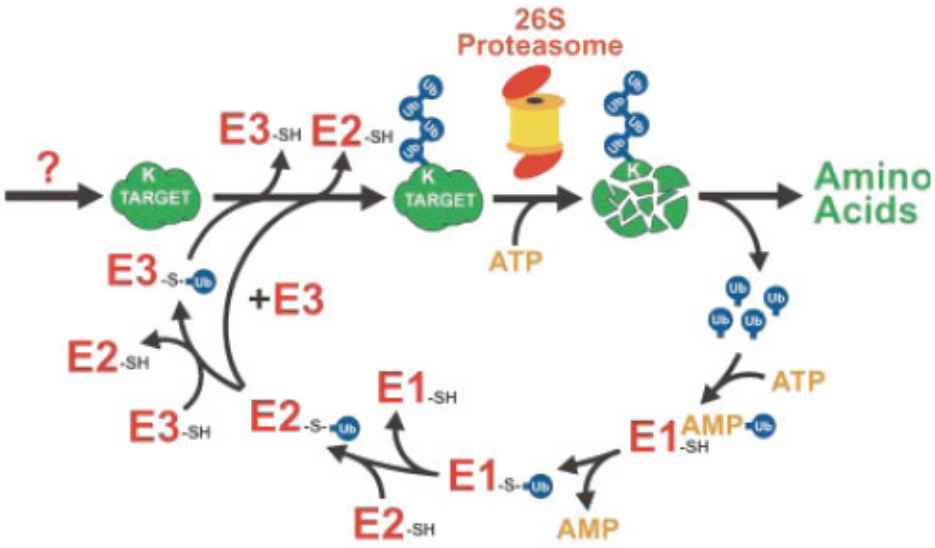

Figure 2. Ubiquitin/ 26S proteasome pathway. (Figure from Smalle and Vierstra, 2004)

2.1.1. E1s or Ub-activating enzymes

E1s or Ub-activating enzymes initiate the ubiquitination. They have high catalytic activity so even low enzyme concentrations are sufficient to activate Ubs (Pickart, 2001). Only two isoforms of E1, encoded by two specific genes, are expressed in *Arabidopsis* (Hatfield *et al.*, 1997; Vierstra *et al.,* 2003.).

2.1.2. E2s or Ub-conjugating enzymes

E2s or Ub-conjugating enzymes form Ub-E2 intermediates and deliver Ub to a corresponding E3 and therefore shuttles between E1s and E3s (Haas and Siepmann, 1997). E2s form a large gene family in plants and the *Arabidopsis* genome contains approximately 37 E2 (or UBC) genes (Bachmair *et al*., 2001). No plant E2 mutants have yet been identified, which has made functional studies difficult. This is the main reason why the function of E2s in plants is not fully understood.

2.1.3. E3s or Ub-protein ligases

E3s or Ub-protein ligases are responsible for recognition of target proteins (Smalle and Vierstra, 2004). They are the most numerous and diverse of the Es. The *Arabidopsis* genome contains more than 1300 genes that encode for E3s or E3 subunits (Smalle and Vierstra, 2004). In plants, there are four types of E3s categorized according to their structure and mechanisms of action. The plant E3s are classified as Homologous to E6AP C terminus (HECT) (Downes *et al*., 2003), Real Interesting New Gene (RING)/ U-Box (Azeveco *et al*., 2001), a complex of Skp1, Cullin (or CDC53) and F-Box protein (SCF) (Gagne *et al*., 2002), and Anaphase-

promoting complex (APC) (Capron *et al*., 2003). Due to their relevance to this thesis, Ub-protein ligases, especially SCF-containing E3s, will be covered in further detail.

HECT E3s have conserved C-terminal region and additional upstream motifs that participate in target recognition, Ub binding and/or localization. These upstream motifs include Armadillo, IQ calmudulin-binding, C-type lectin binding, transmembrane, Ub-interacting motif, Ub-associated and Ub-like domains (Downes *et al*., 2003). APC is an essential element for degrading mitotic cyclins and controlling the half-life of other factors crucial for mitotic progression and exit (Haper *et al*., 2002).

RING/U-Box E3s are not fully understood. Their structure consists of either a RING-like motif or a U-Box motif (Mayer and Hardtke, 2002). They play a role in plant physiology, including photomorphogenesis (Holm *et al.,* 2002), auxin signaling (Xie *et al*., 2002), cold sensing (Lee *et al.,* 2001), self incompatibility (Stone *et al.,* 2003), wax biosynthesis and removal of misfolded polypeptides (Yan *et al*., 2003).

The initial discovery of SCF-dependent proteolysis comes from cell division analysis of the budding yeast *Saccharomyces cerevisiae* (Patton *et al*., 1998). Cell division cycle mutants, *cdc4, cdc34* and *cdc53* are arrested with unreplicated DNA at non-permissive temperatures (Schwob *et al*., 1994; Willems *et al*., 2004.). Studies in these cell cycle mutants indicate that Cdc53 and Cdc4 interact with two other proteins, Skp1 and Rbx1 to form an E3 ubiquitin ligase complex (i.e. SCF-dependent Ub ligases) (Koepp *et al*., 1999). The SCF-dependent Ub ligases are composed of Cullin (Cdc53), Rbx and Skp proteins. The organization and structure of SCF E3s are shown in **Figure 3**. Cullins function as scaffold proteins for E3s (Patton *et al*., 1998).

Rbx, a RING-finger protein, interacts with cullin scaffold protein at the C-terminal global domain and functions as a dock for Ub/E2 conjugate (Petroski and Deshaies, 2005). Skp interacts with cullin scaffold at the N-terminal region and binds to substrate specific proteins called F-box proteins (Petroski and Deshaies, 2005). F-box proteins recruit target proteins to be ubiquitinated and are highly diverse (Gagne *et al.*, 2002; Deshaies, 1999). For example, the *Arabidopsis* genome contains more than 700 F-box proteins (Andrade *et al*., 2001). As soon as the target protein is recognized and attached to E3 complex, an Ub moiety is transferred to a lysine residue on the target protein (reviewed by Pickart, 2001). This cycle repeats several times resulting in a poly ubiquitin tail addition to the target protein. After polyubiquitination the target protein is destined for proteolytic degradation in 26S proteasome complex and ubiquitin is recycled (**Figure 2**).

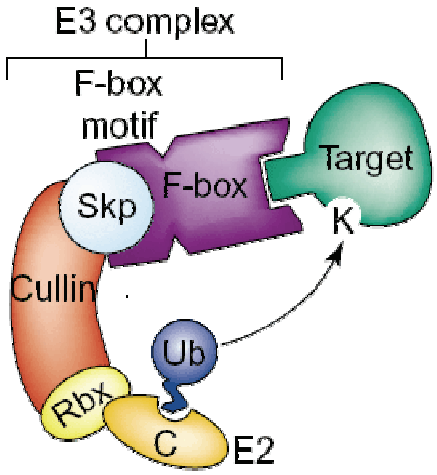

Figure 3. Organization and structure of SCF-dependent ubiquitin ligase (Figure from Vierstra, 2003.)

Cullin are a family of proteins characterized by the presence of a distinct globular C-terminal domain (cullin homology domain) and a series of N-terminal repeats of a five-helix bundle (cullin repeats) (Petroski and Deshaies, 2005). The Cullin family in humans has seven different members (CUL1, 2, 3, 4A, 4B, 5 and 7) (Petroski and Deshaies, 2005). In plants six homologs to cullin members are expressed (CUL1, 2, 3A, 3B, 4 and 5) (Shen *et al*., 2002). Each type of cullin family is a component of specific ubiquitin ligase complexes. Phylogenetic analyses have shown that the *Arabidopsis Cul1* and *Cul2* genes are not orthologous to animal *Cul1* and *Cul2* (Risseeuw *et al*., 2003). Among the plant cullins, Cullin1 is the most extensively studied one. It has a very important role in plant development and null mutants for *cul1* are embryonic lethal in *Arabidopsis* (Shen *et al*., 2002). Mutations of binding site of Cullin1 for other components of SCF complex also affect the action of Cullin1 as well as overall SCF functions (Zheng *et al*., 2002). For example, a single amino acid substitution in binding site of Cullin1 for ASK (ASK in plants for *Arabidopsis* SKP1) causes inactivation of SCF function (Hellmann *et al*., 2003). The transgenic plants that have inactivated SCF complex by a single amino acid substitution have shown lethality at two cotyledon stage (Hellmann *et al*., 2003). The small number of transgenic plants that survived has shown altered organogenesis including an apical meristem with a pin-like structure (Hellmann *et al.,* 2003).

2.1.4. 26S Proteasome Complex

The last component of the Ub/26S proteasome pathway is 26S proteasome. The 26S proteasome is an ATP-dependent proteolytic complex, composed of the 20S

core protease and the 19S regulatory particle (Hartmann-Peterson *et al*., 2003; Voges *et al*., 1999). The 20S core protease forms a cylindrical structure and the 19S regulatory particles form lids at both ends of the complex in order to regulate entry and exit of molecules through the 20S core protease (**Figure 4**) (reviewed by Smalle and Vierstra, 2004). This structural organization separates the degradation process from the cellular environment and only targeted proteins are proteolytically degraded while the cellular proteins are kept safe (Groll *et al*., 2000). The polyubiquitinated target proteins enter the complex at the regulatory particle. As the protein moves along the core particle ATP-dependent proteolytic degradation occurs (Groll *et al*., 2000). The end products of degradation, amino acids, are discharged from the other core particle end of the complex (Groll *et al*., 2000). The 26S proteasome is able to distinguish between a target protein and the polyubiquitin tail such that only the target protein can pass through the regulatory particle while the ubiquitin tail is kept out of the complex (Hartmann-Peterson *et al*., 2003). The Ubiquitin tail is dissociated into individual ubiquitin proteins, which are to be used in the next round of Ub cycle.

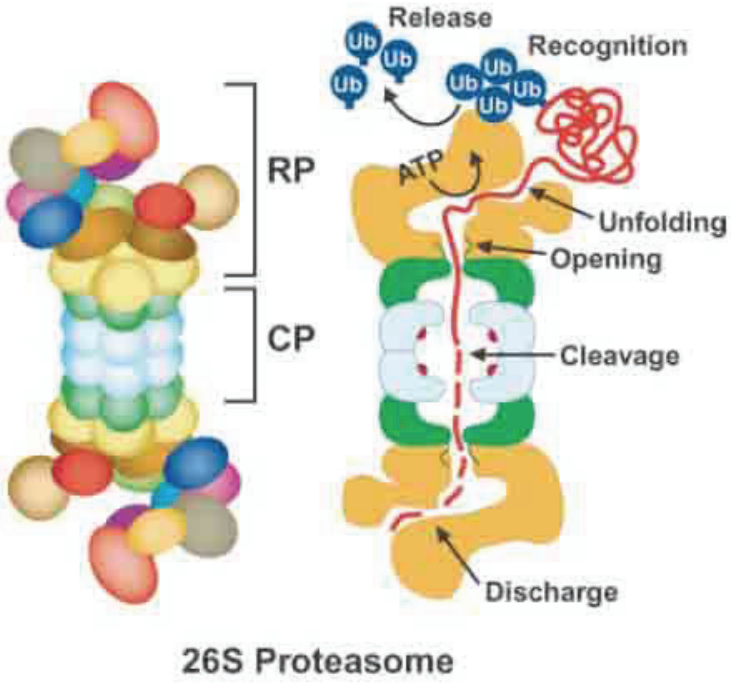

Figure 4. Organization and structure of 26S proteasome (Figure from Smalle and Vierstra, 2004)

2.2. Ubiquitin-like Protein Modifiers (SUMO, APG12 and RUB1)

Although ubiquitin was the first protein modifier found, it is not the only one present in nature. Additional protein modifiers include SUMO, APG12 and RUB. All Ubiquitin-like modifiers resemble ubiquitin in their mechanisms of substrate conjugation (Haas and Siepmann, 1997; Vierstra and Callis, 1999). Like ubiquitin, these modifiers are small polypeptides which modify proteins by conjugation. Moreover, these modifiers also have their own activating and conjugating enzymes (Hochstrasser, 2000). Similar to ubiquitin, they require energy input for the activation step (Hochstrasser, 2000). Besides their similar actions, the function of ubiquitin-like modifiers are diverse as well as their target proteins (Haas and Siepmann, 1997). While a polyubiquitin tail is required to target proteins for proteolysis, conjugation of a single molecule is sufficient for the function of other ubiquitin-like modifiers (Haas and Siepmann, 1997). Unlike ubiquitin, which targets proteins for proteolytic degradation, the ubiquitin-like proteins have regulatory functions, which do not include proteolytic degradation of targets (Lammer et al., 1998).

Little is known about function of SUMO (Small ubiquitin-like modifiers) in plants; however, some assumptions have been made based on their homology to animal SUMO. In animals, SUMO modifiers are believed to target nuclear proteins and function in their localization (Vierstra and Callis, 1999; Hochstrasser, 2000). It was proposed that addition of SUMO alters the localization, conformation or protein interactions of its target (Hochstrasser, 2000). SUMO is likely to have roles in protein trafficking, especially that of nuclear-localized proteins (review by Vierstra and Callis, 1999). APG12 (Autophagy-defective-12) proteins target lysosomal proteins

and are involved in autophagy processes since APG12 mutants of yeast are shown to be defective in autophagy (Mizushima *et al.,* 1998). Although several homologous APG12 genes exist in the *Arabidopsis* genome, there has been limited research on their function.

RUB (Related-to-Ubiquitin) is also known as Nedd8 (i.e. short for neuronal precursor cell expression developmentally down-regulated in mammals and *Schizosaccharomyces pombe*). Similar to Ubiquitin, RUB is found in all eukaryotes (Hochstrasser, 1998). The RUB conjugation pathway is also similar to that of Ubiquitin. Both RUB and Ubiquitin attach to their target proteins by covalent bonds through a series of activating and conjugating enzymes to achieve modification of their targets (Haas and Siepmann, 1997; Vierstra and Callis, 1999). However, the targets of RUB1 are the Cullin subunit of SCF-dependent ubiquitin ligases (Hochstrasser, 1998). Attachment of a single RUB1 to Cullin regulates E3 function by modifying assembly and disassembly of SCF-dependent E3s by binding to Cullins (**Figure 5**) (del Pozo and Estelle, 1999; Hori *et al*., 1999).

In *Arabidopsis thaliana*, there are three RUB proteins (Rao-Naik *et al*., 1998). The RUB1 and RUB2 proteins vary by a one amino acid. RUB3, which has 16 amino acid differences to RUB1 and RUB2, is more divergent from the other two proteins (Bostick *et al*., 2004). The RT-PCR studies have shown that the expression of *RUB1* and *RUB2* are present in all plant organs while *RUB3* expression is reduced compared to *RUB1* and *RUB2* (Rao-Naik *et al.,* 1998). RUB1 proteins and their conjugating enzymes are functionally conserved across species (Liakopoulos *et al*., 1998). This

conservation was proved by a study where human RUB1 successfully conjugated to yeast Cdc53 (target protein in yeast) (Liakopoulos *et al*., 1998).

It has been shown that *Arabidopsis* RUB1 and RUB2 are functionally redundant and the presence of at least one functional RUB-encoding gene is sufficient for proper RUB function (Bostick *et al*., 2004). While single *RUB1* or *RUB2* mutant plants are viable and have wild type phenotype, no double mutant seedlings were recovered after screening more than 300 progeny (Bostick *et al*., 2004). This indicates that RUB1 and RUB2 proteins are not only structurally similar, but they are also functionally redundant.

RUB1, like ubiquitin, requires activating and conjugating enzymes in order to covalently attach to target proteins (Hochstrasser, 1998). RUB1 activating and conjugating enzymes were initially identified in *S. cerevisiae* (Hochstrasser, 1998). The yeast RUB1 activating enzyme, Uba3-Ula1, is a heterodimeric protein (Hochstrasser, 1998). In *Arabidopsis*, the RUB1 activating enzyme is composed of AXR1 and ECR1 proteins (del Pozo *et al.,* 1998). AXR1 and ECR1 are expressed in growing tissues while little RNA or protein is detected in non-growing tissues (del Pozo *et al.,* 1998). AXR1 and ECR1 are involved in auxin responses in plants. Mutations in *AXR1* alter auxin responses and auxin-related growth and development in *Arabidopsis* (del Pozo *et al.,* 2002). This suggests that reduction in regulation of Cullins by RUB1 results in deficiencies in auxin response.

The RUB1 conjugating enzyme is termed Ubc12p and HsUbc12 in yeast and human, respectively (Liakopoulos *et al*., 1998; Osaka *et al.,* 1998). Like in human, RUB1 conjugating enzyme in *Arabidopsis* was found based on sequence similarity to

yeast Ubc12p and was called RCE1 (RUB1 conjugating enzyme1) (del Pozo and Estelle, 1999b). Transgenic *Arabidopsis* plants expressing a recessive mutation in the *RCE1* show deficiencies in ethylene biosynthesis (Larsen and Cancel, 2004). The *rce1* mutants displayed features of the ethylene-mediated triple response even in absence of ethylene (Larsen and Cancel, 2004). Moreover, these mutants produced small leaves and fewer seeds. The *rce1* mutants have also displayed impaired induction of basic chitinase and plant defensin (Larsen and Cancel, 2004). Given the fact that regulatory proteins of both the ethylene biosynthesis and jasmonic acid pathways are subject to ubiquitination, these findings suggest that regulation of Cullin proteins by RUB1 is important in ethylene and jasmonic acid responses.

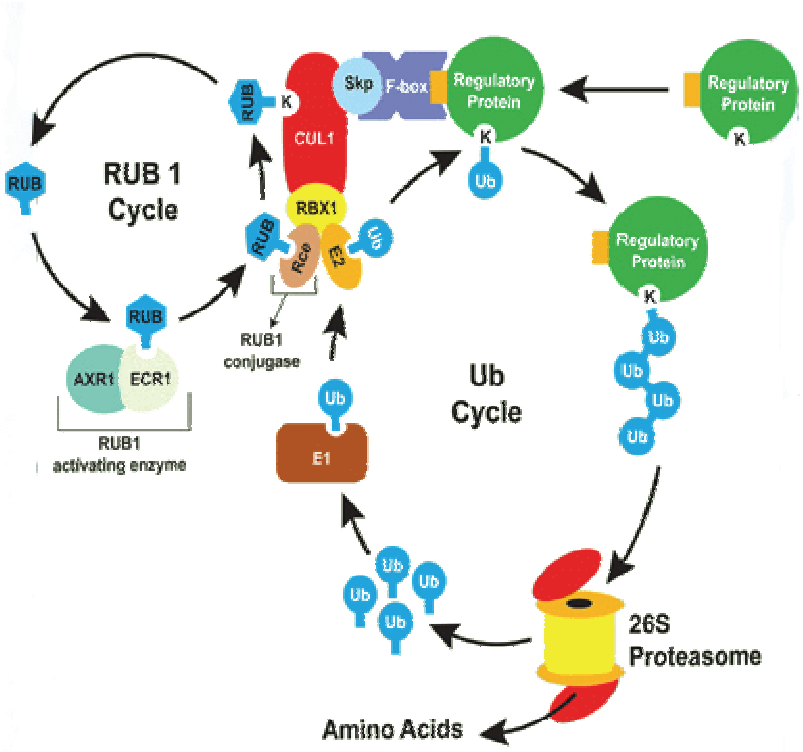

Figure 5. RUB1 and Ubiquitin cycles. Ubiquitin cycle is modified and regulated by RUB1 protein, which attaches covalently to Cullin subunit of E3 ligases. (Figure modified from Smalle and Vierstra, 2004)

2.3. Ubiquitin/ 26S Proteasome Pathway and Plant Development

The Ubiquitin/26S proteasome pathway contributes to a wide variety of developmental processes in plants. These include cell cycle, embryogenesis, photomorphogenesis, circadian rhythms, hormone signaling, disease resistance, and senescence (reviewed by Smalle and Vierstra, 2004). In *Arabidopsis*, more than 1400 genes encode for components of Ubiquitin/26S proteasome pathway, which constitutes approximately 5% of the proteome (Smalle and Vierstra, 2004). The amount of cellular resources and energy allotted to this pathway indicates the importance of this pathway to plant development.

Among the components of the pathway, E3 ligases are the most diverse. Specific E3 ligases are associated with specific cellular and physiological processes (**Figure 6**) (Moon *et al.,* 2004). In *Arabidopsis*, RING and SCF E3s are more abundant than HECT E3s (Vierstra, 2003). For example, the *Arabidopsis* genome encodes for only seven HECT E3s (Downes *et al*., 2003). One of these, UPL3 (for Ubiquitin Protein Ligase3), has been extensively studied and appears to be involved in gibberellin-mediated trichome development in plants (Perazza *et al*., 1998). The *Arabidopsis* genome contains a large number of genes encoding for RING E3s, including COP1 has been extensively studied. COP1 is a key component in photomorphogenesis and is a negative regulator of light responses (Deng *et al.,* 1991) by targeting activators of light response for degradation (Osterlund *et al*., 2000).

The SCF-dependent E3s are highly diverse in the *Arabidopsis* genome (Vierstra, 2003). This diversity is a result of F-box subunit, which targets substrates. SCF E3 targets include transcription factors, cell cycle regulators, and regulatory

proteins involved in development and signal transduction (reviewed by Smalle and Vierstra, 2004). Proteolytic degradation of these targets is important for many processes including hormone response, photomorphogenesis, circadian rhythms, floral development, and senescence (Smalle and Vierstra, 2004). The best characterized SCF E3 in plants is SCF^{TIR1}, which targets regulatory AUX/IAA proteins for proteolytic degradation (Gray *et al.,* 1999). The AUX/IAA protein acts as a negative regulator of auxin responses by forming a complex with ARF (Auxin Related Factor) transcription factor (Gray *et al.,* 1999). The proteolytic degradation of AUX/IAA dissolves AUX/IAA-ARF complex and allows the ARF (Auxin Related Factors) to initiate transcription of auxin responsive genes (Gray *et al*., 2001).

SCF-dependent E3s also play a role in gibberellic acid (GA) responses in plants. Similar to auxin, GA initiates GA-specific SCF E3s, including SCF^{SLY}, which targets negative regulators of GA response for degradation (Fu *et al*., 2004). The targets of SCF^{SLY} are GAI and RGA proteins (Dill *et al.,* 2004). As a result of removal of negative regulators of GA responsive genes, the GA responsive genes are made available to transcription machinery.

Ethylene is another plant hormone whose biosynthesis and signaling are affected by proteolytic degradation. The components of ethylene signaling pathway have been extensively studied. The signaling pathway includes the ethylene receptors, ETR1, ETR2 and EIN4, Raf-like kinase CTR1, EIN2 protein, and the transcription factor EIN3 (Guo and Ecker, 2004). The transcriptional activator of ethylene, EIN3, is a target of Ub/26S proteasome pathway. In response to ethylene, degradation of EIN3 via SCF^{EBF} is inhibited resulting in the release of the transcription activator,

which becomes available to activate ethylene responsive genes (Guo and Ecker, 2003).

Although Ubiquitin/26S proteasome pathway plays many roles in plant physiological processes, its role in woody plant dormancy has yet to be identified. A cDNA-AFLP study using wild-type and *Arabidopsis etr1-1* expressing poplars has shown differential expression of 10 Ubiquitin/26S proteasome pathway specific genes during dormancy (Coleman *et al*., unpublished data). This suggests that this pathway may play a role in poplar bud dormancy. This thesis research aims to identify the roles of several components of Ubiquitin/26S proteasome pathway including Cullin, RUB1 conjugase and EIN3-binding F-box (EBF) protein in poplar bud development and dormancy. Along with RUB1 conjugase and Cullin1, EBF was selected because EBF F-box protein has been shown to involve in ethylene signaling pathway through degradation of the EIN3 transcription factor by Ubiquitin/26S proteasome pathway (Gagne *et al*., 2004; Guo and Ecker 2003; Potuschak *et al*., 2003). Because poplars expressing a mutant allele of ethylene receptor (i.e. *etr1-1*) have altered dormancy and the ethylene signaling involves targeted protein degradation by Ubiquitin/26S proteasome pathway, the study of EBF gene expression could provide a link between dormancy and involvement of ethylene signaling in this process.

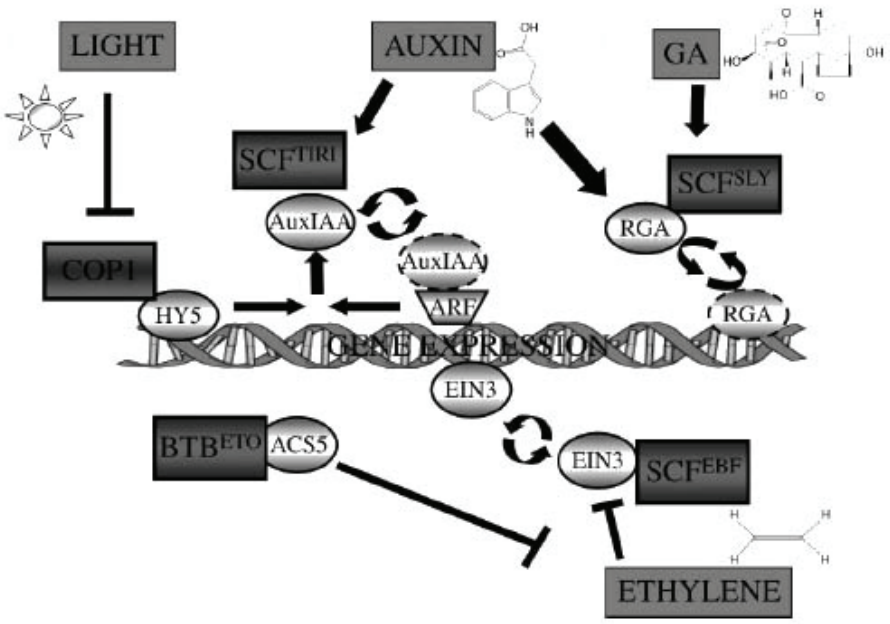

Figure 6. Various physiological and cellular processes are controlled by targeted protein degradation. (Figure from Moon *et al.,* 2004)

MATERIALS AND METHODS

1. Plant Material

The hybrid poplar (*Populus tremula* X *Populus alba*) clone 717-B4, obtained from INRA, France, was used to study vegetative bud development and dormancy. The hybrid poplar clone 717 was transformed with *Arabidopsis* ethylene receptor gene ETR1 carrying the negative dominant mutation *etr1-1*. The *Arabidopsis etr1-1* mutant allele was provided by Harry Klee, University of Florida. The *Arabidopsis etr1-1* mutant allele was cloned into a modified pGPTV-BAR under the control of 35S promoter vector with restriction enzyme digestions and ligations. The orientation of *etr1-1* with respect to 35S promoter was verified by H*ind*III/E*co*RI and H*ind*III/S*ac*I double digestions. The modified vector was transferred to *Agrobacterium* strain C58/pMP90 by freeze-thaw method. Poplar transformations were done as described by Leple *et al* (1992) except that selection of transformants was with the herbicide BASTA (5mg/L).

Plants were maintained in tissue culture until rooted. Rooted plants were transferred to soil with gradual acclimatization to air. Plants were fertilized with Peters 20-20-20 at the rate of 50ppm N. Bud formation and dormancy induction were achieved by exposing plants to 8h light/16h dark (short day photoperiod) for 12 weeks, whose last four weeks were at 10^{o}C during the day and 4^{o}C during the night. In Coleman's research group, bud development and dormancy is studied in three developmental stages. Stage 1 is bud formation which occurs during the first three weeks in SD conditions. Stage 2 is bud maturation which occurs during weeks four through six. In stage 3, bud dormancy occurs with exposure to short day conditions

beyond six weeks. The dept of dormancy is increased by exposing plants to low temperatures during last four weeks of bud dormancy stage. Tissue samples from terminal buds, axillary buds, bark, the fifth, tenth and the fifteenth leaves were collected on weekly basis for 13 weeks.

2. RNA Isolation

For RNA isolation, tissue samples from terminal buds, axillary buds, bark, the fifth, tenth and the fifteenth leaves were collected. Collected tissues were immediately frozen in liquid nitrogen and were stored at -80^{o}C until RNA isolation. Total RNA was isolated using RNeasy® total RNA isolation kit (QIAGEN Inc., California, USA) with minor modifications. Tissues were ground to fine powder with a mortar and a pestle that had been baked in oven, and then, pre-cooled in liquid nitrogen. Leaves, bark and axillary buds were resuspended in RNeasy® RLT buffer containing 0.1% (v/v) β-mercapto-ethanol and 0.1% (w/v) polyvinylpyrrolodone-40, and were homogenized by vortexing. Homogenates from leaves, bark and axillary buds were incubated at 56^{o}C for 3 minutes, transferred directly onto RNeasy® QIAshredder spin columns and centrifuged at 14,000 rpm for 2 minutes. The supernatant was transferred to a fresh microcentrifuge tube and mixed with a 0.5X volume of 100% ethanol. The rest of the total RNA isolation procedure was performed as following the manufacturer's procedure.

Terminal bud ground tissue was added to RNeasy® RLT buffer containing 0.1% (v/v) β-mercapto-ethanol, 0.1% (w/v) polyvinylpyrrolodone-40 and 0.4 of volume of 5M Potassium Acetate solution (pH 6.5) was added and mixed by inversion. Terminal bud homogenate was then incubated on ice for 15 minutes

followed by centrifugation at 12,000rpm for 15 minutes at 4°C. The supernatant was transferred to a fresh microcentrifuge tube, followed by 0.5X volume of 100% ethanol and mixed. The solution was then transferred to RNeasy® Spin Columns and the remaining steps of the procedure followed the manufacturer's instructions for plant RNA isolation.

Total RNA was precipitated with a 0.1X volume of 3M Sodium Acetate and a 2X volume of 100% ethanol at -20°C overnight and precipitated at 14,000rpm for 30 minutes at 4°C. Pelleted RNA precipitate was washed twice with 70% ethanol and the RNA pellets were dried in Savant Integrated Speed Vac® at medium heat. The RNA pellets were dissolved in RNase-free water.

RNA concentration was determined by measuring absorbance at 260nm using a spectrophotometer (Perkin Elmer, Lambda Bio UV/VIS spectrometer). RNA samples were stored at -80°C until needed.

3. Computational Analysis of Poplar EST 99 and EST 181

3.1. Retrieval of Gene Models for EST 99 and EST 181

A previous functional genomics study using cDNA-AFLP was performed to identify candidate genes involved in bud development and dormancy of wild-type and *Arabidopsis etr1-1* expressing poplars (Coleman *et al*., unpublished data). Among the 502 differentially expressed ESTs (Expressed Sequence Tags), two ESTs have been chosen to study further detail. The nucleotide sequences of EST 99 (NCBI Accession# CX282586) and EST 181 (NCBI Accession# CX282665) were used to do a BLAST (Basic Local Alignment Search Tool) search of the *Populus* database (JGI *Populus trichocarpa* v1.0) at the Joint Genome Institute web site

(http://www.jgi.doe.gov/). Four different gene model prediction programs (Eugene, Fgenesh, Grail, and Genewise) were used to retrieve predicted protein, transcript, and gene sequences for each EST.

3.2. Multiple Sequence Alignment of Gene Models

Multiple sequence alignments of predicted protein and transcript sequences were performed in order to obtain related consensus sequences for the ESTs. Multiple sequence alignments were performed using ClustalW 1.83 software (Higgins and Sharp, 1988; Higgins *et al*., 1996). Gap opening and gap extension penalties were 10.00 and 0.20, respectively. BLOSUM series and ClustalW 1.6 options were set as protein and DNA weight matrices, respectively. The alignment output was visualized and consensus sequences were created using BioEdit v7.0.4 software (License Agreement for BioEdit v7.0.4: BioEdit v7.0.4 copyright I 1997-2005, Tom Hall).

3.3. Retrieval of Homologous Sequences

Consensus protein and transcript sequences for the ESTs were used to perform protein-protein BLAST (blastp) and nucleotide-nucleotide BLAST (blastn) searches, on non-redundant protein and nucleotide databases at the NCBI web site (http://www.ncbi.nlm.nih.gov/). Complete or near-complete homologous protein and transcript sequences were obtained. Sequences with a homology of e^{-20} or better e-value were retrieved and used for phylogenetical analysis.

3.4. Phylogenetic Analysis

Phylogenetic analysis of EST 99 and EST 181 was performed for gene annotation. The homologous protein sequences identified in the prior BLAST

searches were saved in FASTA format and aligned to EST 99 and EST 181 consensus protein sequences using ClustalW 1.83 sequence alignment software program. Gap opening (10.00) and gap extension (0.20) penalties were applied. BLOSUM series were chosen as protein weight matrix.

The alignment output was edited using the BioEdit v7.0.4 software program (Hall, 1997). The gaps at the ends and/or within the alignments were filled in with question marks (?) as suggested by the phylogenetic analysis software program. The alignment was edited to extract the best aligned regions. By eliminating poorly aligned regions, the length of alignment was reduced to a manageable-length, which could efficiently be processed by phylogenetic analysis software programs. However, the edited alignment still contained a high degree of diversity in terms of nucleotide inversions, transitions, additions, and deletions, which are essential for determining phylogenetic relationships among sequences. The edited alignment files were written in and saved as PHYLIP format.

Phylogenetic analysis of the EST 99 and EST 181 based on amino acid sequence were carried out using distance (Neighbor Joining) and maximum parsimony (MP) methods in PHYLIP 3.63 (Felsenstein, 2002). Support for each node was tested with 100 bootstrap analysis, using random input order for each replicate. Amino acid substitution models were used whenever possible. In distance methods, the Kimura amino acid substitution model was chosen. In MP methods, search-for-best-tree option was set and in distance methods, neighbor-joining option was chosen over UPGMA (Unweighted Pair Group Method with Arithmetic mean) option.

Each method produced 100 different trees which were, then, condensed to a consensus tree using "consense.exe" option of the PHYLIP 3.63 software. Trees were rooted using the out group species *Cryptosporidium hominis* and *Plasmodium berghei* for EST 99 and EST 181, respectively. These species had the most divergent sequences in their alignment, and yet, their sequences shared a certain degree of similarity to the rest of the sequences. This made them good candidates for out group species. Consensus trees were drawn using the TreeView v.1.6.6 software program (Page, 1996).

4. Expression Analysis of Poplar RUB1 Conjugase and Cullin1 Genes

4.1. cDNA Synthesis and Reverse Transcription-Polymerase Chain Reaction (RT-PCR)

RNA samples were treated with DNase prior to cDNA synthesis using RQ1 RNase-free DNase (Promega Corp., WI, USA). Reverse transcription reactions, were performed using ImProm-II™ Reverse Transcription System (Promega Corp, WI, USA). Approximately 800ng of total RNA was used to synthesize cDNA following the manufacturer's instructions and the optional ribonuclease inhibition using 20 units of RNasin® ribonuclease inhibitor step was included in the procedure.

Gene specific primers for RUB1 conjugase and Cullin1 genes were designed using Primer Select™ 5.51 sequence analysis software (DNASTAR Inc.). All the primers used in this thesis were synthesized by Invitrogen. The gene specific forward and reverse primers for RUB1 conjugase gene were 5'-GTGGCGTGCCGATCAAGAAGC-3' and 5'-CCACAT ACCCGCCAGTCATAG-3', respectively. The gene specific forward and reverse primers for Cullin1 gene were

5’-ATGGGGCAGATGGATTATTATGAA-3’ and 5’-AGCCAACCACGTCCTTTTTATCT-3’, respectively.

Poplar Ubiquitin was used as an internal control in the gene expression studies. The forward and reverse primers for Ubiquitin-like protein (UBQL) gene were 5’-CCAGACCAGCAGAGGTTGA-3’and 5’-GATCTTGGCCTTCAGGTTGT-3’, respectively. These primer pairs amplified a 207 bp fragment of the Ubiquitin transcript. Although ubiquitin was used as an internal control, the PCR reactions took place in different tubes. The main reason for not having the reactions take place in a single tube was that the primers for Ubiquitin-like protein amplified three different UBQLs; one of the amplified products had a size conflict with the amplified fragments of RUB1 conjugase and Cullin1 genes. Another reason was that the genes studied required different numbers of PCR cycles to reach the linear range, which prevented having the reactions take place in a single tube.

In order to assure semi-quantitative analysis of gene expression, the number of PCR cycles was determined empirically to find the linear range of amplification. RUB1 conjugase, Cullin1, and Ubiquitin cDNAs were amplified 25, 30, 35 and 40 number of PCR cycles. The linear range of amplification was at 25 cycles for both RUB1 conjugase and Ubiquitin genes and that was at 30 cycles for Cullin1 gene.

PRC reaction mixes were prepared by combining 1X Takara *Ex Taq*™ DNA polymerase buffer, 200µM dNTP mix, 0.2 µM gene specific forward and reverse primers, 2mM $MgCl_2$, 90ng template cDNA, and 1.25 units of *Ex Taq*™ DNA polymerase in a total volume of 50µl. The PCR conditions for amplification of RUB1 conjugase included denaturation at 94^{o}C for 30 seconds, annealing at 55^{o}C for 30

seconds, and synthesis at 72°C for 1 min. These conditions were cycled 25 times followed by a final elongation step at 72°C for 7 minutes. The PCR conditions for amplification of Cullin1 were the same as those of RUB1 conjugase, except that the number of PCR cycles was 30. The PCR conditions for amplification of Ubiquitin were the same as those of RUB1 conjugase.

The RT-PCR products were separated through a 1.2% (w/v) agarose gel using 1X TAE (TRIS Base-Acetic Acid-EDTA pH 8.0) buffer and stained with 0.1μg/ml Ethidium Bromide. Gels were run at 3 V/cm. DNA was visualized under ultra violet (UV) light and documented using Kodak 1D imaging analysis software. Gel images were saved as TIFF files.

5. Analysis of RUB1 and Ubiquitin Conjugated Proteins

5.1. Poplar Vegetative Bud Protein Extraction and Quantification

During purification of total RNA from apical buds, the column flow-through solutions from all steps were with an equal volume of 0.1M ammonium acetate in -20°C methanol overnight at -20°C. Pelleted proteins were at 10,000g for 20 minutes at room temperature. The protein pellets were washed three times with 0.1M ammonium acetate in -20°C methanol and once with -20°C acetone. Protein pellets were air dried and resuspended in 1X sodiumdodecylsulfate (SDS) buffer (0.025M TRIS, 0.192M Glycine, 0.1% SDS, pH 8.3) and 1mM dithiothreitol (DTT).

Bud proteins were quantified using the Bicinchoninic acid (BCA) protein assay. Prior to performing BCA protein assay interfering substances such as DTT were removed by precipitating the proteins using trichloroacetic acid (TCA) by mixing the aliquots with 72% (w/v) trichloroacetic acid and 0.15% (w/v) sodium

deoxycholate (SDS). The mixtures were incubated at 25°C for 10 minutes after which the samples were centrifuged at 14,000rpm at room temperature for 10 minutes. The supernatants were discarded and the protein pellets were dissolved in 5% (w/v) SDS. Protein samples were mixed with a solution of 50:1 ratio of BCA reagent A to BCA reagent B (Pierce, IL, USA). Samples were incubated at 37°C for 30 minutes and the absorbance at 562nm was measured using a spectrophotometer. BSA was used as standards to prepare a calibration curve. The equation of the calibration curve was used for determination of concentration of bud proteins.

5.2. SDS Polyacrylamide Gel Electrophoresis (SDS-PAGE) of Proteins and Western Blot Analysis

Proteins were separated by SDS-PAGE using 12% resolving gel (1.5M TRIS pH 8.8) and 5% stacking gel (1.0M TRIS pH 6.8). Proteins were first denatured at 100°C for 3 minutes. Each lane was loaded 5µg of protein in sample loading buffer (1X SDS and bromophenol blue). Protein markers (Pierce, BlueRanger® prestained protein molecular weight marker mix, IL, USA) used in this experiment were myosin (216 kD), phosphorylase B (119 kD), BSA (83.8 kD), ovalbumin (49.7 kD), carbonic anhydrase (32.7 kD), trypsin inhibitor (26.2 kD), and lysozyme (18.1 kD). Protein gels were run at 200V until the loading dye ran out of the gels.

After SDS-PAGE, the proteins were transferred to 0.45µm nitrocellulose membranes (Trans-Blot®, Bio-Rad Laboratories, CA, USA) using Genie Electrophoretic Blotter. The transfer buffer was 25mM TRIS-HCl/192mM Glycine (pH 8.3) in 20% (v/v) methanol. The proteins were transferred to the membrane by applying a voltage of 24V for 40 minutes. After the transfer, the membranes were

washed once with water and once with TRIS Buffered Saline (TBS) (10 mM Tris, 150 mM NaCl, pH 7.4) for 5 minutes. Membranes were blocked with 3% BSA in TBS overnight at 4^{o}C with gentle shaking. Then, membranes were washed twice with 1X TBS buffer containing 1% Tween20 (TTBS) for 5 minutes.

Membranes were incubated with primary antibodies overnight at 4^{o}C with gentle shaking. The primary antibodies were RUB1 and Ubiquitin polyclonal antibodies, both of which were raised in rabbit. RUB1 polyclonal antibody (Orbigen Cat. No. PAB-11608) was diluted 1,000 times with 1% BSA in TTBS buffer. Ubiquitin polyclonal antibody (Santa Cruz Biotechnology, Inc. Cat. No. Ub (FL-76): sc-9133) was diluted 500 times with 1% BSA in TTBS buffer. After washing twice with TTBS, membranes were then incubated with secondary antibody at 25^{o}C for one hour. Anti-rabbit IgG antibody was used as secondary antibody and diluted 7,500 times with 1% BSA in TTBS. Membranes were washed three times with TTBS, once with TBS and twice with an alkaline phosphatase buffer (100mM NaCl, 5mM $MgCl_2$ and 100mM TRIS-Cl, pH 9.5) for 5 minutes. Color was developed with 66µl of NBT (50mg/ml, Nitro-blue tetrazolium chloride, ImmunoPure®, Promega, USA) and 33µl of BCIP (50mg/ml, 5-Bromo-4-Chloro-3'-Indolyphosphate p-Toluidine Salt, ImmunoPure®, Promega, USA) in the alkaline phosphatase buffer. Color development was stopped with water. Digital images of the membranes were made and saved as TIFF files.

6. Expression of EBF-like (ein3-binding F-box protein like) Gene during Vegetative Bud Development

Using gene loci identification numbers for *Arabidopsis EBF1* (At2g25490) and *EBF2* (At5g25350) the *Populus* database (JGI *Populus trichocarpa* v1.0) at the Joint Genome Institute web site (http://www.jgi.doe.gov/) was searched for poplar EFB homologs. The protein sequences for poplar gene models were retrieved and aligned with *Arabidopsis EBF* sequences. The ClustalW tree was used as a guide to select poplar homologs to *Arabidopsis EBF* genes. The transcript sequences from the filtered models for putative poplar *EBF* genes on linkage groups LG XVIII and LG VI were used to design poplar *EBF* specific primers using Primer Select™ 5.51 sequence analysis software (DNASTAR Inc.). The forward and reverse primers for poplar *EBF*-like gene were 5'-TGCCCGGGGGTGAAGAGA-3' and 5'-GCGGGGCATTGGGAAAGAT-3', respectively. Ubiquitin was used as an internal control in semi-quantitative RT-PCR. The PCR reactions for amplification of *EBF*-like genes were 94^{o}C for 30 seconds, 57^{o}C for 30 seconds, and 72^{o}C for 1 min. PCR reactions were run for 35 cycles which was followed by an elongation step at 72^{o}C for 7 minutes. The PCR conditions for amplification of ubiquitin were the same except 25 cycles were used.

The products of RT-PCR were separated through 1.2% (w/v) agarose gel with 1X TAE (TRIS Base-Acetic Acid-EDTA pH: 8.0) buffer and stained with 0.1µg/ml Ethidium Bromide. Gels were run at 3V/cm. The PCR products were visualized under ultra violet (UV) light and gel images were taken using Kodak 1D imaging analysis software.

7. The Effects of the Ethylene Precursor ACC and Inhibitor AVG on Expression of RUB1 Conjugase Gene

Stem cuttings from 10 week old poplars were used to determine whether the ethylene precursor ACC or the inhibitor AVG affected RUB1 conjugase expression. Four levels (0μM, 25μM, 50μM, 100μM) of both ACC (1-aminocyclopropanecarboxylic acid) and AVG ((*E*)-L-2-[2-(2-aminoethoxy)vinyl]glycine) were used. Stem cuttings of 30cm from wild type poplars and poplars expressing *Arabidopsis etr1-1* were placed into solutions immediately after cutting. The top of bottles were wrapped tightly with parafilm to prevent evaporation. Apical meristems were collected after 6 days of treatment under long day conditions (16 hours of light and 8 hours of dark) at 20^{o}C. RNA isolation, cDNA preparation, and RT-PCR procedures were as previously detailed for RUB1 conjugase.

8. Obtaining Full Length cDNA for the RUB1 Conjugase Gene

Full length cDNA sequence for RUB1 conjugase was obtained using RT-PCR with gene specific 5'-end and 3'-end primers designed from the predicted gene sequence. cDNA synthesis and PCR conditions were the same as those for the RUB1 conjugase expression study except for the primers. In order to obtain the complete cDNA sequence, the primers included putative start and stop codons. The RUB1 conjugase gene specific 5'-end primer and 3'-end primers were 5'-ATGATTCGGCTATTTAAAGTGAAGG-3' and 5'-CTAAATACACCGTGGAAAGAAGG-3', respectively.

The PCR products were cloned into the pGEM®-T Easy vector (Promega Corporation, WI, USA) according to manufacturer's instructions. The ligation

reaction was incubated at 4^{o}C overnight to increase the ligation efficiency. JM109 high efficiency competent cells were transformed with the ligation reaction and grown on Luria Broth (LB) plates with 100mg/L Ampicillin, 100µl of 100mM IPTG, and 20µl of 50µg/ml X-Gal. After incubation overnight at 37^{o}C, white colonies were selected and grown in liquid LB medium with 100mg/L Ampicillin for plasmid DNA isolation.

Plasmid DNA was isolated using the Wizard® *Plus* DNA purification system (Promega Corporation, WI, USA) following the manufacturer's instructions. Putative RUB1 conjugase full length cDNA was first digested with *Eco*RI or *Pst*I or a double digested of N*co*I and S*ac*I restriction enzymes. Digestions were performed using 5µg of plasmid DNA, 20 units of digestion enzyme, and 1X restriction enzyme buffer in a total volume of 10µl. The digestions were done at 37^{o}C for 1 hour. The digestion products were separated through 1.2% (w/v) agarose gel with 1X TAE buffer and stained with Ethidium Bromide. DNA was visualized with UV-light and the gel images were saved as TIFF files.

Plasmid DNA containing a RUB1 conjugase full length cDNA insert was sequenced at the core sequencing facility of the University of Maryland Biotechnology Institute Center for Biosystems Research (5129 Plant Sciences Building, College Park, MD).

RESULTS

1. Computational Analysis of EST 99

1.1. Retrieval of gene models and consensus sequences associated with EST 99

The BLAST search at JGI *Populus* database using the EST 99 sequence have indicated that there are three possible genes coding for the EST 99. One is on linkage group VII (LG_VII), the second is on scaffold 57 (Sc_57) and third is on linkage group IX (LG_IX). Sequence similarity of EST 99 to the gene on LG_VII is 100%, while that is 93.33% to the genes on Sc_57 and 82.47% to the genes on LG_IX. **Table A1** in the appendix lists the gene models associated with EST 99 for all three locations in the poplar genome. Multiple sequence alignment of predicted transcript sequences from the gene models are represented in the appendix **Figure A1**, **Figure A2** and **Figure A3**. Predicted protein alignments are placed in the appendix sections **Figure A4**, **Figure A5** and **Figure A6**. The transcript and protein consensus sequences created from the alignments are represented in the appendix. The pairwise alignments of consensus protein and transcript sequences have shown that the genes represented at LG_VII, LG_IX and Sc_57 are similar to each other. The sequence similarities are high at protein level (~90%) while that is more diverged at nucleotide level (~84%) (**Figure 7 and Figure 8**).

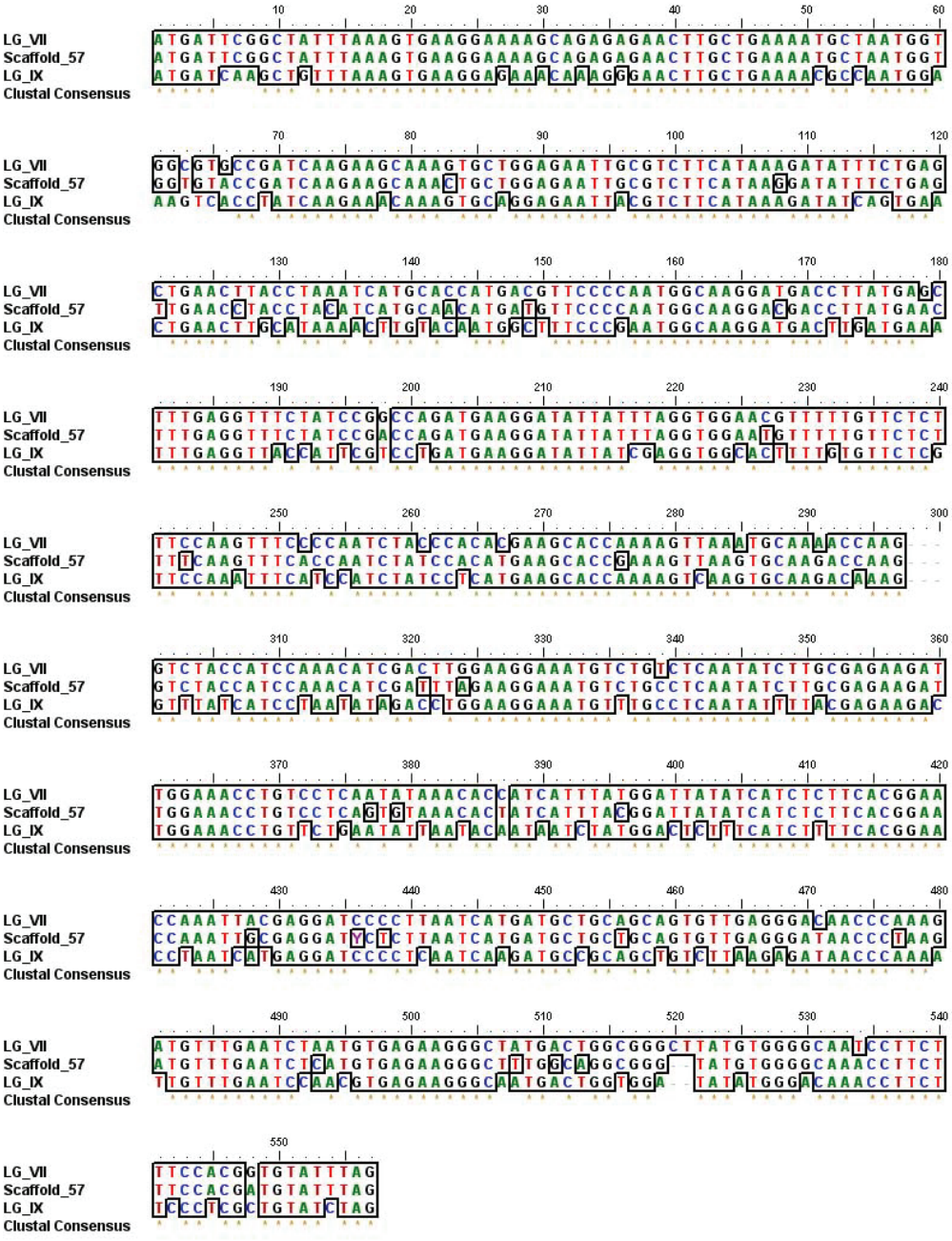

Figure 7. Multiple sequence alignment of consensus transcript sequences for the genes encoding EST 99 at LG_VII, LG_IX and Scaffold_57. 5'- and 3'- UTRs (Untranslated Regions) have been excluded from the sequences. Clustal consensus sequences are labeled "*" indicating identical or conserved residues in all sequences; ":"shows conserved substitutions and "." indicates semi-conserved substitutions.

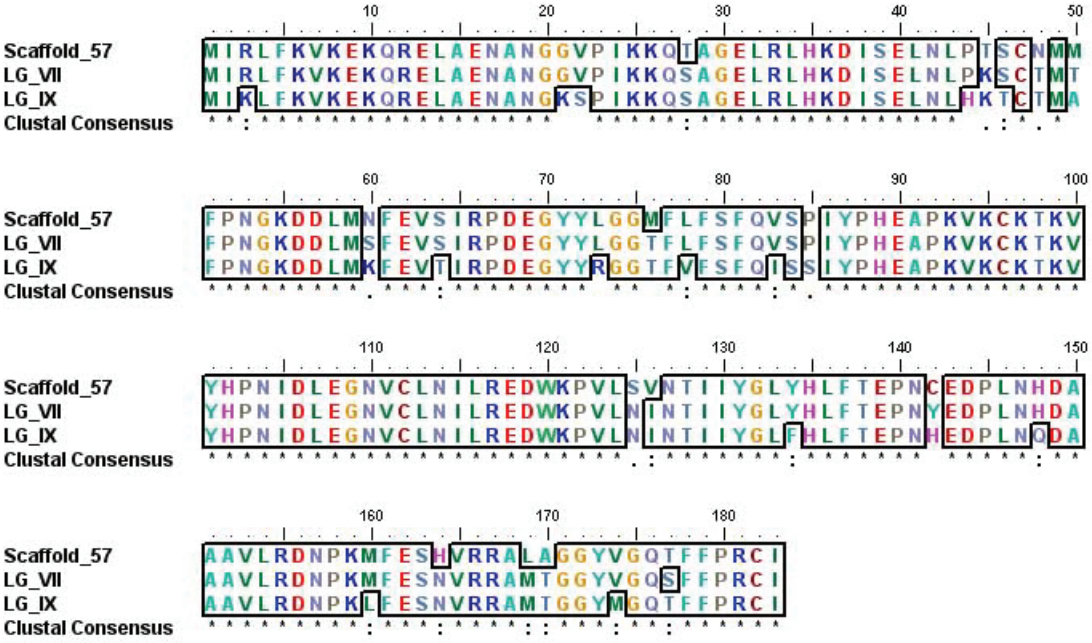

Figure 8. Multiple sequence alignment of consensus protein sequences for the genes encoding for EST 99 at LG_VII, LG_IX and Scaffold_57. Clustal consensus sequences are labeled "*" indicating positions which have a single, fully conserved residue; ":" shows one of the strong groups is fully conserved; and "." indicates that one of the weaker groups is fully conserved.

1.2. EST 99 encodes for an RUB1 conjugase-like protein in poplar

Gene annotation can be accomplished using two different approaches either by functional studies or by homology to a previously identified gene. In this study, the homology approach was used for annotation of EST 99. The results of BLAST search on NCBI protein (**Table 1**) and nucleotide (**Table2**) databases revealed that EST 99 shared similarity to both RUB1 conjugase and E2 ubiquitin conjugase.

Although RUB1 conjugase and E2 ubiquitin conjugase both are components of Ubiquitin/ 26S proteasome pathway, they have diverse functions. Since EST 99 shares a high degree of similarity to both enzymes, it would be erroneous to annotate the gene solely by the results of BLAST search. For accurate annotation of the gene, phylogenetical analyses were performed.

47 protein sequences were aligned and edited before using for PHYLIP phylogenetic analysis (**Figure 9**). The results of phylogenetic analysis using distance and maximum parsimony approaches were similar with the poplar protein located in the same branch as the RUB1 conjugase from other organisms (**Figures 10 and 11**). In both cases, the branches are highly supported by bootstrap values of 95% for neighbor joining approach and 100% for maximum parsimony approach. This suggests that EST 99 encodes for an RUB1 conjugase-like gene in poplar.

Table 1. The results of BLAST (blastp-nr) search on NBCI protein database using consensus protein sequence for EST 99 as query. E-value cut-off is e-15

NCBI Accession Number	**Organism Name**	**Abbreviation used in Phylogenetic Trees**	**Description of Hit Protein**	**E-value**
AAN75193.1	*Olea europa*	O. eu RUB1	RUB1 conjugating enzyme	9e-96
AAG23847.1	*Lycopersicon esculentum*	L. es RUB1	RUB1 conjugating enzyme	6e-82
CAA51821.1	*Lycopersicon esculentum*	L. es E2	E2 conjugating enzyme	5e-18
AAA64427.1	*Pisum sativum*	P. sa E2	E2 conjugating enzyme	6e-18
AAD12207.1	*Arabidopsis thaliana*	A. th RUB1	RUB1 conjugating enzyme	5e-86
NP_568008.1	*Arabidopsis thaliana*	Not used	RUB1 conjugating enzyme (RCE1)	5e-28
AAM63316.1	*Arabidopsis thaliana*	A. th UBC11	E2 conjugating enzyme (UBC 11)	3e-19
AAM63837.1	*Arabidopsis thaliana*	A. th E2	E2 conjugating enzyme	1e-20
CAC27113.1	*Arabidopsis thaliana*	A. th E2(1)	E2 conjugating enzyme	6e-20
CAA78716.1	*Arabidopsis thaliana*	A. th E2(2)	E2 conjugating enzyme	2e-19
CAA78715.1	*Arabidopsis thaliana*	A. th E2(3)	E2 conjugating enzyme	3e-19
AAM44985.1	*Arabidopsis thaliana*	A. th UBC10	E2 conjugating enzyme UBC10	2e-20
CAB79598.1	*Arabidopsis thaliana*	A. th UBC9	E2 conjugating enzyme (UBC9)	6e-20
NP_567791.1	*Arabidopsis thaliana*	A. th UBC9(1)	Ub conjugating enzyme (UBC9)	6e-20

Table 1 continued.

NCBI Accession Number	Organism Name	Abbreviation used in Phylogenetic Trees	Description of Hit Protein	E-value
NP_568595.2	*Arabidopsis thaliana*	A. th UBC8	Ub conjugating enzyme (UBC8)	9e-20
AAL34248.1	*Arabidopsis thaliana*	A. th UBC8(1)	Ub conjugating enzyme (UBC8)	2e-19
AAV34697.1	*Arachis hypogaea*	A. hy E2	Ub conjugating enzyme	7e-19
AAD51109.1	*Mesembryanthenum crystallinum*	M. cr UBC2	Ub conjugating enzyme 2	7e-19
AAL99225.1	*Gossypium raimondii*	G. ra E2	Ub conjugating enzyme E2	1e-18
AAL99221.1	*Gossypium hirsutum*	G. hi E2	Ub conjugating enzyme E2	8e-18
AAL99223.1	*Gossypium arbereum*	G. ar E2	Ub conjugating enzyme E2	2e-18
AAN03469.1	*Glycine max*	G. ma E2	Ub conjugating enzyme E2	3e-17
AAP52544.1	*Oryza sativa*	O. sa E2	Ub conjugating enzyme	4e-84
XP_463908.1	*Oryza sativa*	O. sa E2(1)	Ub conjugating enzyme	1e-19
BAD34325.1	*Oryza sativa*	O. sa E2(2)	Ub conjugating enzyme	2e-19
NP_915993.1	*Oryza sativa*	O. sa E2(3)	Ub conjugating enzyme	4e-19
XP_482060.1	*Oryza sativa*	O. sa RUB1	Ub conjugating enzyme	2e-80
BAD36217.1	*Oryza sativa*	O. sa RUB1(1)	Ub conjugating enzyme	2e-75
XP_464900.1	*Oryza sativa*	O. sa UBC5b	Ub conjugating enzyme UBC5b	7e-19
BAB89354.1	*Oryza sativa*	O. sa UBC5a	Ub conjugating enzyme UBC5b	1e-18
AAT01622.1	*Zea mays*	Z. ma RUB1	RUB1 conjugating enzyme	4e-83

Table 1 continued,

NCBI Accession Number	Organism Name	Abbreviation used in Phylogenetic Trees	Description of Hit Protein	E-value
AAB88617.1	*Zea mays*	Z. ma E2	Ub conjugating enzyme	2e-19
AAP80608.1	*Triticum aestivum*	T. ae RUB1	RUB1 conjugating enzyme	9e-67
AAU82109.1	*Triticum aestivum*	T. ae E2	Ub conjugating enzyme	2e-18
AAP04430.1	*Hordeum vulgare*	H. vu E2	Ub conjugating enzyme	2e-19
AAR83891.1	*Capsicum annuum*	C. an E2	Ub conjugating enzyme	3e-18
XP_577006.1	*Rattus norvegicus*	R. no E2	Ub conjugating enzyme	5e-17
NP_001008382.1	*Rattus norvegicus*	R. no NEDD8	NEDD8-conjugating enzyme	2e-15
XP_528640.1	*Pan troglodytes*	P. tr UBC12	Ub conjugating enzyme UBC12	9e-56
XP_516184.1	*Pan troglodytes*	P. tr NEDD8	NEDD8-conjugating enzyme	7e-22
XP_497504.1	*Homo sapiens*	H. sa UBC12	Ub conjugating enzyme UBC12	2e-55
AAH66917.1	*Homo sapiens*	H. sa E2	Ub conjugating enzyme	3e-16
CAD21285.1	*Neurospora crassa*	N. cr E2	Ub conjugating enzyme	3e-48
CAA17917.1	*Schizosaccharomyces pombe*	S. po UBC4	Ub conjugating enzyme UBC4	2e-18
XP_757129.1	*Ustlilago maygis*	U. ma UBC1	Ub conjugating enzyme UBC1	9e-19
EAK98832.1	*Candida albicans*	C. al E2	Ub conjugating enzyme	5e-42
NP_013409.1	*Saccharomyces cerevisiae*	S. ce UBC12p	Ub conjugating enzyme UBC12p	1e-36
NP_010344.1	*Saccharomyces cerevisiae*	S. ce UBC5p	Ub conjugating enzyme UBC5p	2e-18
NP_009638.1	*Saccharomyces cerevisiae*	S. ce UBC4p	Ub conjugating enzyme UBC5p	2e-18

Table 1 continued,

NCBI Accession Number	Organism Name	Abbreviation used in Phylogenetic Trees	Description of Hit Protein	E-value
EAL47583.1	*Entamoeba histolytica*	E. hi E2	Ub conjugating enzyme UBC5p	4e-27
EAL49024.1	*Entamoeba histolytica*	E. hi E2(1)	Ub conjugating enzyme	1e-23
EAL37293.1	*Cryptosporidium hominis*	C. ho E2	Ub conjugating enzyme	4e-23
AAH21792.1	*Mus musculus*	M. mu E2	Ub conjugating enzyme	5e-60
NP_080730.1	*Mus musculus*	M. mu NEDD8	NEDD8 conjugating enzyme	2e-22
XP_613823.1	*Bos taurus*	B. to NEDD8	NEDD8 conjugating enzyme	7e-19
CAH76282.1	*Plasmodium chabaudi*	P. ch E2	Ub conjugating enzyme	6e-20
NP_701795.1	*Plasmodium falciparum*	P.fa E2	Ub conjugating enzyme	6e-20

Table 2. The results of BLAST (blastn-nr) search on NBCI nucleotide database using consensus transcript sequence for EST 99 as query. E-value cut-off is e-10. cds: coding sequence.

NCBI Accession Number	**Organism Name**	**Description of Hit Nucleotide**	**E-value**
AY004247	*Lycopersicon esculentum*	RUB1 conjugating enzyme (RCE1) mRNA (partial cds)	1e-57
AY157723	*Olea europaea*	RUB1 conjugating enzyme (ORCE) mRNA (complete cds)	1e-48
NM_119844	*Arabidopsis thaliana*	RUB1-conjugating enzyme, putative (RCE1)(At4g36800) mRNA (complete cds)	8e-31
AF202771	*Arabidopsis thaliana*	RUB1 conjugating enzyme (RCE1) mRNA (complete cds)	8e-31
BT005005	*Arabidopsis thaliana*	putative RUB1-conjugating enzyme (At2g18600) mRNA, complete cds.	3e-30
CAR299066	*Cicer arietinum*	partial mRNA for ubiquitin-conjugating enzyme E2	2e-22
AY591341	*Zea mays*	putative RUB1 conjugating enzyme mRNA, complete cds	1e-14
NM_195275	*Oryza sativa*	putative ubiquitin-conjugating enzyme (OSJNBb0038H12.1), mRNA	2e-10

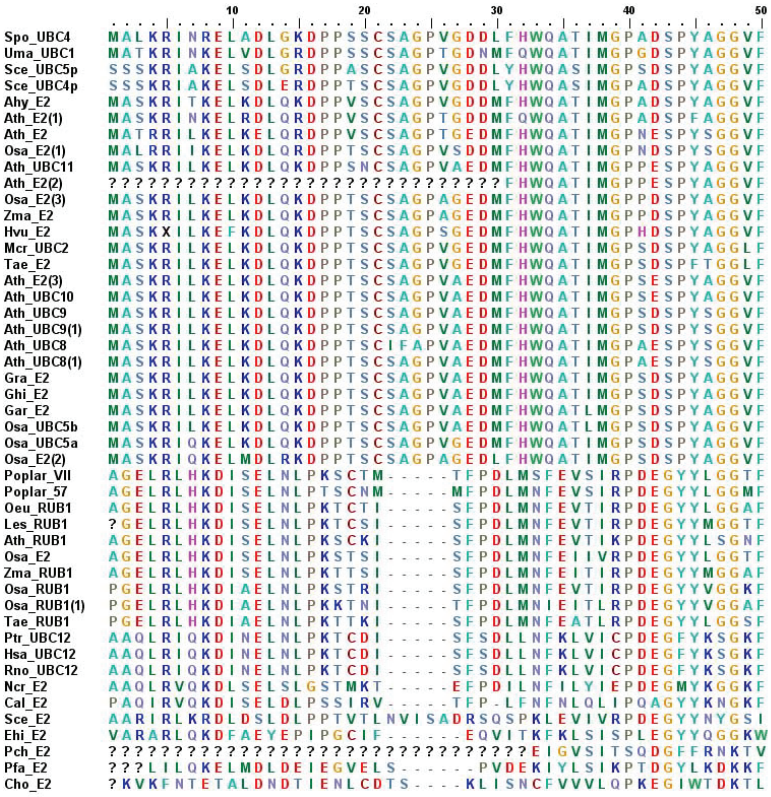

Figure 9. E2 conjugase and RUB1 conjugase protein sequences were aligned using ClustalW. The alignment was edited using BioEdit to manage the end gaps. The first column shows the abbreviation of species (first letter of genus name and the next two letters of species name) and gene designation (E2, RUB1, UBC). The alleles are shown either in letters (A, B, C) or in parenthesis ([1], [2], [3]).

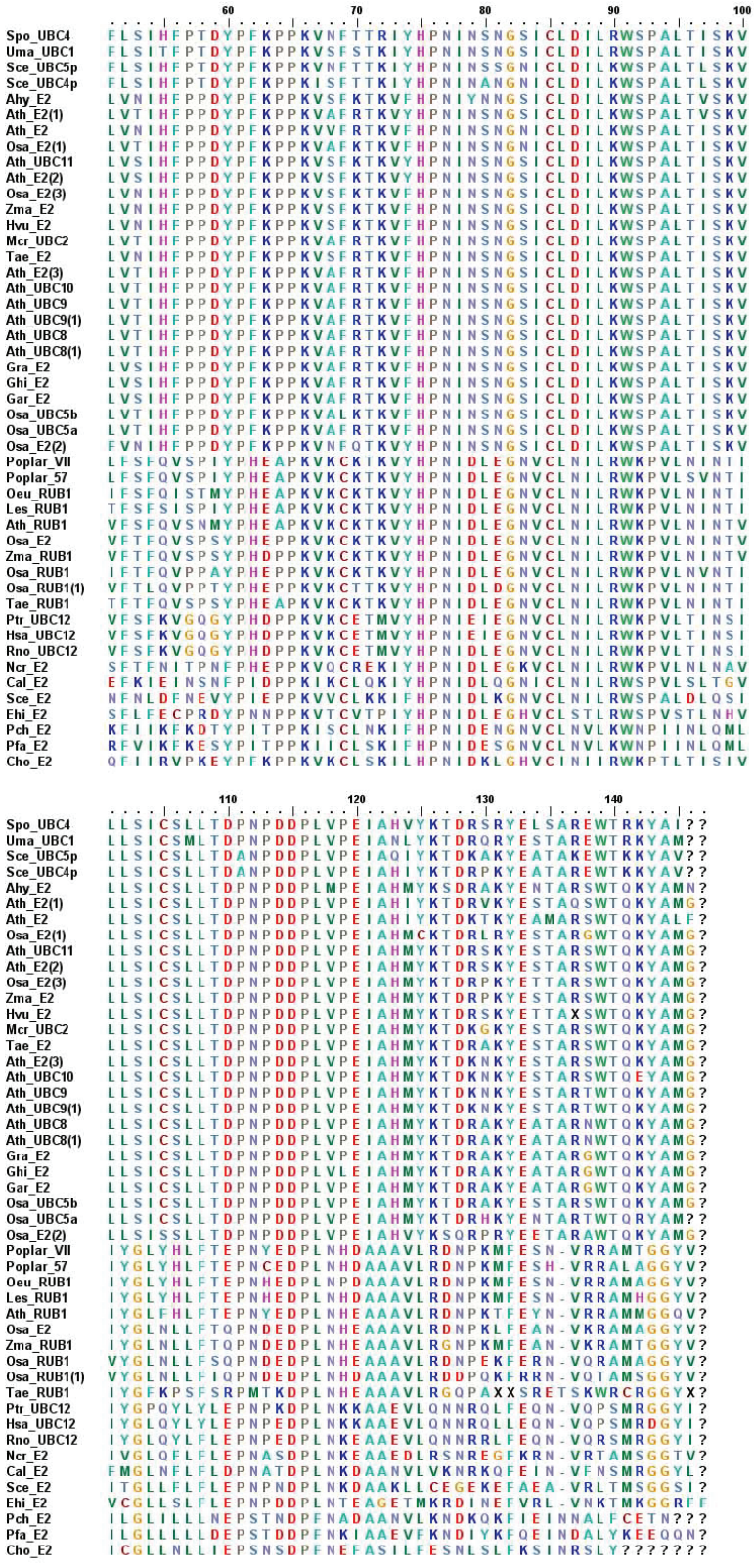

Figure 9 continued.

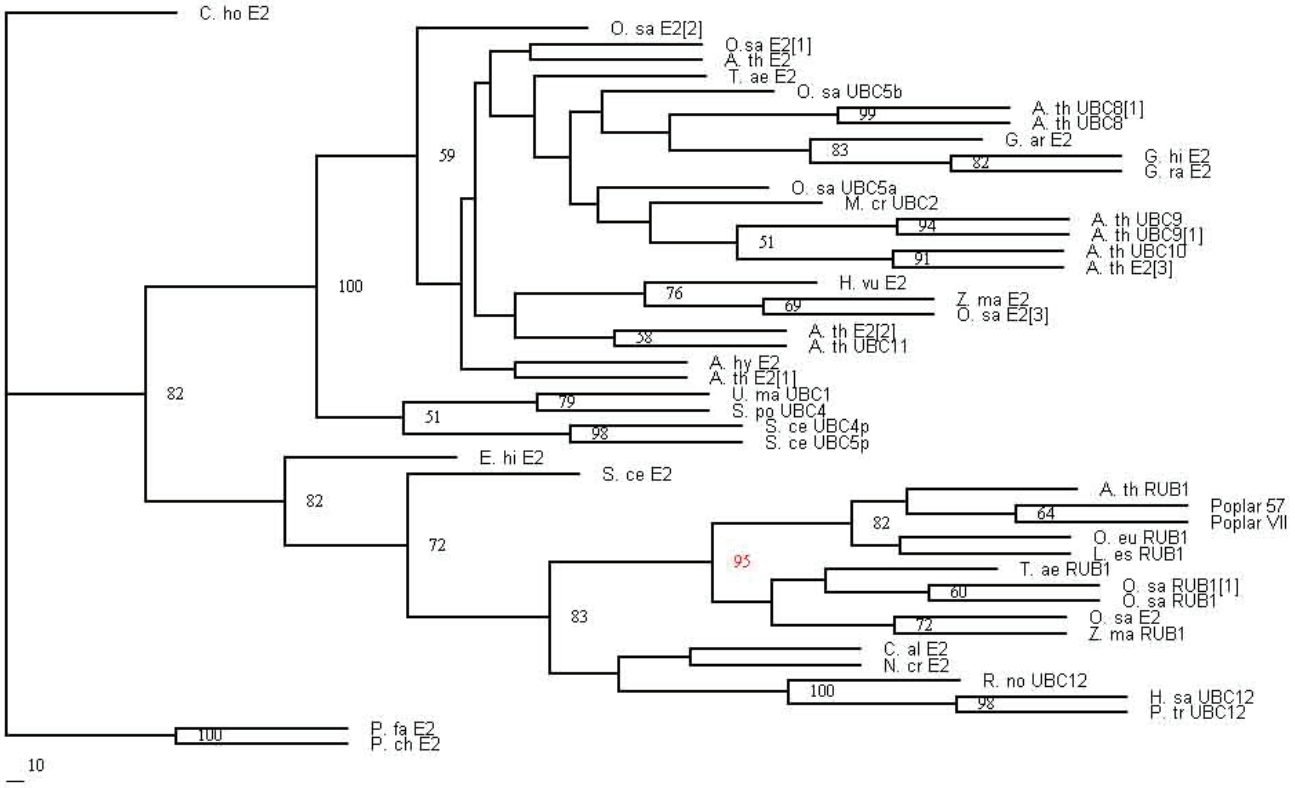

Figure 10. Molecular phylogeny of E2 conjugase and RUB1 conjugase sequences, obtained by distance and neighbor-joining methods. Significant bootstrap support (>50%) is shown next to the respective nodes. Bootstrap value for the clade containing poplar sequences is in red color. Bar scale shows the number of amino acid substitutions.

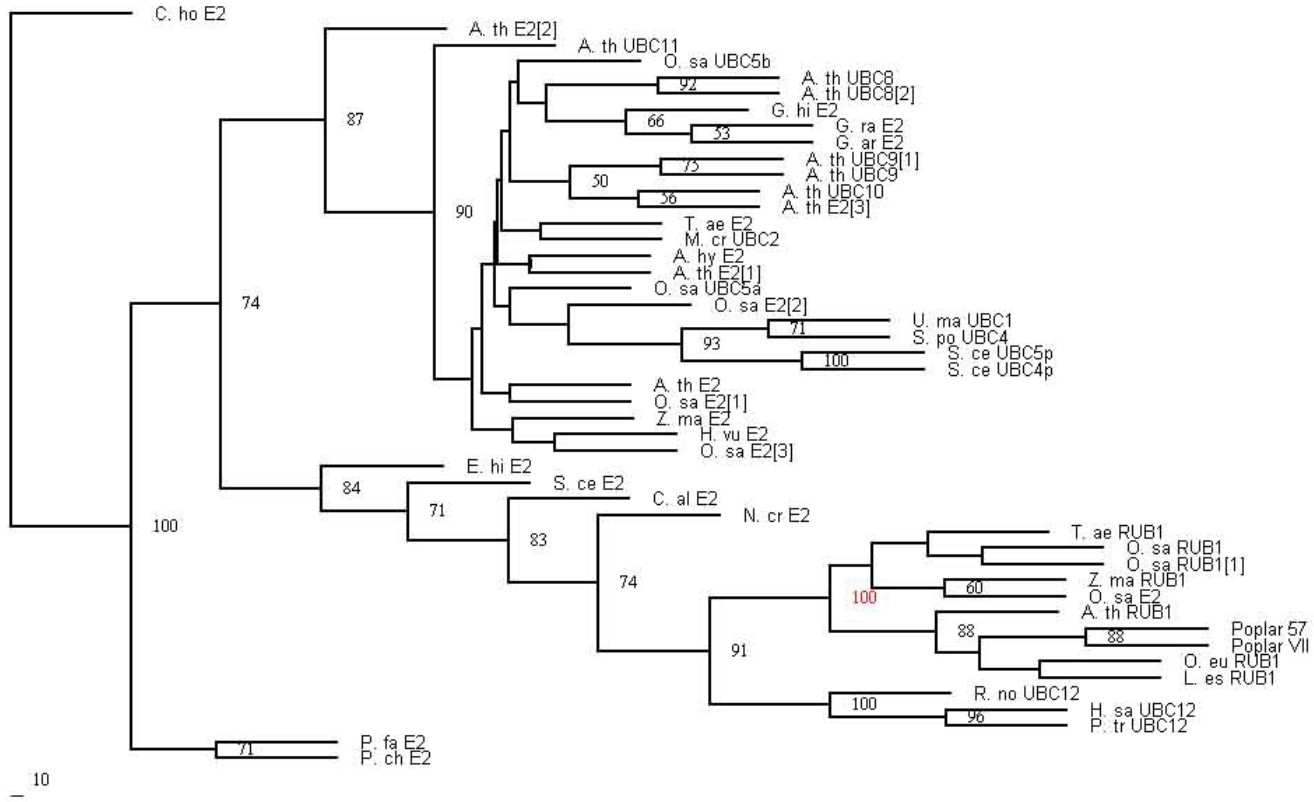

Figure 11. Molecular phylogeny of E2 conjugase and RUB1 conjugase sequences, obtained by maximum parsimony methods. Significant bootstrap support (>50%) is shown next to the respective nodes. Bootstrap value for the clade containing poplar sequences is in red color. Bar scale shows the number of amino acid substitutions

2. Computational Analysis of Poplar EST 181

2.1. Retrieval of gene models and consensus sequences associated with EST 181

The results of BLAST search at JGI *Populus* database using EST 181 sequence have shown that it is homologous to two different locations in poplar genome. This suggests that there are two possible genes coding for EST 181, one of which is on linkage group X (LG_X) and the other one is on scaffold 132 (Sc_132). The sequence similarity of EST 181 to the predicted gene on LG_X is 94.20%, while that is 97.83% for the predicted gene located on Sc_132. **Table A2** in appendices section shows the gene models associated with EST 181 for both locations in the poplar genome. Multiple sequence alignment of predicted transcript sequences from gene models are shown in the appendices **Figure A7** and **Figure A8**. Predicted protein sequence alignments are shown in the appendices **Figure A9** and **Figure A10**. The consensus sequences created from alignments are also included in the appendices figures. The pairwise alignments of consensus protein and transcript sequences are shown in **Figures 12 and 13**, respectively.

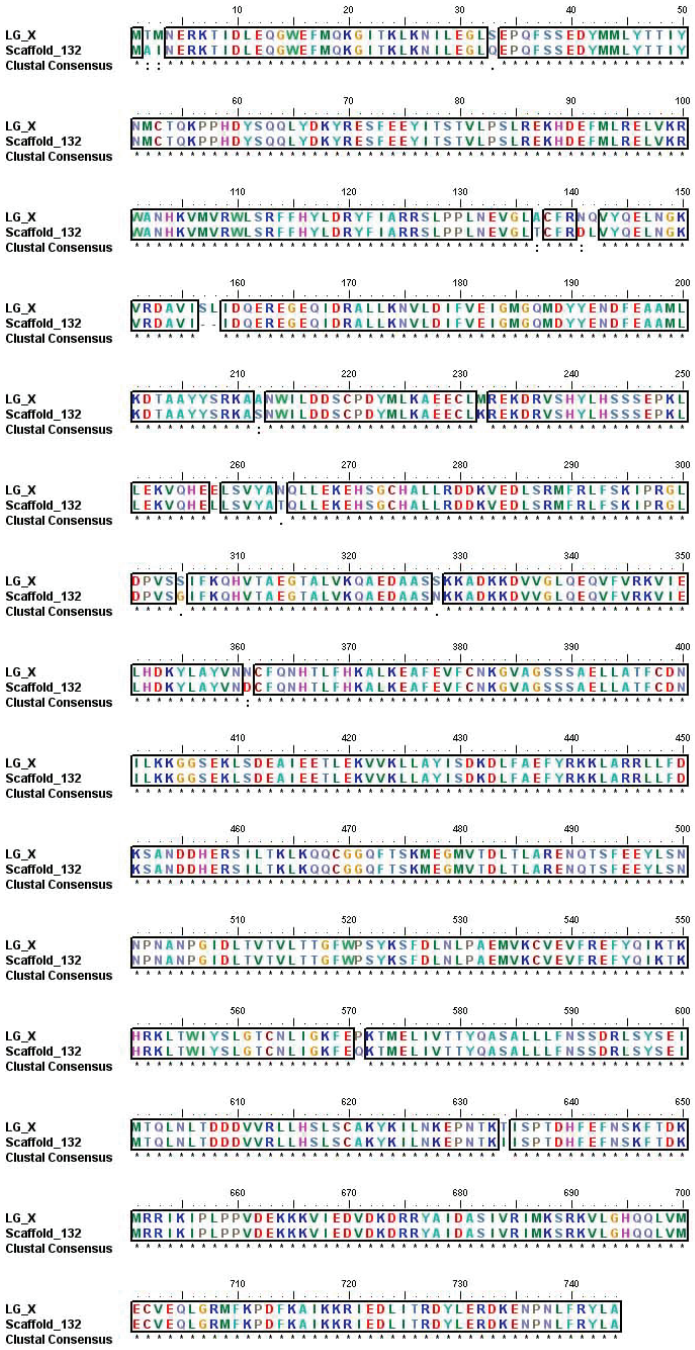

Figure 12. Pairwise alignment of consensus protein sequences for the genes encoding for EST 181 on LG_X and Scaffold_132. Clustal consensus sequences are labeled "*" indicating positions which have a single, fully conserved residue; ":" shows one of the strong groups is fully conserved; and "." indicates that one of the weaker groups is fully conserved.

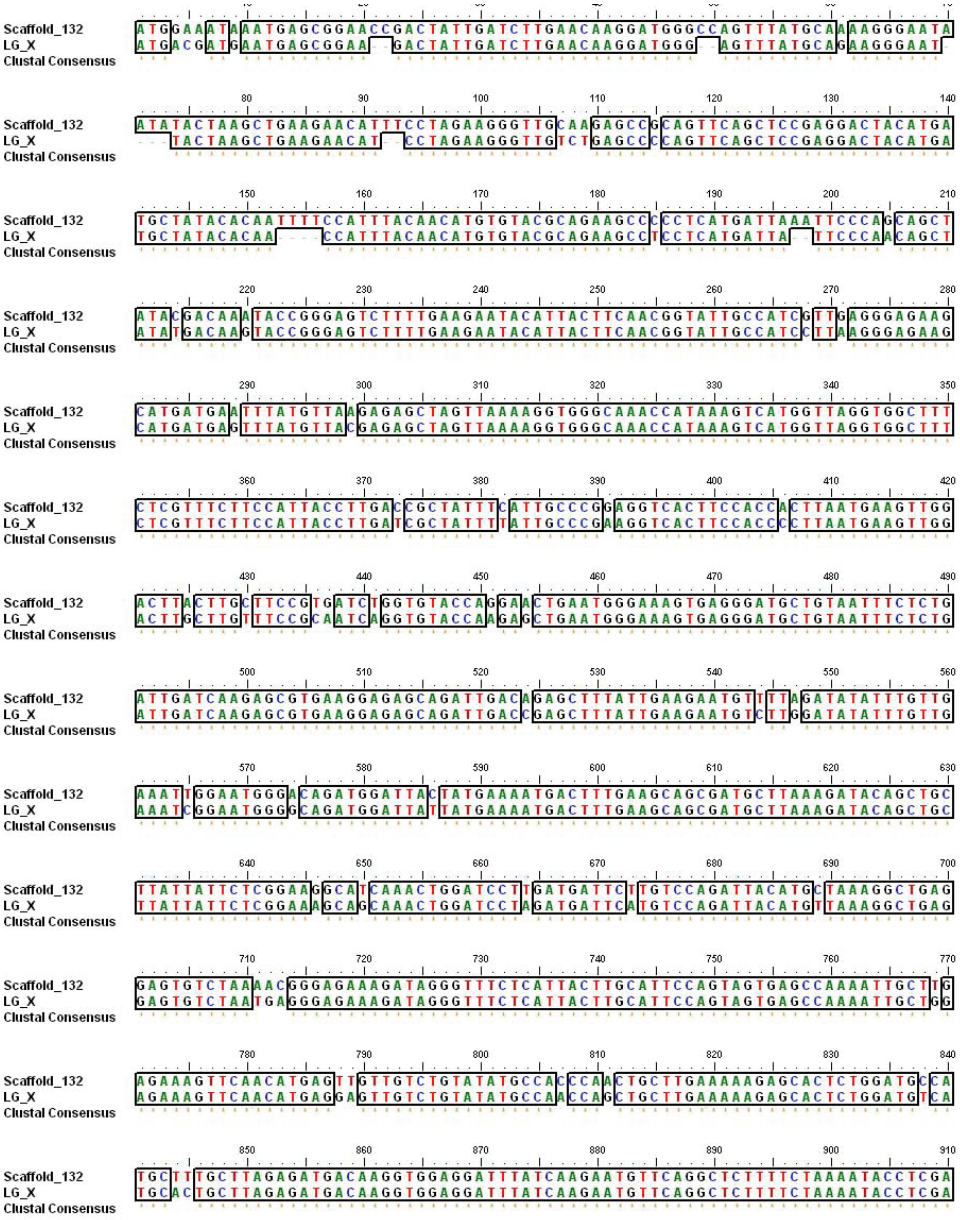

Figure 13. Pairwise alignment of consensus transcript sequences for the genes encoding for EST 181 at LG_X and Scaffold_132. Clustal consensus sequences are labeled "*" indicating identical or conserved residues in all sequences; ":"shows conserved substitutions and "." indicates semi-conserved substitutions

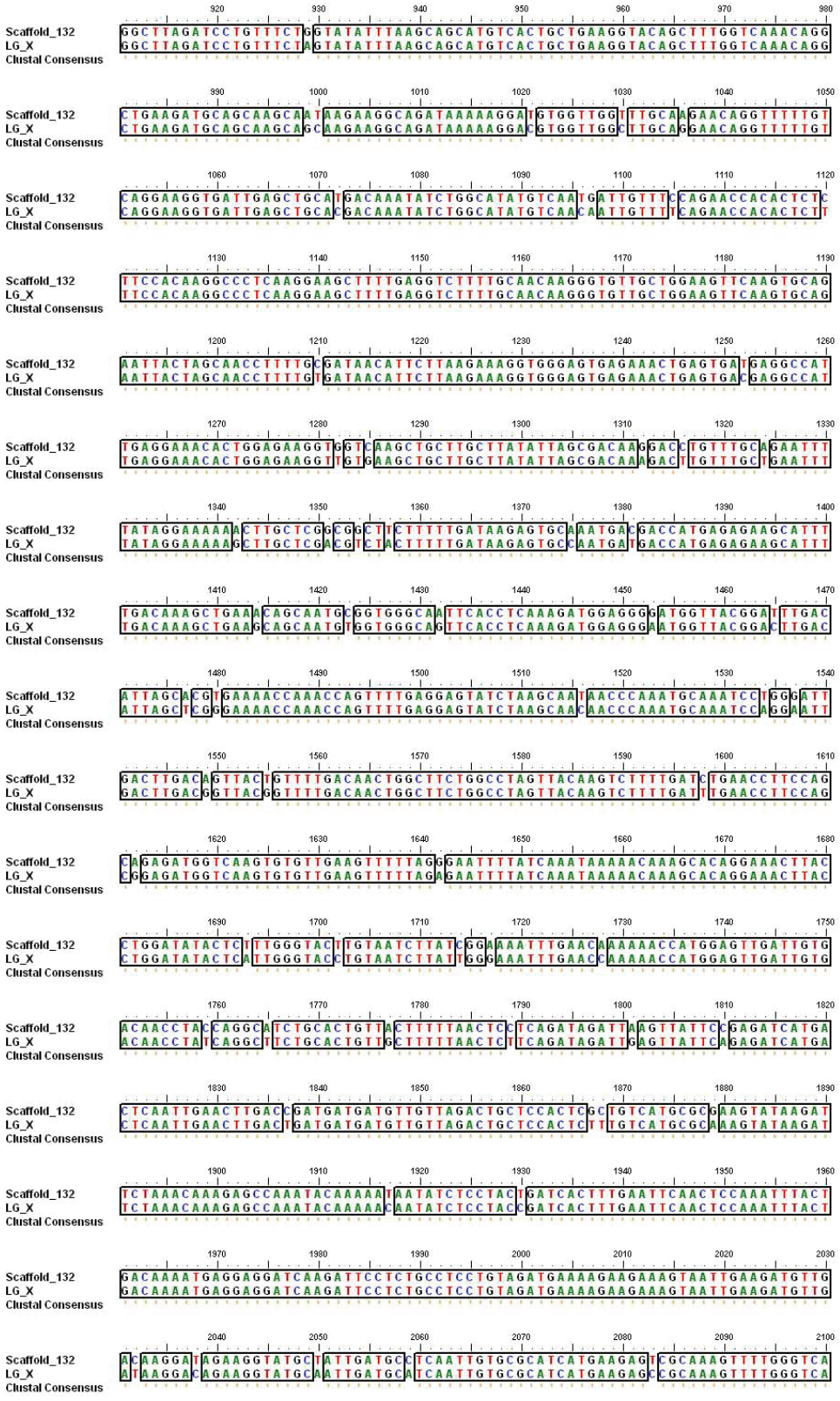

Figure 13 continued.

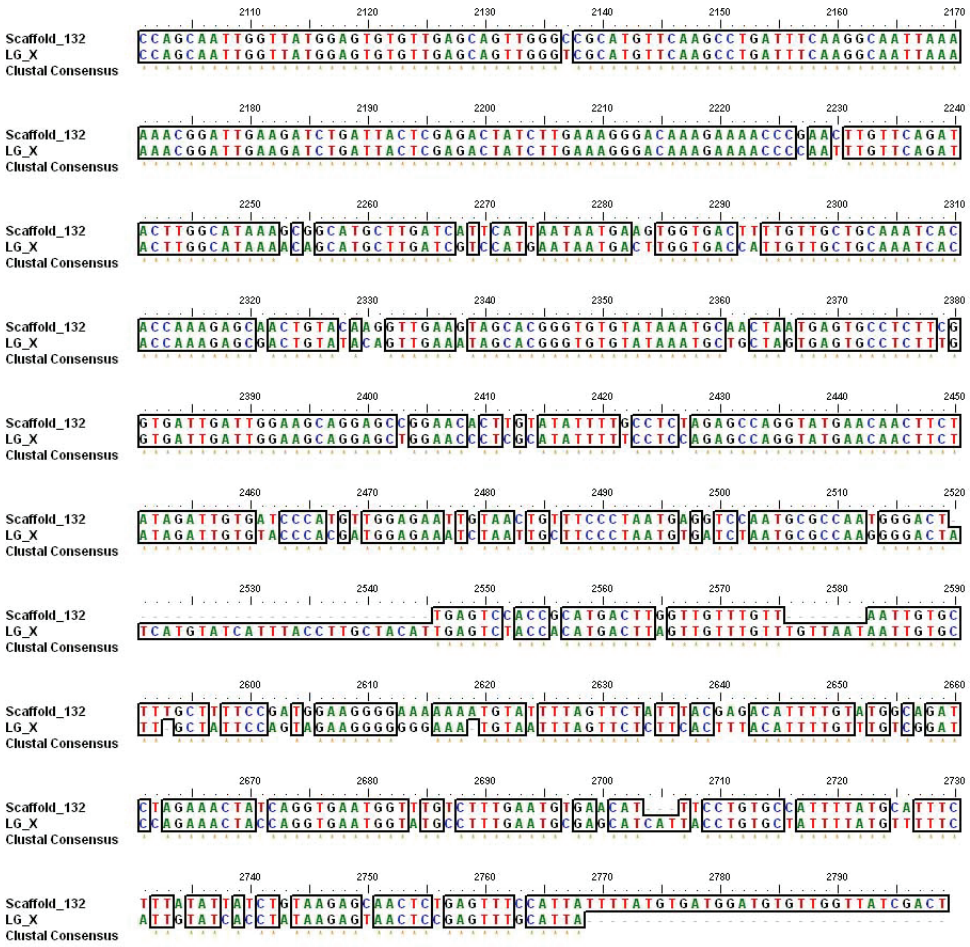

Figure 13 continued.

2.2. EST 181 encodes for a Cullin1-like protein in poplar

Gene annotation of EST 181 was based on protein homology. The results of BLAST search on NCBI protein (**Table 3**) and cDNA (**Table 4**) non-redundant databases indicate that EST 181 is a member of Cullin gene family. Cullin is a multi gene family involved in formation of SCF-type ubiquitin ligases. The results of BLAST search using the protein database showed that poplar EST 181 has certain similarity to all six members of Cullin gene family. Since each family member is involved in a distinct physiological process, it was essential to identify to which Cullin gene poplar EST 181 is most similar. For this purpose, phylogenetic analysis was performed. **Figure 14** shows the edited Cullin protein sequence alignment.

Figure 15 and **Figure 16** show the results of phylogenetic analysis of Cullin sequences. For both Neighbor Joining (**Figure 15**) and Maximum Parsimony (**Figure 16**) trees, the poplar cullin sequence grouped with Cullin 1 sequences. The bootstrap support for the clade having poplar cullin sequences is 100%. Moreover, the organization of sequences in the clade makes biological sense, in that, the sequences from monocots and dicots clustered in distinct clades. This suggest that the poplar cullin sequence is most similar to Cullin1 protein, thus, EST 181 is likely to encode a Cullin 1 protein in poplar. Although most of the Cullin 1 sequences are clustered in the same clade, some Cullin1 sequences appeared in some clades with other Cullin sequences. However, this incidence does not falsify the finding that the poplar cullin gene is a Cullin 1 gene but it suggests that this phenomenon is due to historical nomenclature of some Cullin genes.

Table 3. The results of BLAST (blastp-nr) search on NBCI protein database using consensus protein sequence for EST 181 as query. E-value cut-off is e-15

NCBI Accession Number	Organism Name	Abbreviation used in Phylogenetic Trees	Description of Hit Protein	E-value
CAC87837	*Nicotiana tabacum*	N. ta C1C	cullin 1C	3e-165
CAC87836	*Nicotiana tabacum*	N. ta C1B	cullin 1B	9e-156
CAC87835	*Nicotiana tabacum*	N. ta C1A	Cullin 1A	4e-155
BAC10548	*Pisum sativum*	P. sa C1	cullin-like protein1	3e-165
AAK53839	*Oryza sativa*	O. sa C(2)	Putative cullin	e-155
BAD61452	*Oryza sativa*	O. sa C1	Cullin 1	e-155
AAU44033	*Oryza sativa*	O. sa C1(1)	putative cullin 1	e-152
XP_467770	*Oryza sativa*	O. sa C3	putative cullin 3	8e-63
XP_480292	*Oryza sativa*	O. sa C3B	putative cullin 3B	2e-81
CAB80750	*Arabidopsis thaliana*	A. th C1	putative cullin-like 1 protein	3e-154
CAC85265	*Arabidopsis thaliana*	A. th C4	cullin 4	1e-68
AAM14063	*Arabidopsis thaliana*	A. th C	putative cullin	1e-68
CAC87120	*Arabidopsis thaliana*	A. th C3A	cullin 3a	4e-61
CAC87839	*Arabidopsis thaliana*	A. th C3B	cullin 3B	4e-60
AAL27655	*Olea europaea*	O. eu C	putative cullin protein	1e-49
BAD93235	*Homo sapiens*	H. sa C4A	cullin-4A	9e-68
CAI41370	*Homo sapiens*	H. sa C4B	Cullin-4B	9e-68
NP_003581	*Homo sapiens*	H. sa C3	cullin 3	4e-55
AAC36682	*Homo sapiens*	H. sa C3 [1]	cullin 3	8e-55
NP_003582	*Homo sapiens*	H. sa C2	cullin 2	6e-46
XP_341543	*Rattus norvegicus*	R. no C2	Predicted: similar to Cul2 protein	7e-46
XP_228689	*Rattus norvegicus*	R. no C4B	similar to cullin 4B	1e-66
XP_342680	*Rattus norvegicus*	R. no C1	similar to SCF complex protein cul-1	2e-46

Table 3 continued,

NCBI Accession Number	Organism Name	Abbreviation used in Phylogenetic Trees	Description of Hit Protein	E-value
XP_217454	*Rattus norvegicus*	R. no mKIAA0617	PREDICTED: similar to mKIAA0617 protein	3e-55
NP_082564	*Mus muculus*	M. mu C4B	cullin 4B	3e-66
NP_666319	*Mus muculus*	M. mu C4A	cullin 4A	3e-66
NP_057925	*Mus muculus*	M. mu C3	Cullin 3	3e-55
NP_036172	*Mus muculus*	M. mu C1	Cullin 1	2e-46
NP_083678	*Mus muculus*	M. mu C2	Cullin 2	1e-35
NP_082083.1	*Mus muculus*	M. mu C5	Cullin 5	2e-27
AAQ98010	*Danio rerio*	D. re C3	Cullin 3	8e-56
NP_955953.2	*Danio rerio*	D. re C1	Cullin 1	2e-46
AAH54607.1	*Danio rerio*	D. re C4A	Similar to cullin 4A	7e-46
BAA32428.2	*Schizosaccharomyces pombe*	S. po C1	Pcu1 (Cullin1)	3e-07
CAA90847.1	*Schizosaccharomyces pombe*	S. po C3	Pcu3 (cullin3)	2e-54
CAB16383.1	*Schizosaccharomyces pombe*	S. po C4	Pcu4 (Cullin 4)	4e-47
AAC47123.1	*Caenorhabditis elegans*	C. el C4	CUL-4	6e-46
AAC47122.1	*Caenorhabditis elegans*	C. el C3	CUL-3	3e-43
Q17390	*Caenorhabditis elegans*	C. el C2	CUL2_CAEEL Cullin-2	1e-34
XP_625899.1	*Cryptosporidium parvum*	C. pa C	Cullin-like protein of probable plant origin	9e-39
AAH77239.1	*Xenopus laevis*	X. la C3	Cul3-protein	3e-56
XP_534586.2	*Canis familiaris*	C. fa C3	PREDICTED: similar to Cullin-3	7e-15

Table 3 continued,

NCBI Accession Number	Organism Name	Abbreviation used in Phylogenetic Trees	Description of Hit Protein	E-value
XP_394044.2	*Apis mellifera*	A. me C1	PREDICTED: similar to Cullin homolog 1	1e-46
XP_519463.1	*Pan troglodytes*	P. tr C1	PREDICTED: similar to Cullin homolog 1	2e-46
AAK14056.1	*Emericella nidulans*	E. ni C1	SCF complex protein cul-1 homolog	2e-44
CAA76074.1	*Lycopersicon esculentum*	L. es C	Putative cullin protein	8e-50
AAS21399.1	*Oikopleura dioica*	O. di C	Cullin	6e-40
XP_678784.1	*Plasmodium berghei*	P. be C	Cullin-like protein	putative
NP_011517	*Saccharomyces cerevisiae*	S. ce C3	The cullin family with similarity to Cdc53p and human CUL3	3e-27
NP_502412.1	*Caenorhabditis elegans*	C. el C6	Cul-6	1e-34

Table 4. The results of BLAST (blastn-nr) search on NBCI nucleotide database using consensus transcript sequence for EST 181 as query. E-value cut-off is e-10. cds: coding sequence.

NCBI Accession Number	**Organism Name**	**Description of Hit Nucleotide**	**E-value**
AB080190.1	*Pisum sativum*	cul1 mRNA for cullin-like protein1, complete cds	0.0
AJ344533.1	*Nicotiana tabacum*	mRNA for cullin 1A (cul1A gene)	1e-72
AJ344534.1	*Nicotiana tabacum*	mRNA for cullin 1B (cul1B gene)	1e-54
AJ344535.1	*Nicotiana tabacum*	partial mRNA for cullin 1C (cul1C gene)	0.0
AJ344536.1	*Nicotiana tabacum*	partial mRNA for cullin 1D (cul1D gene)	1e-26
AY336990.1	*Oryza sativa*	CUL1 mRNA, complete cds	5e-57
AJ318017.1	*Arabidopsis thaliana*	mRNA for cullin 1 (cul1 gene)	4e-39
NM_116491.2	*Arabidopsis thaliana*	cullin family protein (At4g02570) mRNA, complete cds	4e-39

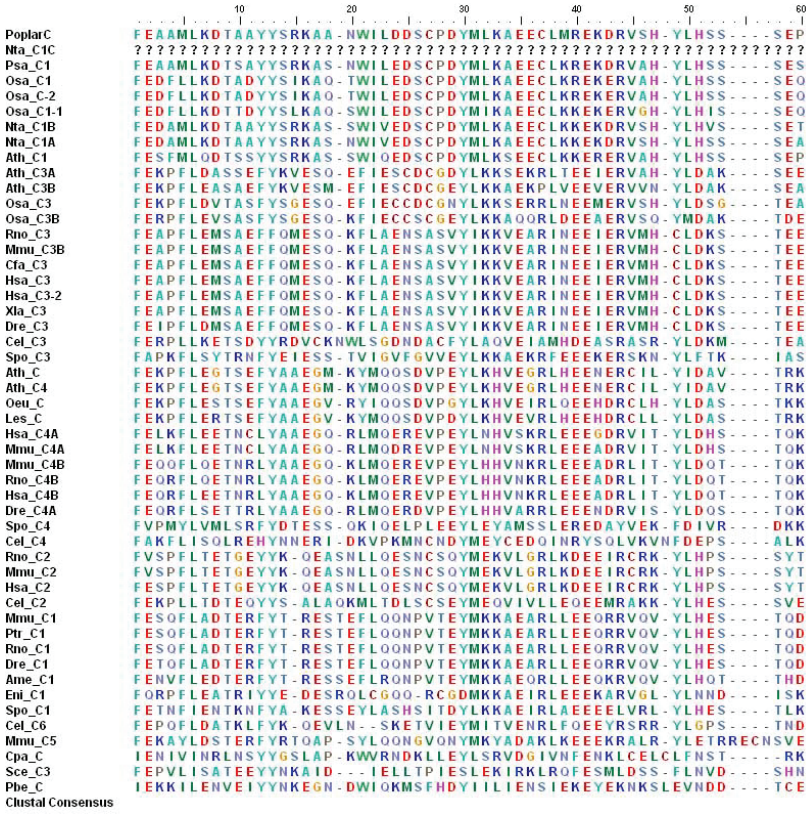

Figure 14. The homologous Cullin protein sequences were aligned using ClustalW. The alignment was edited using BioEdit to manage the gaps at the ends. The first column shows the abbreviation for species (first letter of genus name and the next two letters of species name) and cullin gene designation (C1-C6). The alleles are shown in letters (A, B, C) or in numbers (1, 2, 3).

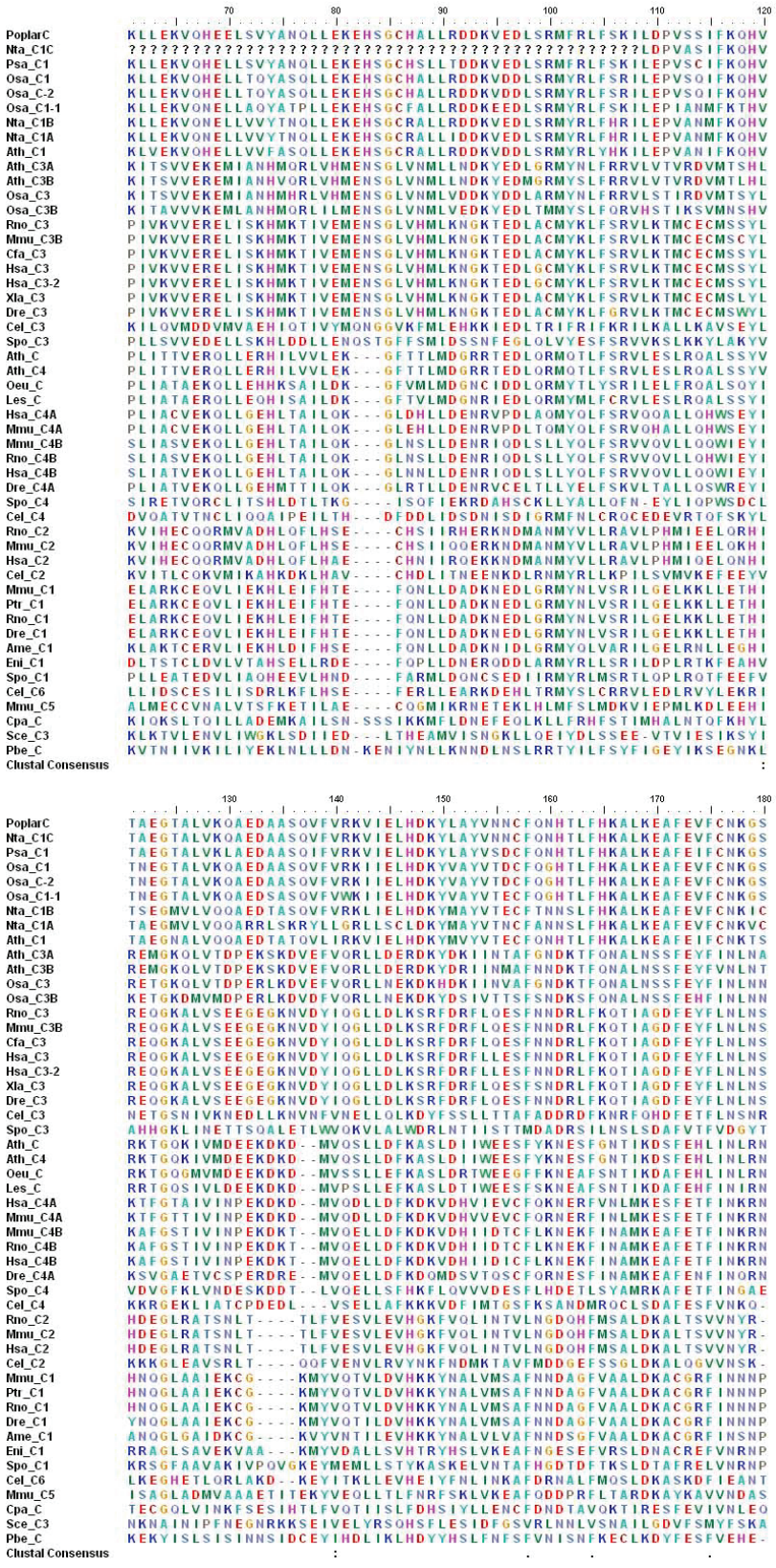

Figure 14 continued.

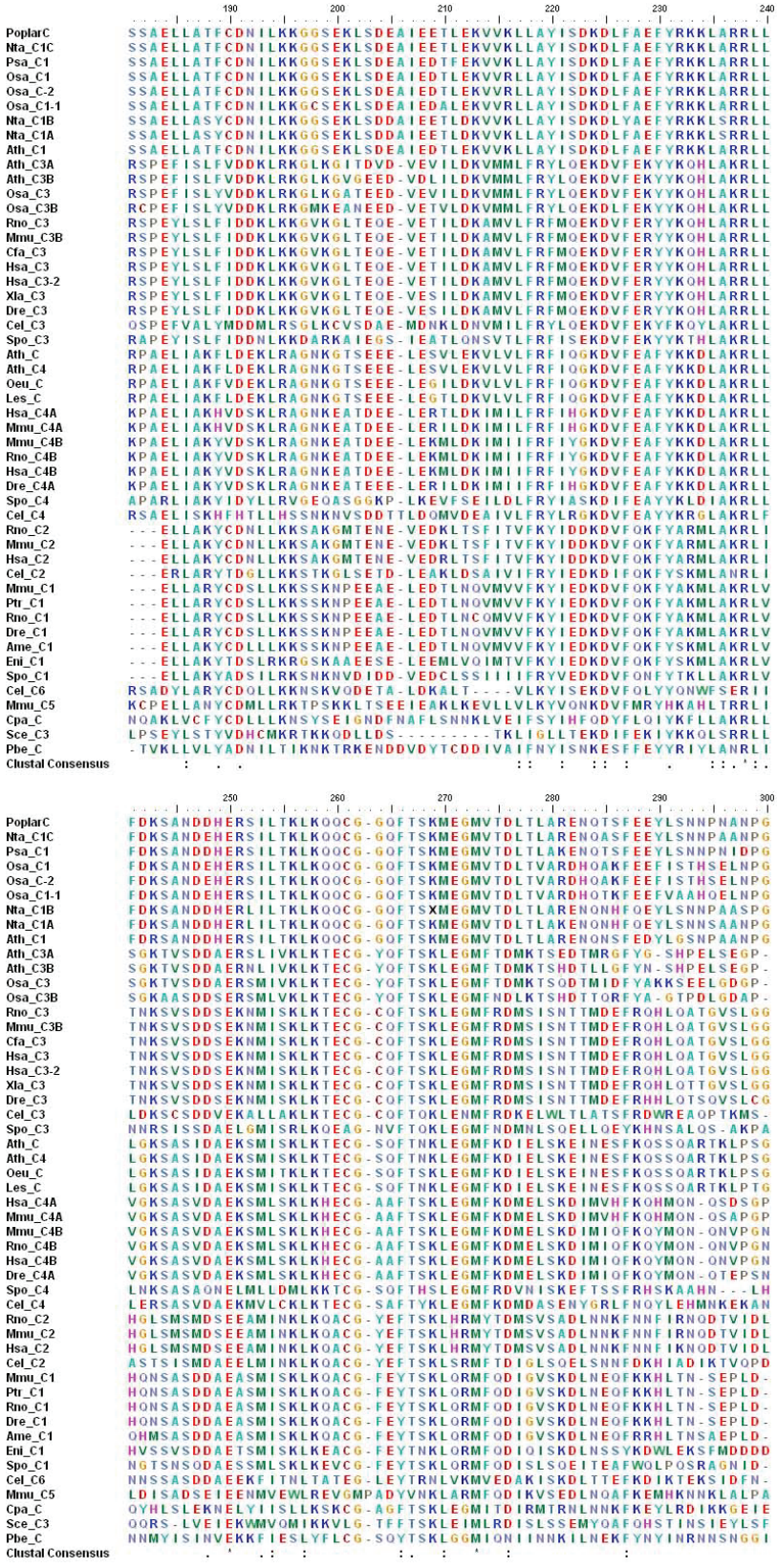

Figure 14 continued.

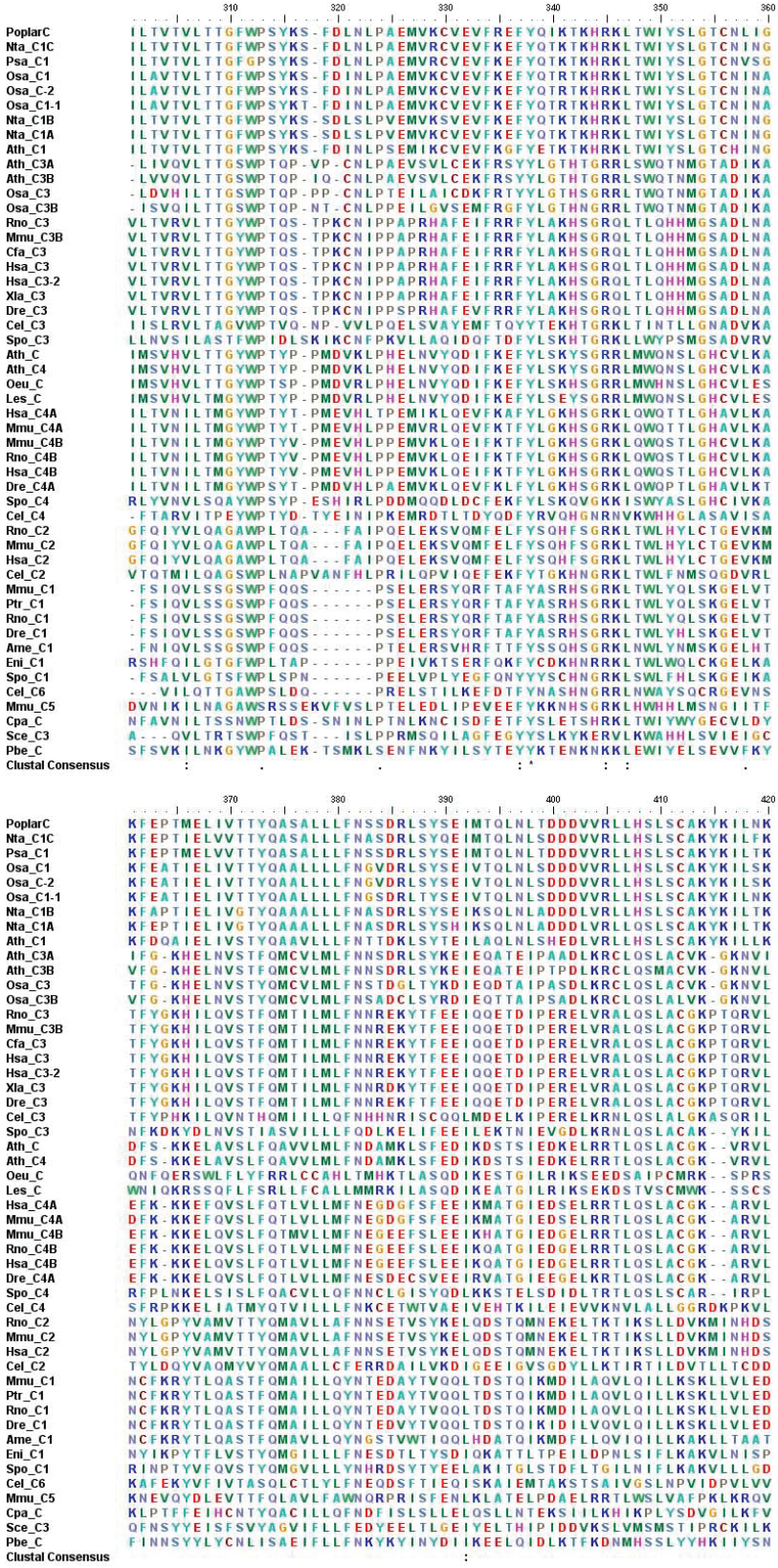

Figure 14 continued.

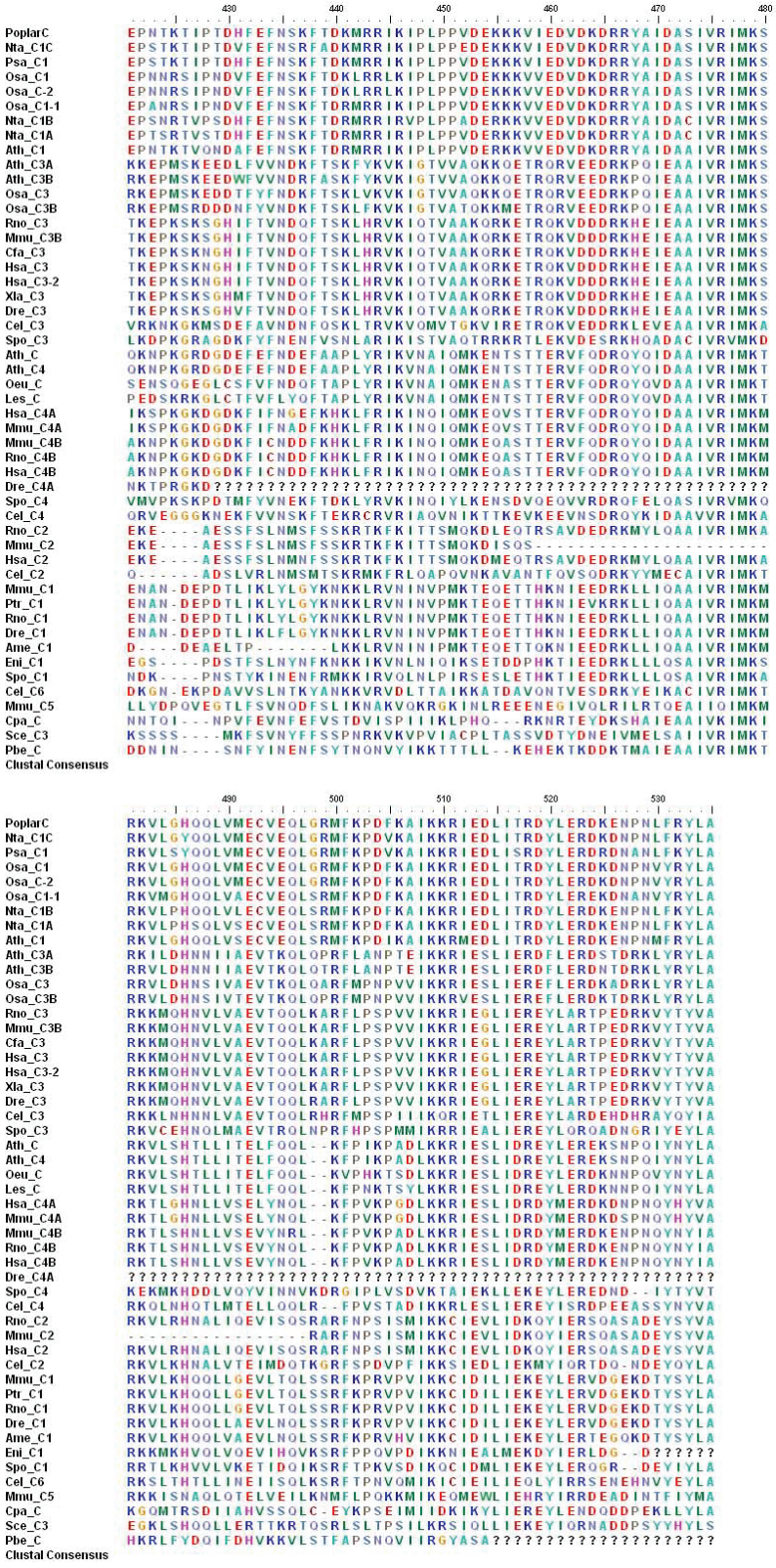

Figure 14 continued.

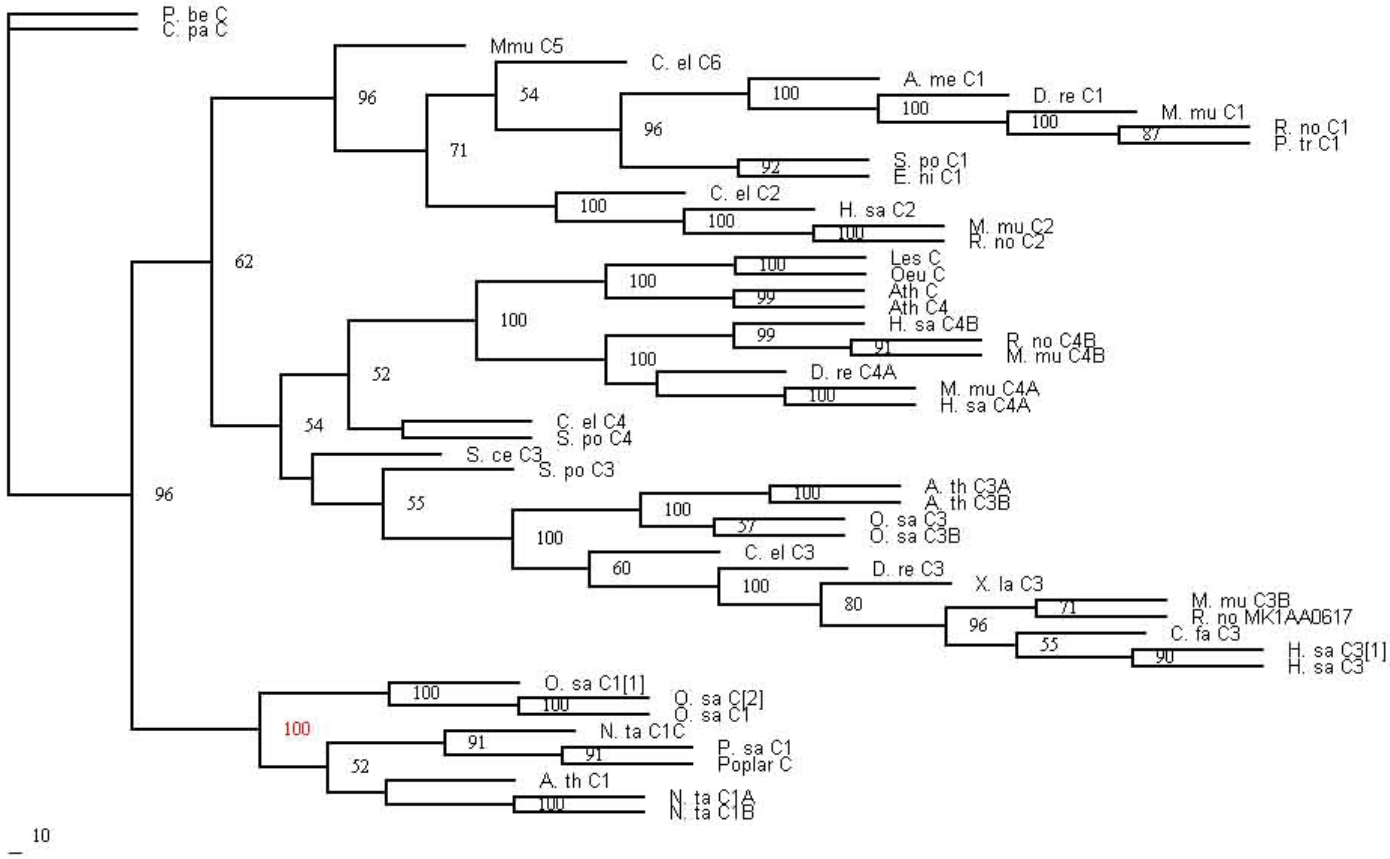

Figure 15. Molecular phylogeny of Cullin protein sequences, obtained by distance and neighbor-joining methods. Significant bootstrap support (>50%) is shown next to the respective nodes. Bootstrap value for the clade containing poplar sequence is in red color. Bar scale shows the number of amino acid substitutions.

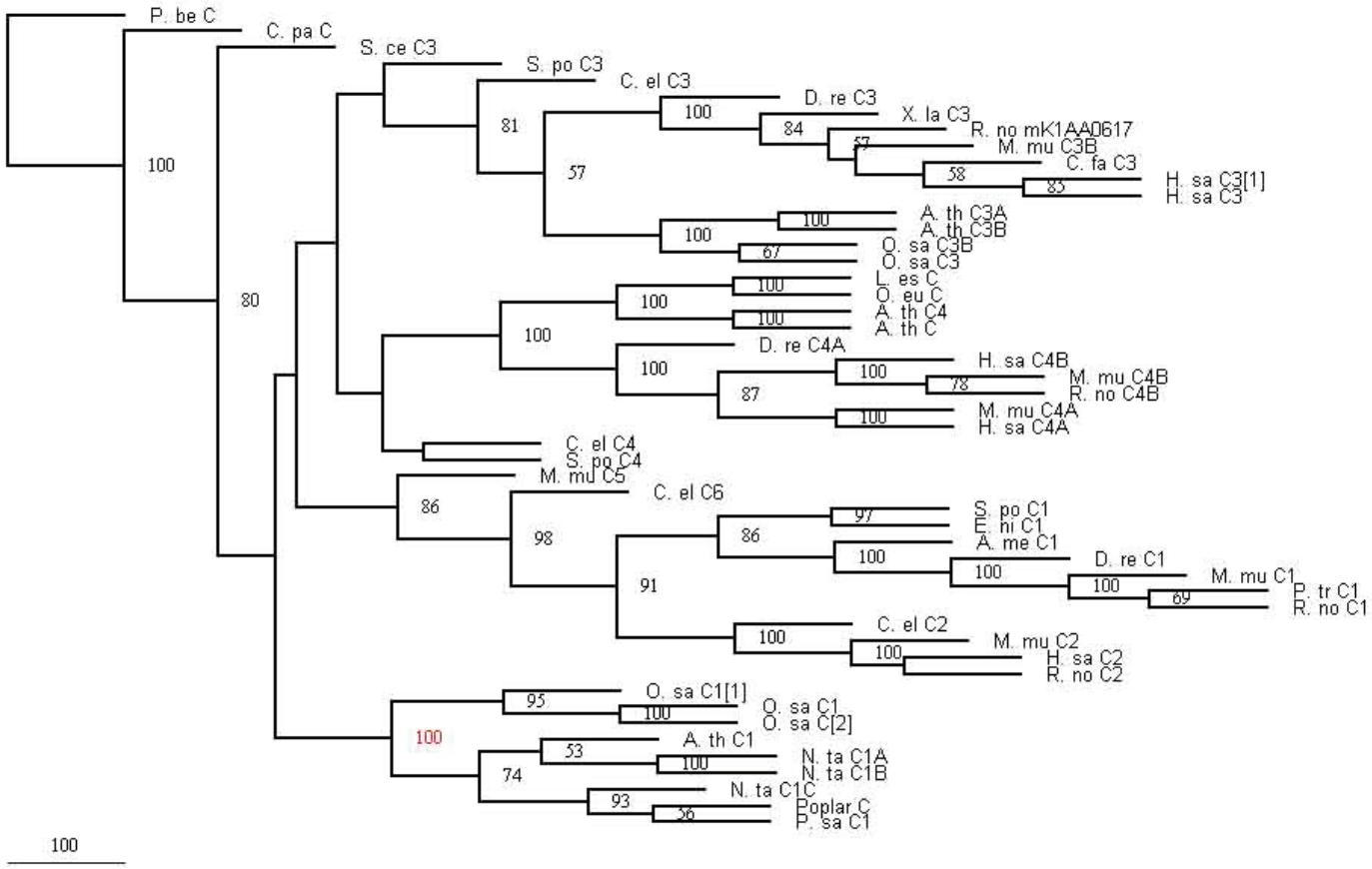

Figure 16. Molecular phylogeny of Cullin protein sequences, obtained by maximum parsimony method. Significant bootstrap support (>50%) is shown next to the respective nodes. Bootstrap value for the clade containing poplar sequence is in red color. Bar scale shows the number of amino acid substitutions.

3. Expression Analysis of poplar RUB1 conjugase and Cullin 1 genes

3.1. Expression analysis of RUB1 conjugase gene during vegetative bud development

In a previous cDNA-AFLP study (Coleman *et. al.,* unpublished results) RUB1 conjugase expression was observed in apical buds of wild type poplar during bud development and dormancy but was not detected in poplars expressing *Arabidopsis etr1-1* mutant allele. To further characterize RUB1 conjugase expression RT-PCR analysis using apical buds, axillary buds, bark, and leaves from both wild type poplars and the poplars expressing *Arabidopsis etr1-1* mutant allele, during bud development and dormancy were performed. As previously observed, RUB1 conjugase was expressed in apical buds during bud development and dormancy (**Figure 17**) but not detected in apical buds of *etr1-1* expressing poplars. In addition, reduced transcript abundance was also observed in axillary buds, leaves and bark of *etr1-1* expressing poplars compared to wild type plants (**Figure 17**). From this, it can be deduced that the reduction in RUB1 conjugase gene expression may also affect functions of RUB1 cycle, resulting in possible impairments in regulation of Cullin1 subunit of Ubiquitin/26S proteasome pathway.

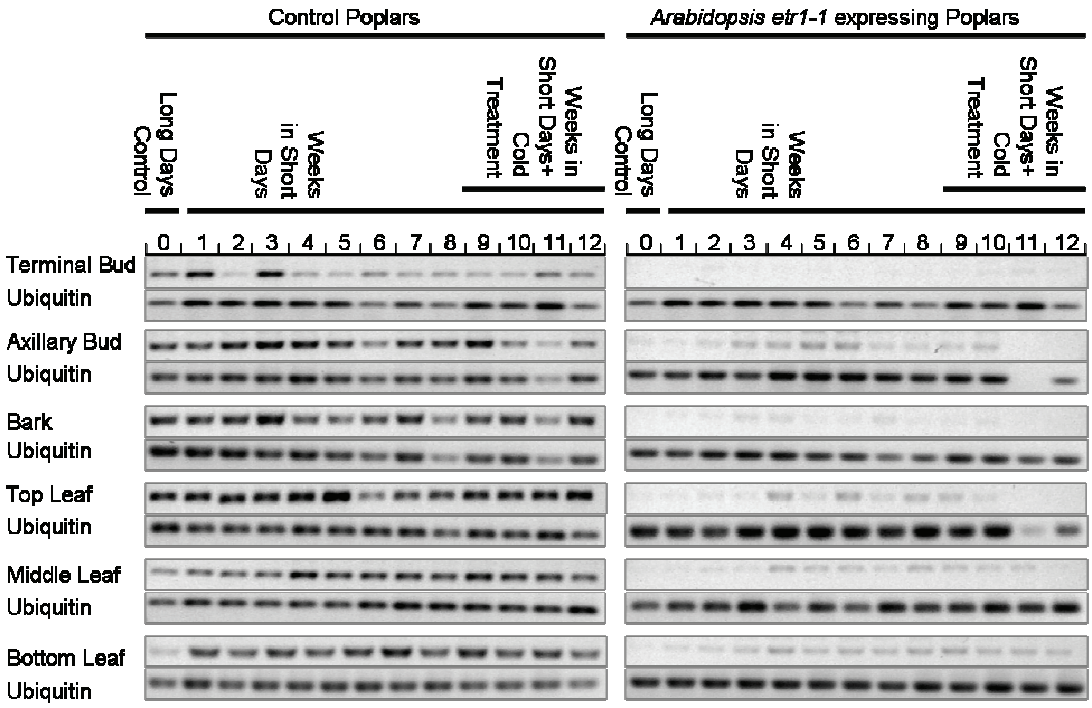

Figure 17. Expression of RUB1 conjugase in poplar tissues. Transcript abundance was determined using semi-quantitative RT-PCR. For dormancy induction, both control poplars and *Arabidopsis etr1-1* expressing poplars were put under short day conditions for 12 weeks whose last four weeks were in cold. Tissue samples were collected on weekly basis for RNA isolation. Ubiquitin was an internal control.

3.2. Expression analysis of Cullin1 gene during vegetative bud development

In order to determine whether the reduction of RUB1 conjugase gene expression affected expression of the Cullin1 gene, the abundance of Cullin1 transcripts in different tissues of wild type and *etr1-1* expressing poplars was compared by RT-PCR. Although the Cullin1 expression did not display significant difference among most of the tissues, its expression increased notably in middle and bottom leaves during short day treatments in wild type poplars (**Figure 18**). This suggests that Cullin1 expression can be senescence associated in older leaves. Interestingly, the expression of Cullin1 did not vary between wild type and *etr1-1* expressing poplars (**Figure 18**). This suggests that introduction of the *Arabidopsis etr1-1* mutant allele to poplar genome had no effect on Cullin1 gene function. Since RUB1 and Ubiquitin cycles function at the protein level, it is also hard to infer, at the gene level, whether RUB1-mediated Cullin1 regulation had been impaired in *etr1-1* expressing poplars.

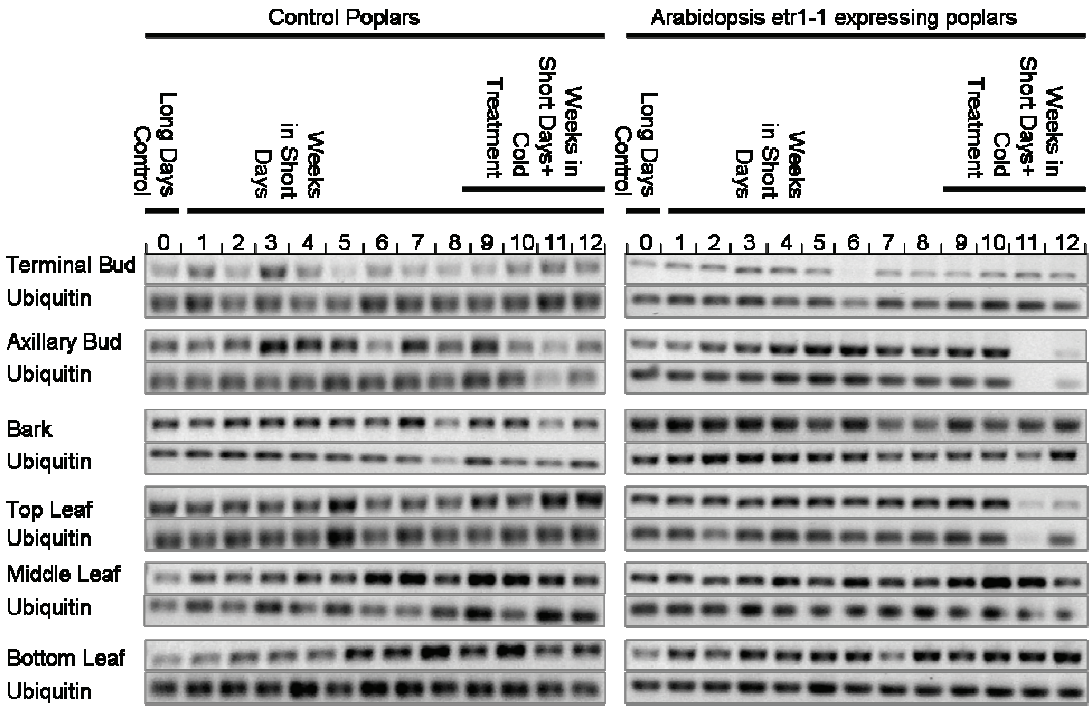

Figure 18. Expression of Cullin1 gene in poplar tissues. Transcript abundance was determined using semi-quantitative RT-PCR. For dormancy induction, both control poplars and *Arabidopsis etr1-1* expressing poplars were put under short day conditions for 12 weeks whose last four weeks were in cold. Tissue samples were collected on weekly basis for RNA isolation. Ubiquitin was an internal control.

4. Analysis of RUB1 and Ubiquitin Conjugated Proteins

The presence of RUB1 and Ubiquitin conjugated proteins during dormancy in both wild-type and the *Arabidopsis etr1-1* expressing poplars was compared by protein gel blot analysis. In both control poplars and *Arabidopsis etr1-1* expressing poplars, numerous proteins are conjugated to Ubiquitin at all stages of dormancy. The abundance of ubiquitination indicates extensive involvement of Ubiquitin/26S proteasome pathway in bud development and dormancy. It also suggests that ubiquitin conjugations play a role in poplar bud development and dormancy. Although, both control poplars and those expressing *etr1-1* mutant allele had shown similar conjugation patterns, there was a slight difference in conjugation of two small proteins (~28kD and ~30kD) (**Figure 19**). These protein conjugations appeared in last three weeks of the dormancy period in control poplars. The appearance of these proteins with cold treatment suggests that cold has initiated ubiquitination of new proteins. While the 30kD protein was still present in poplars expressing *Arabidopsis etr1-1* mutant allele, the 28kD was no longer present. This protein is either not produced in *etr1-1* expressing poplars or not targeted for ubiquitination, which may suggest that loss of ethylene receptor function in poplars has initiated a different ubiquitination profile during cold treatments of dormancy period.

In contrast to Ubiquitin conjugated proteins, the RUB1 conjugated proteins were less abundant. This was expected because RUB1 is associated with a limited set of proteins, most of which are in RUB1 cycle. The pattern of RUB1 conjugated proteins changed little throughout the dormancy period, but the abundance of conjugated proteins increased (**Figure 20**). There was a difference in conjugation of

two proteins (~84kD and ~140kD) (**Figure 20**). The 84kD protein is present only in control poplars. The abundance of 84kD protein increases with cold treatment. The 140kD protein is present only in control poplars during cold treatment. The absence of these two protein conjugations from *etr1-1* expressing poplars suggests that these proteins either are not produced or fail to conjugate with RUB1. In latter case, the absence of these conjugations from *etr1-1* expressing poplars may prevent proper functioning of the RUB1 cycle, leading to impairments in regulation of Ubiquitin cycle.

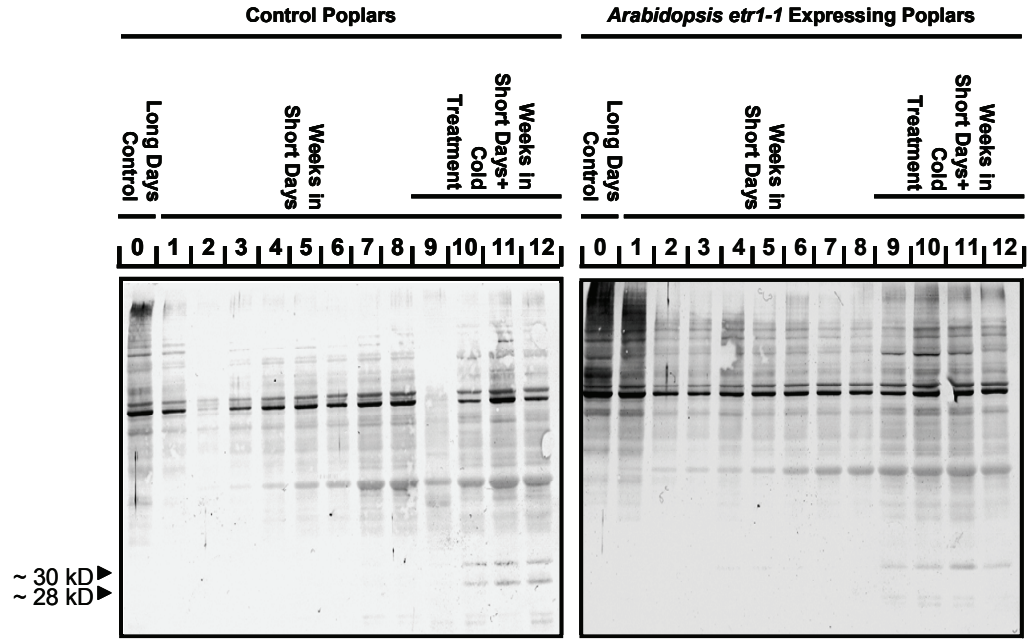

Figure 19. Western blots. Ubiquitin conjugated proteins during vegetative bud development and dormancy. For dormancy induction, both control poplars and *Arabidopsis etr1-1* expressing poplars were put under short day conditions for 12 weeks whose last four weeks were in cold. Protein was isolated from terminal buds in weekly basis for 13 weeks.

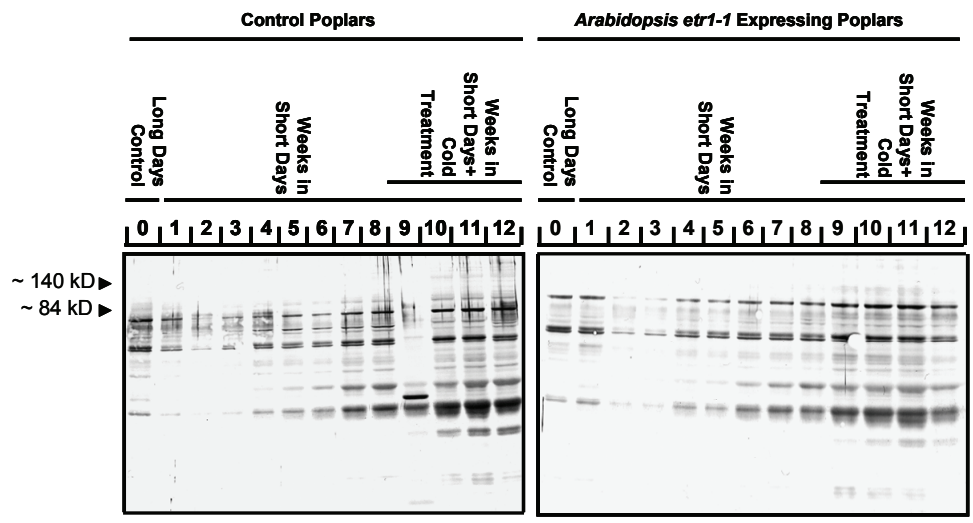

Figure 20. Western blots. RUB1 conjugated proteins during vegetative bud development and dormancy. For dormancy induction, both control poplars and *Arabidopsis etr1-1* expressing poplars were put under short day conditions for 12 weeks whose last four weeks were in cold. Protein was isolated from terminal buds in weekly basis for 13 weeks.

5. Expression of EBF-like gene during vegetative bud development

Because of the differences in RUB1 conjugase between wild type and *etr1-1* expressing poplars and the changes in ubiquitination and RUB1 conjugation of proteins during dormancy, it was determined whether other components of Ubiquitin/26S proteasome pathway are expressed differentially. Among several components of the pathway, EBF, an F-box protein, was selected because EBF F-box protein has been shown to involve in ethylene signaling pathway through degradation of the EIN3 transcription factor by Ubiquitin/26S proteasome pathway (Gagne *et al*., 2004; Guo and Ecker 2003; Potuschak *et al*., 2003). Because poplars expressing a mutant allele of ethylene receptor (i.e. *etr1-1*) have altered dormancy and the ethylene signaling involves targeted protein degradation by Ubiquitin/26S proteasome pathway, the study of EBF gene expression could provide a link between dormancy and involvement of ethylene signaling.

The *Arabidopsis* EBF gene was used to retrieve homologous EBF gene sequences from the poplar genome. The poplar genome has two EBF genes located on LG XVIII and LG VI. Since these two genes have high sequence similarity, a common set of primers were designed to study expression of poplar EBF1/2-like gene during vegetative bud development and dormancy.

No difference in expression was detected in wild type and *etr1-1* expressing poplar during bud development and dormancy. Poplar EBF-like gene has shown an abundant expression in wild type and *etr1-1* expressing poplar terminal bud tissues at all steps of dormancy. This indicates that the vegetative bud development and dormancy does not affect the EBF-like gene expression (**Figure 21**). Moreover, there

is little difference between the control poplars and the poplars expressing *Arabidopsis etr1-1* mutant allele in EBF gene expression. It can be deduced that introduction of a mutant ethylene hormone receptor to poplars, although it created alterations in dormancy, had little effect on expression of EBF-like F-box protein.

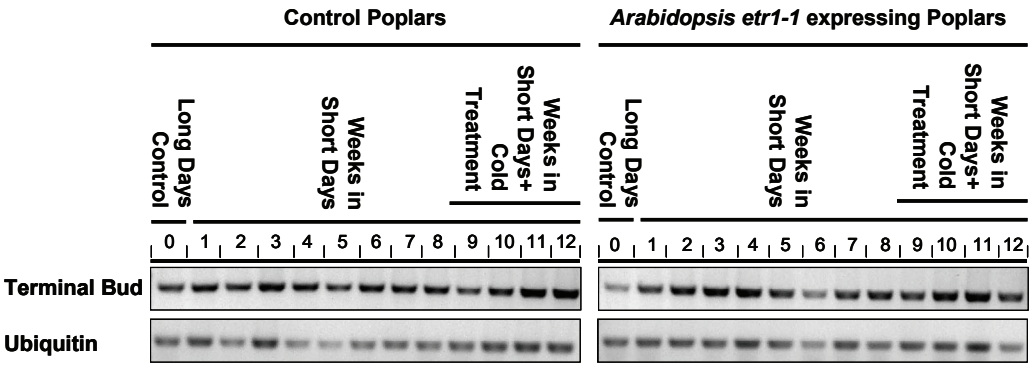

Figure 21. Expression analysis of poplar EBF-like gene in terminal bud tissues using semi-quantitative RT-PCR technique. For dormancy induction, both control poplars and *Arabidopsis etr1-1* expressing poplars were put under short day conditions for 12 weeks whose last four weeks were in cold. Terminal buds were collected on weekly basis for RNA isolation. Ubiquitin was an internal control

6. The Effects of ACC and AVG Treatments on Expression of RUB1 Conjugase Gene

The effect of the ethylene precursor ACC and the ethylene inhibitor AVG on RUB1 conjugase gene expression was studied to investigate the factors affecting RUB1 conjugase gene expression in poplars. Cut stems of both control poplars and poplars expressing *Arabidopsis etr1-1* were treated with four levels (0μM, 25μM, 50μM, 100μM) of ACC and AVG. The results of RT-PCR using RUB1 conjugase gene specific primers are shown in **Figure 22**. In control poplars, neither ACC nor AVG treatments had any effect on expression of RUB1 conjugase gene. In poplars expressing *Arabidopsis etr1-1* mutant allele, AVG treatments displayed no effect on RUB1 conjugase expression. ACC treatments, on the other hand, have influenced RUB1 conjugase gene expression. A reduction in RUB1 conjugase expression was observed when *etr1-1* expressing poplars were treated with 50μM ACC (**Figure 22**).

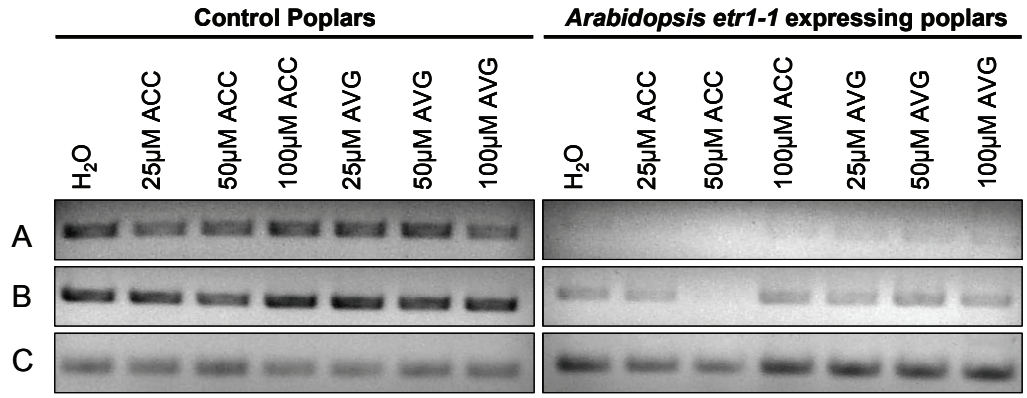

Figure 22. Effect of ACC and AVG treatments on RUB1 conjugase gene expression in control and *Arabidopsis etr1-1* expressing poplars by semi quantitative RT-PCR. H_2O was used as control. **A:** 28 PCR cycles. **B:** 35 PCR cycles, and **C:** Ubiquitin as internal control (25 PCR cycles). Plants were kept under long day conditions throughout the experiment.

7. Full Length cDNA Poplar RUB1 Conjugase-like Gene

Full length cDNA for poplar RUB1 conjugase-like gene was obtained using gene specific 3'-end and 5'-end primers. The poplar RUB1 conjugase cDNA has a nucleotide length of 552bp, which translates to a predicted protein of 184 amino acids. Poplar RUB1 conjugase cDNA sequence is 75% and 78% similar mRNA sequences of *Arabidopsis thaliana* (NCBI Accession number: AC006135) and of Olive tree (NCBI Accession number: AY157723.1), respectively (**Figure 23**).

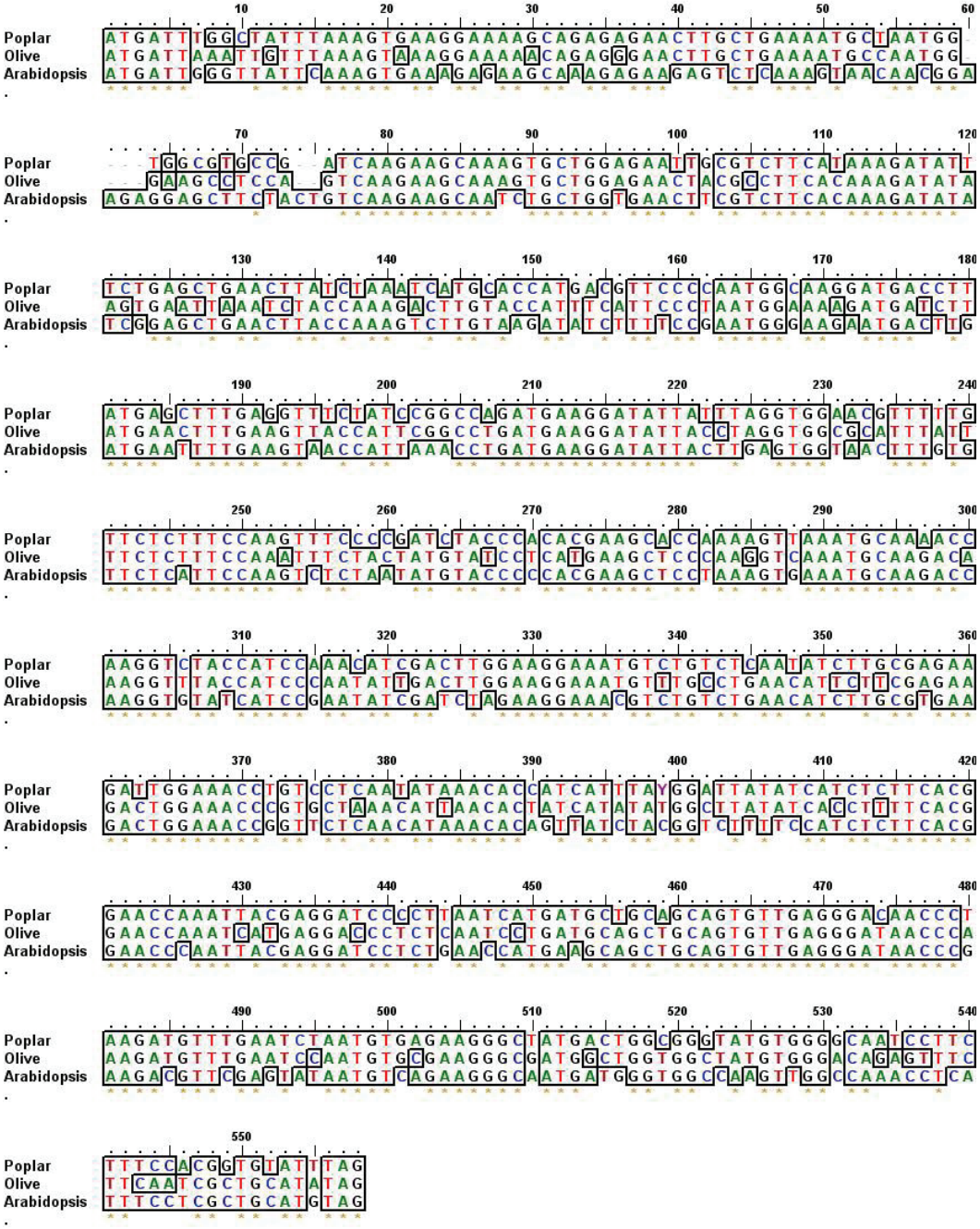

Figure 23. Multiple sequence alignment of Poplar RUB1 conjugase full length cDNA, Olive tree (*Olea europaea*) RUB1 conjugase mRNA and *Arabidopsis thaliana* RUB1 conjugase mRNA. The sign "." stands for Clustal Consensus sequence. The sign "*" indicates identical or conserved residues in all sequences.

DISCUSSION

In this thesis, the role of RUB1 and Ubiquitin cycles was studied in woody plant bud development and dormancy. Previous cDNA-AFLP studies comparing control poplars and poplar expressing *Arabidopsis etr1-1* mutant allele identified several genes involved in these two cycles (Coleman *et al.,* unpublished results). The number of differentially expressed genes and their expression patterns suggests that RUB1 and Ubiquitin cycles may be involved in woody plant bud development and dormancy. From these genes, two candidate genes, RUB1 conjugase and Cullin1, were studied further. RUB1 conjugase is a member of RUB1 cycles and is involved in the regulation of Cullin-dependent ubiquitin ligases (del Pozo and Estelle, 1999; Hori *et al*., 1999). This regulatory relationship, together with their expression pattern observed in the cDNA-AFLP study, made these two genes interesting to study in more detail.

To determine the tissue specificity of these genes, an analysis of expression in different tissues during vegetative bud development and dormancy was conducted. The results show that RUB1 conjugase and Cullin1 gene were not only expressed in apical buds but also expressed in axillary buds, leaves and bark. Moreover, RUB1 conjugase was expressed at high levels in control poplars compared to poplars expressing *Arabidopsis etr1-1* mutant allele. This suggests that the reduction in RUB1 conjugase gene expression may also affect the function of RUB1 cycle, resulting in possible impairments in the regulation of Cullin subunit of SCF-dependent ubiquitin ligases in poplars.

In order to investigate the factors affecting RUB1 conjugase gene expression and to establish a connection between ethylene signaling, ubiquitination, and dormancy, the effects of the ethylene precursor ACC and ethylene inhibitor AVG was determined. Since *etr1-1* expressing poplars have a dominant ethylene receptor mutation, the effects of ACC and AVG on RUB1 gene expression would provide such a connection. While RUB1 conjugase gene expression was not affected by AVG treatments, its expression was ceased by 50μM ACC treatment in *etr1-1* expressing poplars. The decline of RUB1 conjugase expression in these plants indicates that there may be interactions or feedbacks between RUB1 cycle and ethylene signaling pathway in poplars.

Since RUB1 and Ubiquitin cycles function at the protein level, it is hard to infer, at the gene level, whether RUB1-mediated Cullin regulation had been impaired in *etr1-1* expressing poplars. In order to investigate this possibility, the presence of RUB1 and Ubiquitin conjugated proteins were determined. In both cases, a number of conjugated proteins were determined. However, the pattern of conjugated proteins changed throughout dormancy in both the number and the abundance. The conjugation of four proteins changed notably during short day and cold treatments. The 28kD and 30kD proteins were conjugated to Ubiquitin only during short days and cold treatments in control poplars. Conjugation of the 28kD protein was absent in *etr1-1* expressing poplars. The 84kD and 140kD proteins were conjugated to RUB1 only in control poplars and the abundance of the 84kD protein increased with cold treatment. The 84kD protein has the same molecular weight as the Cullin family member Cul5 (Kipreos *et al*., 1997; Byrd *et al*., 1997). The absence of the 84kD

protein from *etr1-1* expressing poplars indicates that the conjugation of RUB1 and Cul5 protein is impaired. Since RUB1 is a regulator of Cullins (Hochstrasser, 1998), an absence of RUB1 and Cul5 conjugation suggests that regulation of Cullin5-dependent SCF ubiquitin ligases are impaired in transgenic poplars, which express *etr1-1* mutant allele and display altered dormancy. From these, it can be deduced that ethylene signaling pathway whose components, such as EIN3, are targeted for degradation by ubiquitination (Gagne *et al*., 2004; Guo and Ecker 2003; Potuschak *et al*., 2003) has a role in bud development and dormancy in poplars.

In order to investigate the role of components of ethylene signaling pathway in poplar dormancy, the expression of EBF, which targets EIN3 for proteolysis, has been studied. The expression of EBF gene failed to show a significant difference during dormancy between wild type and *etr1-1* expressing poplars. From this, it can also be deduced that introduction of a mutant ethylene hormone receptor to poplars, although it created alterations in dormancy, had little effect on expression of EBF-like F-box protein.

The involvement of ethylene in dormancy has been shown in potato and birch. The role of ethylene in dormancy has been established in potato where endogenous ethylene was shown to be essential for full expression of microtuber endodormancy (Suttle *et al*., 1998). The transgenic ethylene-insensitive birches (*Betula pendula*), which express the dominant *etr1-1* mutation, ceased elongation compared to wild type under short days. The formation of terminal buds was abolished and endodormancy was delayed in birches expressing *etr1-1* mutant allele (Ruonala *et al*., 2006). This study has shown involvement of ethylene in terminal bud formation. In

addition to these studies, the results of this thesis provide insights in understanding the involvement of ethylene signaling in poplar bud development and dormancy. The results of this research not only show a link between ethylene and dormancy, but also suggest the involvement of Ubiquitin/26S proteasome pathway in these processes.

Establishing a link between ethylene signaling, dormancy, and ubiquitination pathway will provide new directions to dormancy studies in poplar. The future studies should focus on characterization of the novel proteins identified in this study. The results of this research indicate that RUB1 conjugase has a role in poplar dormancy. This can further be investigated by creating RUB1 conjugase knock-outs using RNAi technology in wild-type poplars. The role of RUB1 cycle in poplar bud development and dormancy can also be established by overexpressing RUB1 conjugase in wild type and *etr1-1* expressing poplars. Future studies on other components of Ubiquitin/26S proteasome pathway will also help establish a relationship between targeted protein degradation, ethylene signaling, and dormancy in poplars.

APPENDIX

Table A1 shows the gene models associated with EST 99 and their locations in poplar genome. LG: Linkage Group, Sc: Scaffold

LG/ Scaffold	Gene Prediction Model Name	Gene Model ID	Location on Genome
LG_VII	extGenewise	estExt_Genewise1_v1.C_LG_VII3332	Poptr1/LG_VII:10348588-10351194
LG_VII	Fgenesh	fgenesh1_pg.C_LG_VII001011	Poptr1/LG_VII:10349307-10351444
LG_VII	Fgenesh	estExt_fgenesh1_pg_v1.C_LG_VII1000	Poptr1/LG_VII:10349307-10351045
LG_VII	extGenewise	estExt_Genewise1_v1.C_LG_VII3335	Poptr1/LG_VII:10348588-10351045
LG_VII	extGenewise	estExt_Genewise1_v1.C_LG_VII3332	Poptr1/LG_VII:10348588-10351194
LG_VII	extGenewise	estExt_Genewise1_v1.C_LG_VII3333	Poptr1/LG_VII:10348588-10351194
LG_VII	extGenewise	estExt_Genewise1_v1.C_LG_VII3334	Poptr1/LG_VII:10348588-10351194
LG_VII	extGenewise	estExt_Genewise1_v1.C_LG_VII3336	Poptr1/LG_VII:10348588-10351194
LG_VII	Genewise1	gw1.VII.3341.1	Poptr1/LG_VII:10349319-10350838
LG_VII	Genewise1	gw1.VII.3342.1	Poptr1/LG_VII:10349319-10350841
LG_VII	Genewise1	gw1.VII.3343.1	Poptr1/LG_VII:10349319-10350841
LG_VII	Genewise1	gw1.VII.3344.1	Poptr1/LG_VII:10349319-10350841
LG_VII	Genewise1	gw1.VII.3345.1	Poptr1/LG_VII:10349319-10350841
LG_VII	Grail	grail3.0019014801	Poptr1/LG_VII:10348582-10351098
LG_VII	Eugene	eugene3.00071036	Poptr1/LG_VII:10349307-10351095

Table A1 continued.

LG/ Scaffold	Gene Prediction Model Name	Gene Model ID	Location on Genome
Sc_57	Fgenesh	estExt_fgenesh1_pg_v1.C_570205	Poptr1/scaffold_57:1919431-1921739
Sc_57	Fgenesh	fgenesh1_pm.C_scaffold_57000103	Poptr1/scaffold_57:1919651-1921152
Sc_57	Fgenesh	estExt_fgenesh1_pm_v1.C_570101	Poptr1/scaffold_57:1919431-1921739
Sc_57	Fgenesh	fgenesh1_pg.C_scaffold_57000208	Poptr1/scaffold_57:1919651-1921152
Sc_57	Fgenesh	estExt_fgenesh1_pg_v1.C_570205	Poptr1/scaffold_57:1919431-1921739
Sc_57	Genewise	gw1.57.307.1	Poptr1/scaffold_57:1919654-1921152
Sc_57	Genewise	gw1.57.125.1	Poptr1/scaffold_57:1919654-1921152
Sc_57	Genewise	gw1.57.6.1	Poptr1/scaffold_57:1919654-1921152
Sc_57	Genewise	gw1.57.41.1	Poptr1/scaffold_57:1919657-1921152
Sc_57	extGenewise	estExt_Genewise1_v1.C_570047	Poptr1/scaffold_57:1919466-1921739
Sc_57	extGenewise	estExt_Genewise1_v1.C_570229	Poptr1/scaffold_57:1919466-1921739
Sc_57	extGenewise	estExt_Genewise1_v1.C_570313	Poptr1/scaffold_57:1919466-1921739
Sc_57	extGenewise	estExt_Genewise1_v1.C_570348	Poptr1/scaffold_57:1919466-1921739
Sc_57	Grail	grail3.0057018501	Poptr1/scaffold_57:1886016-1930720
Sc_57	Grail	grail3.0057018701	Poptr1/scaffold_57:1919553-1921825
Sc_57	Grail	grail3.0057018702	Poptr1/scaffold_57:1919553-1921825
Sc_57	Eugene	eugene3.00570216	Poptr1/scaffold_57:1919426-1921164
LG_IX	extGenewise	estExt_fgenesh1_pg_v1.C_LG_IX0520	Poptr1/LG_IX:3327839-3329798
LG_IX	Genewise	gw1.IX.1907.1	Poptr1/LG_IX:3328164-3329436

Table A1 continued.

LG/ Scaffold	Gene Prediction Model Name	Gene Model ID	Location on Genome
LG_IX	Genewise	gw1.IX.1908.1	Poptr1/LG_IX:3328164-3329436
LG_IX	Genewise	gw1.IX.1905.1	Poptr1/LG_IX:3328167-3329436
LG_IX	extGenewise	estExt_Genewise1_v1.C_LG_IX1898	Poptr1/LG_IX:3328041-3329798
LG_IX	extGenewise	estExt_Genewise1_v1.C_LG_IX1899	Poptr1/LG_IX:3328041-3329798
LG_IX	extGenewise	estExt_Genewise1_v1.C_LG_IX1900	Poptr1/LG_IX:3328041-3329798
LG_IX	extGenewise	estExt_Genewise1_v1.C_LG_IX1901	Poptr1/LG_IX:3328041-3329798
LG_IX	extGenewise	estExt_Genewise1_v1.C_LG_IX1902	Poptr1/LG_IX:3328041-3329798
LG_IX	Grail	grail3.0001048201	Poptr1/LG_IX:3327930-3329811
LG_IX	Fgenesh	fgenesh1_kg.C_LG_IX000028	Poptr1/LG_IX:3327921-3329794
LG_IX	extGenewise	estExt_fgenesh1_kg_v1.C_LG_IX0025	Poptr1/LG_IX:3327839-3329798
LG_IX	Fgenesh	fgenesh1_pm.C_LG_IX000239	Poptr1/LG_IX:3328161-3329436
LG_IX	extGenewise	estExt_fgenesh1_pm_v1.C_LG_IX0236	Poptr1/LG_IX:3327839-3329798
LG_IX	Fgenesh	fgenesh1_pg.C_LG_IX000526	Poptr1/LG_IX:3327921-3329794
LG_IX	Fgenesh	fgenesh1_pg.C_LG_IX000527	Poptr1/LG_IX:3328161-3329436
LG_IX	extGenewise	estExt_fgenesh1_pg_v1.C_LG_IX0520	Poptr1/LG_IX:3327839-3329798
LG_IX	extGenewise	estExt_fgenesh1_pg_v1.C_LG_IX0521	Poptr1/LG_IX:3327839-3329798
LG_IX	Genewise	gw1.IX.1904.1	Poptr1/LG_IX:3328164-3329349
LG_IX	Grail	grail3.0001048203	Poptr1/LG_IX:3327930-3329811
LG_IX	Eugene	eugene3.00090545	Poptr1/LG_IX:3327826-3329798

Table A1 continued.

LG/ Scaffold	Gene Prediction Model Name	Gene Model ID	Location on Genome
LG_IX	Genewise	gw1.IX.1906.1	Poptr1/LG_IX:3328164-3329436
LG_IX	Grail	grail3.0001048202	Poptr1/LG_IX:3327930-3329811

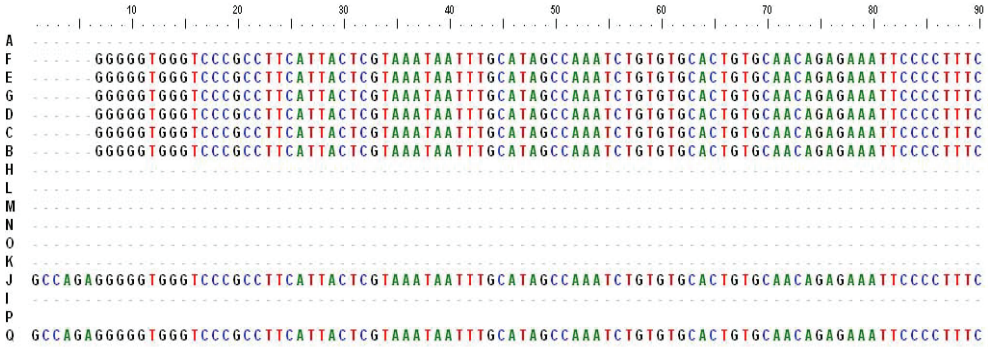

Figure A1. Multiple sequence alignment of predicted transcript sequences from LG_VII for EST 99. Letters **A**-to-**O** are the names of gene models **A:** estExt_Genewise1_LG_VII3334, **B:** estExt_Genewise1_LG_VII3336, **C:** estExt_Genewise1_LG_VII3333, **D:** estExt_Genewise1_LG_VII3332, **E:** estExt_Genewise1_LG_VII3332_2, **F:** estExt_Genewise1_LG_VII3335, **G:** grail3.0019014801, **H:** gw1.VII.3345.1, **I:** gw1.VII.3344.1, J: gw1.VII.3343.1, **K:** gw1.VII.3342.1, **L:** gw1.VII.3341.1, **M:** estExt_fgenesh1_LG_VII1000, **N:** eugene3.00071036, **O:** fgenesh1_LG_VII001011. **P:** Clustal Consensus, **Q:** Consensus transcript sequence

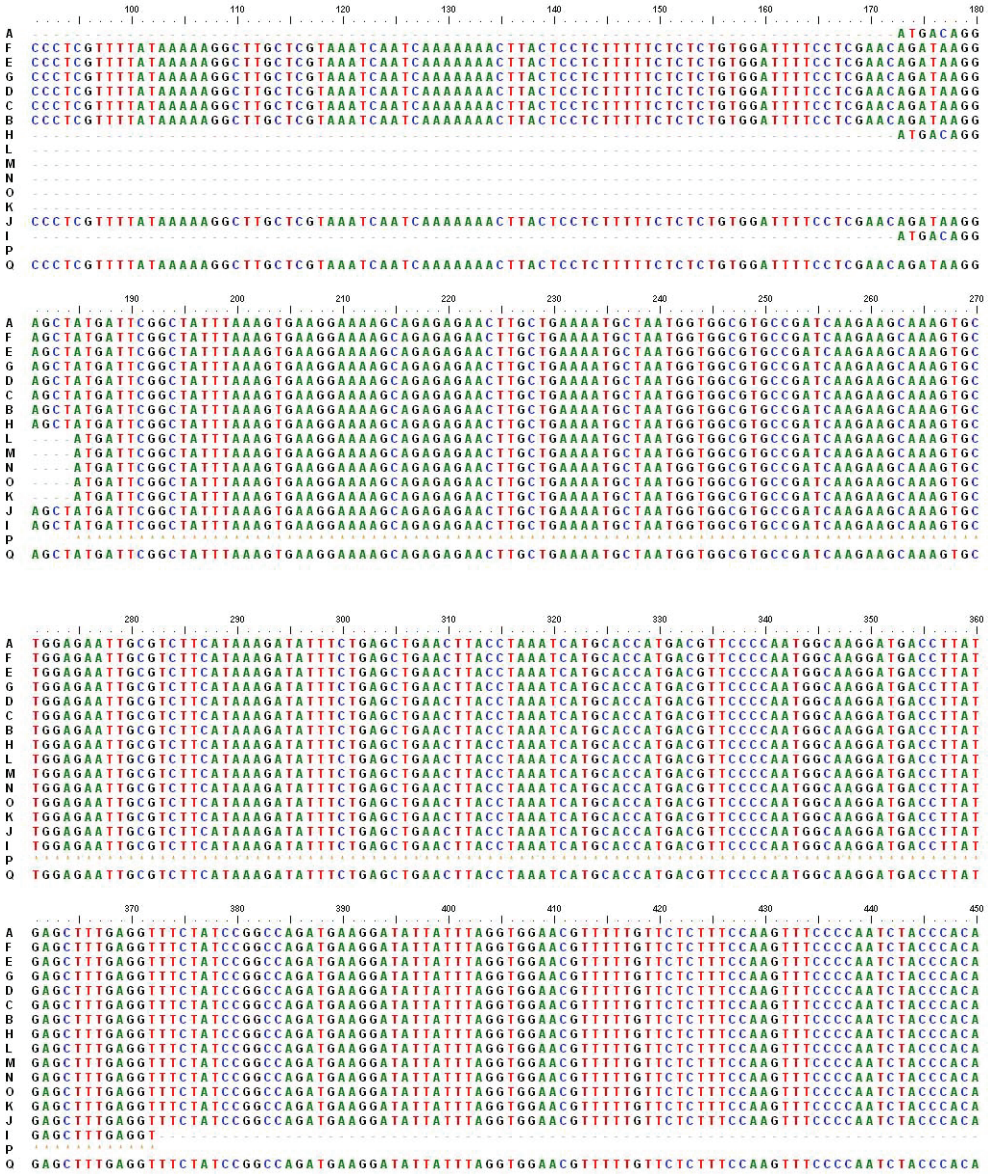

Figure A1 continued.

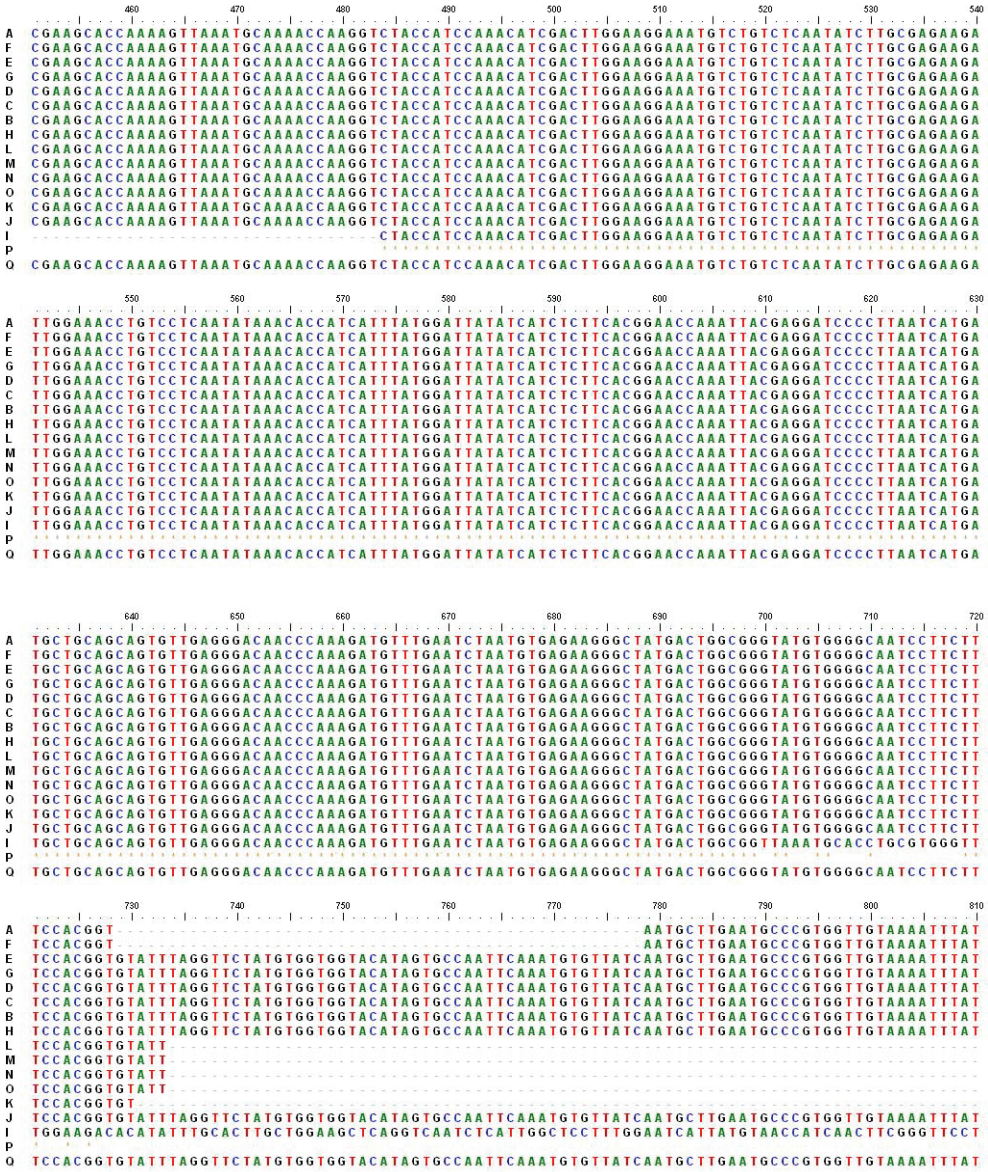

Figure A1 continued.

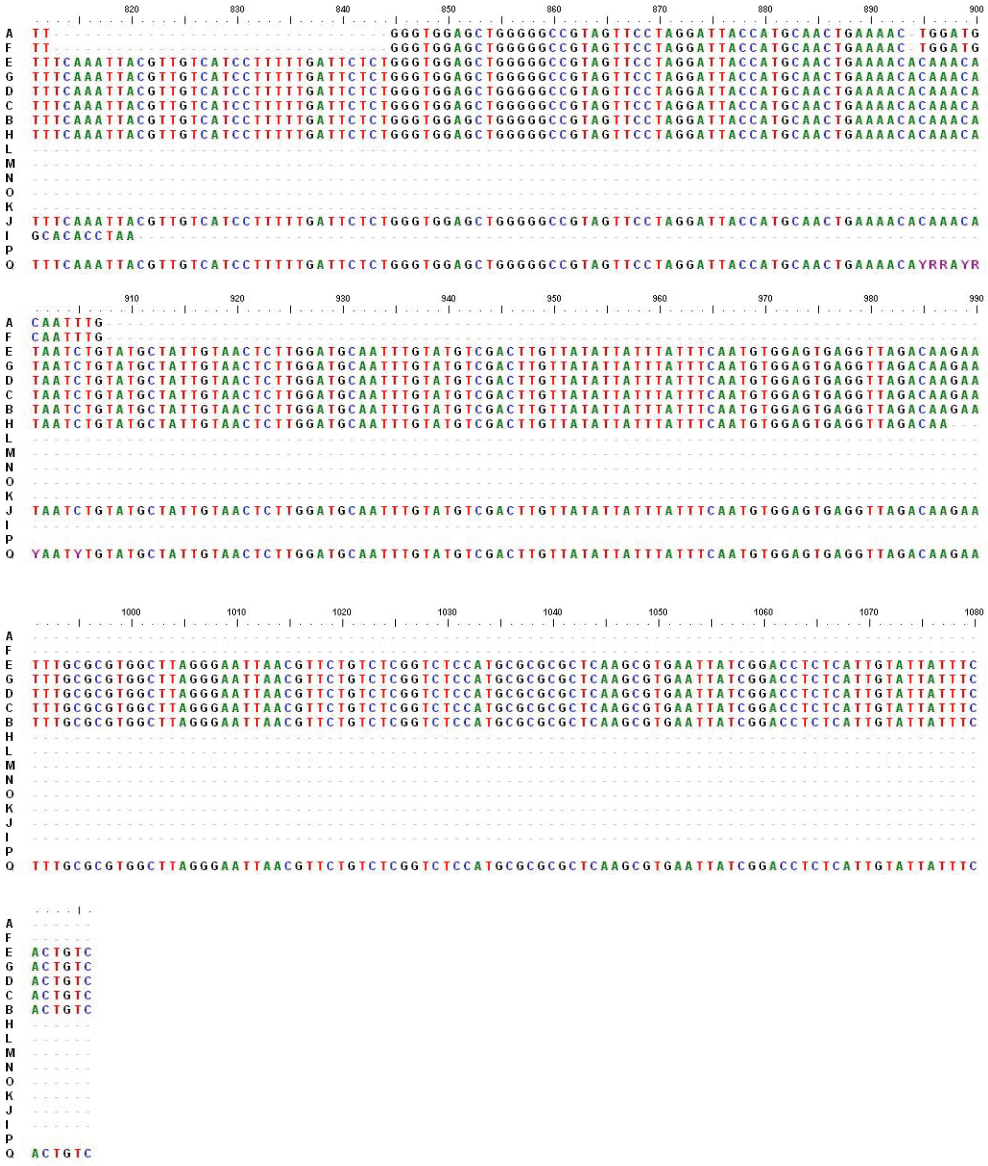

Figure A1 continued.

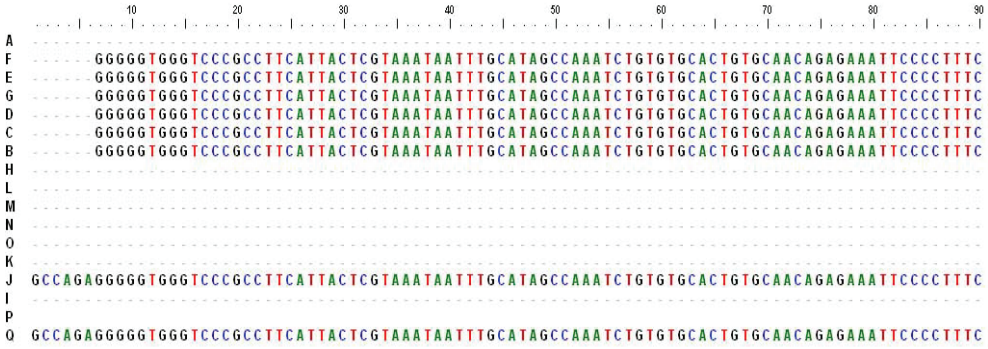

Figure A2. Multiple sequence alignment of predicted transcript sequences from Scaffold_57 for EST 99. Letters **A**-to-**P** are the names of gene models **A:** estExt_fgenesh1_pg_v1.C_570205, **B:** estExt_fgenesh1_pm_v1.C_570101, **C:** estExt_Genewise1_v1.C_570047, **D:** estExt_Genewise1_v1.C_570229, **E:** estExt_Genewise1_v1.C_570313, **F:** estExt_Genewise1_v1.C_570348, **G:** eugene3.00570216, **H:** fgenesh1_pg.C_scaffold_57000208, **I:** fgenesh1_pm.C_scaffold_57000103, **J:** grail3.0057018501, **K:** grail3.0057018701, **L:** grail3.0057018702, **M:** gw1.57.6.1, **N:** gw1.57.41.1, **O:** gw1.57.125.1, **P:** gw1.57.307.1. **Q:** Clustal consensus, **R:** Consensus transcript sequence

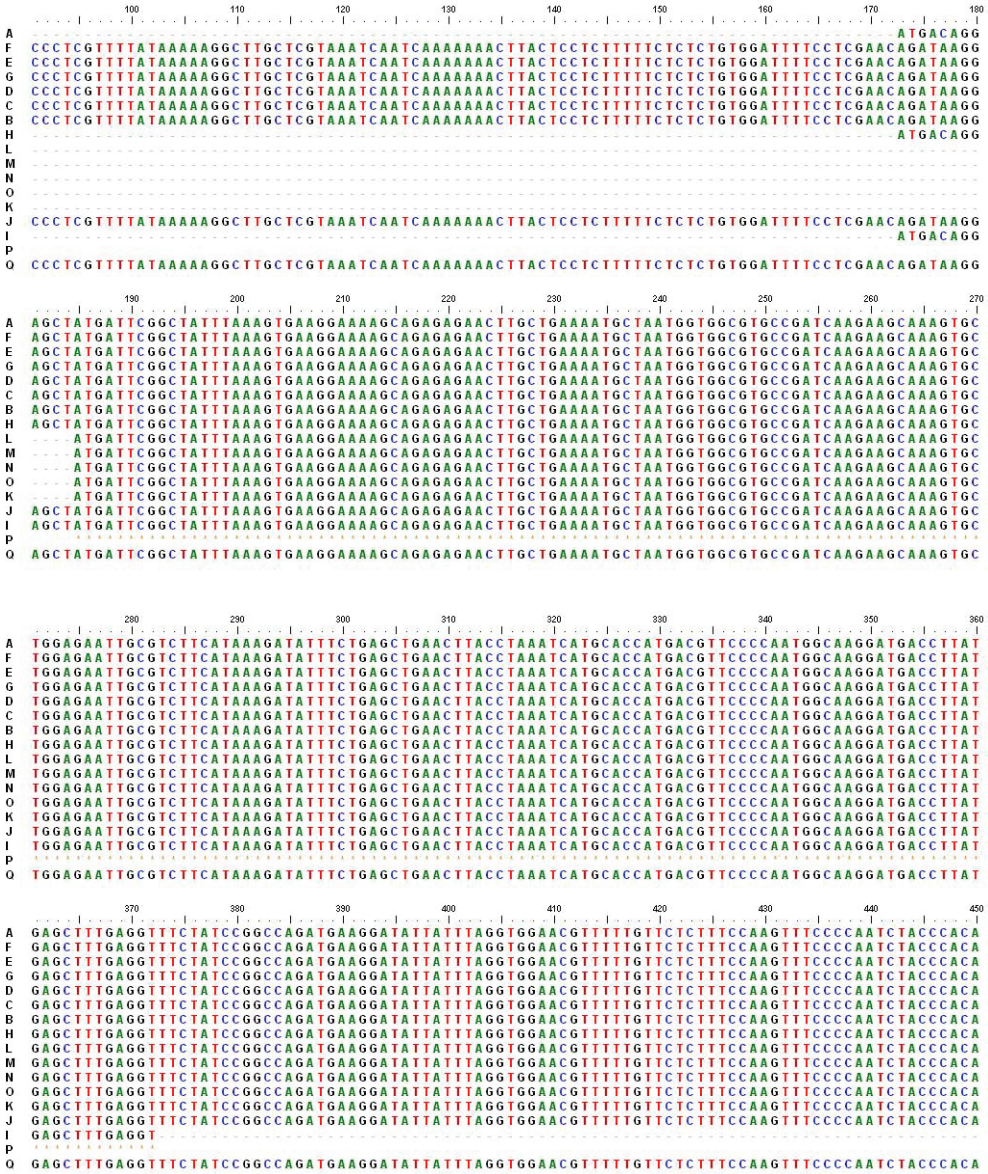

Figure A2 continued.

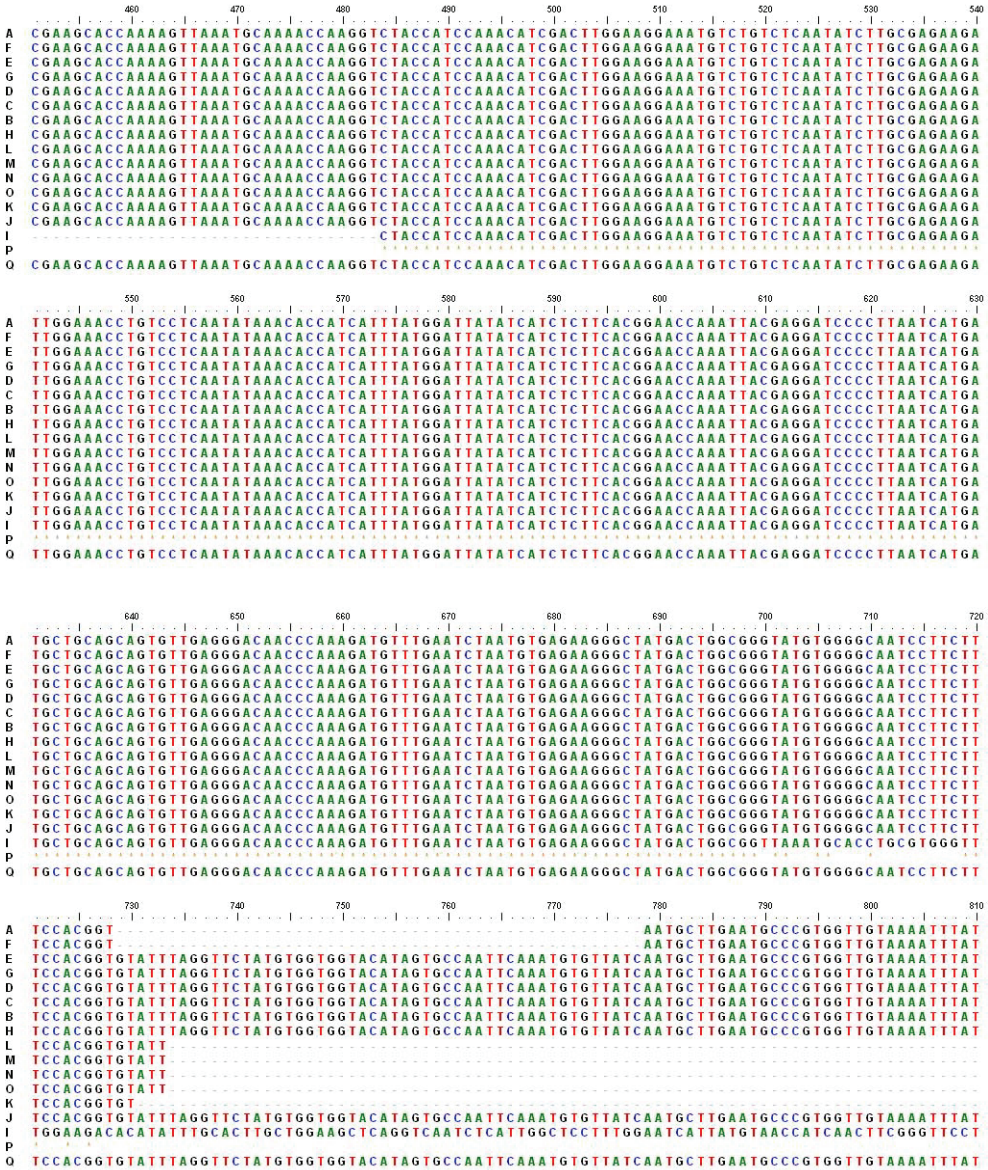

Figure A2 continued.

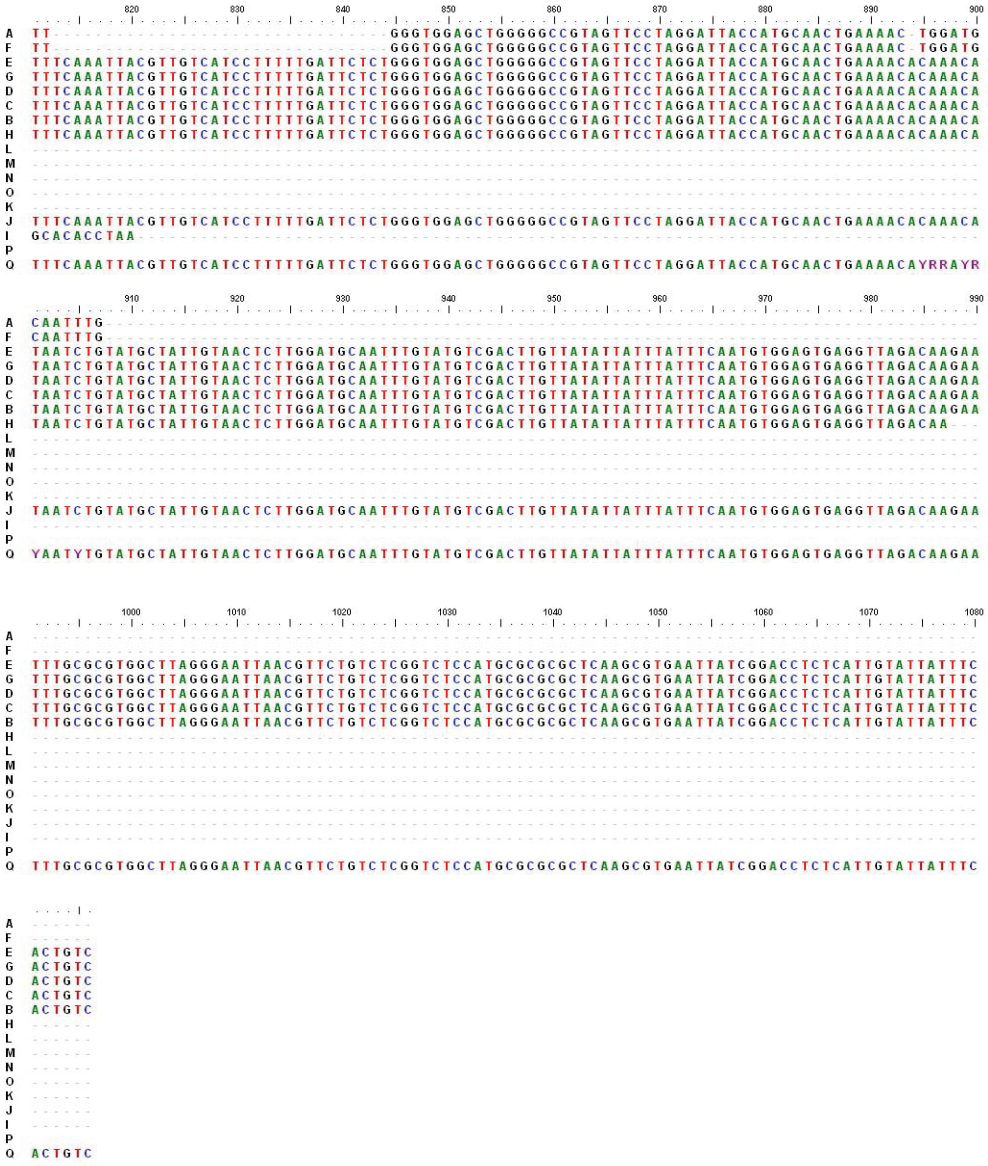

Figure A2 continued.

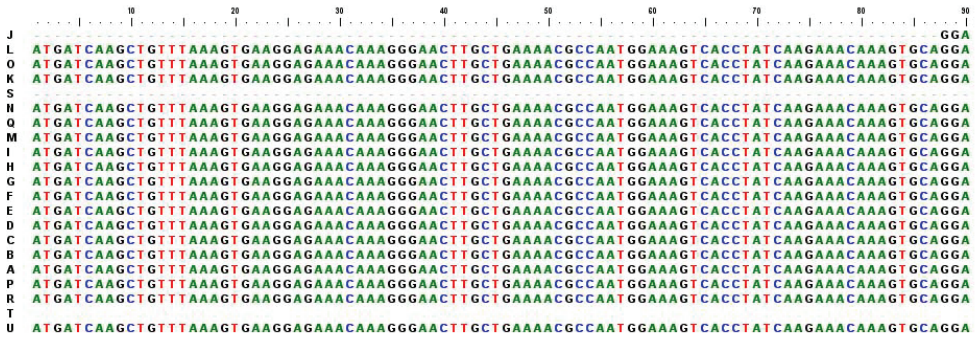

Figure A3. Multiple sequence alignment of predicted transcript sequences from LG_IX for EST 99. Letters **A**-to-**S** are the names of gene models **A.** estExt_fgenesh1_pg_v1.C_LG_IX0520, **B.** fgenesh1_kg.C_LG_IX000028, **C.** estExt_fgenesh1_kg_v1.C_LG_IX0025, **D.** fgenesh1_pm.C_LG_IX000239, **E.** estExt_fgenesh1_pm_v1.C_LG_IX0236, **F.** fgenesh1_pg.C_LG_IX000526, **G.** fgenesh1_pg.C_LG_IX000527, **H.** estExt_fgenesh1_pg_v1.C_LG_IX0520, **I.** estExt_fgenesh1_pg_v1.C_LG_IX0521, **J.** gw1.IX.1904.1, **K.** estExt_Genewise1_v1.C_LG_IX1899, **L.** estExt_Genewise1_v1.C_LG_IX1899, **M.** estExt_Genewise1_v1.C_LG_IX1900, **N.** estExt_Genewise1_v1.C_LG_IX1901, **O.** estExt_Genewise1_v1.C_LG_IX1902, **P.** grail3.0001048201, **Q.** grail3.0001048202, **R.** grail3.0001048203, **S.** eugene3.00090545. **T.** Clustal Consensus. **U.** Consensus transcript sequence

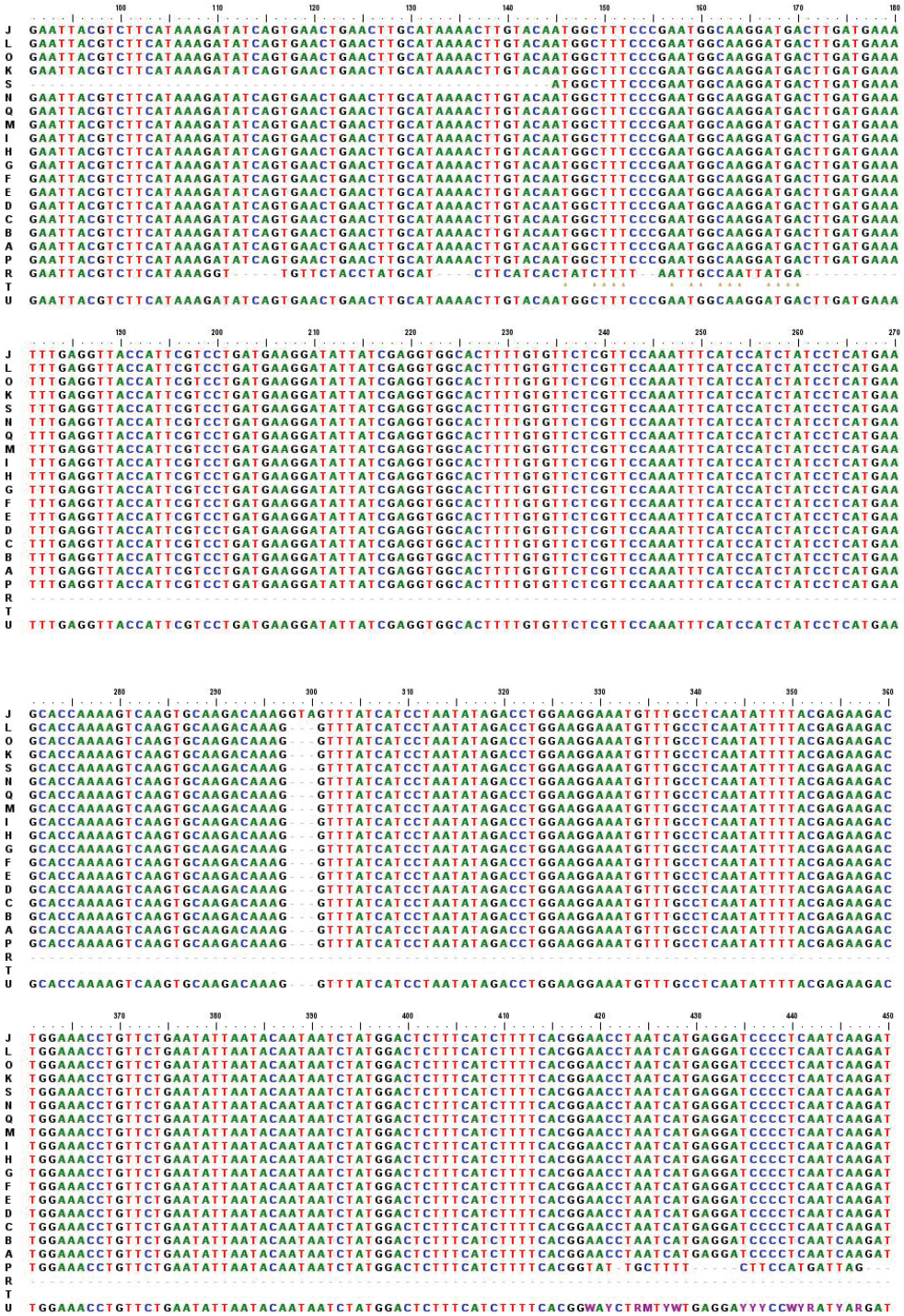

Figure A3 continued.

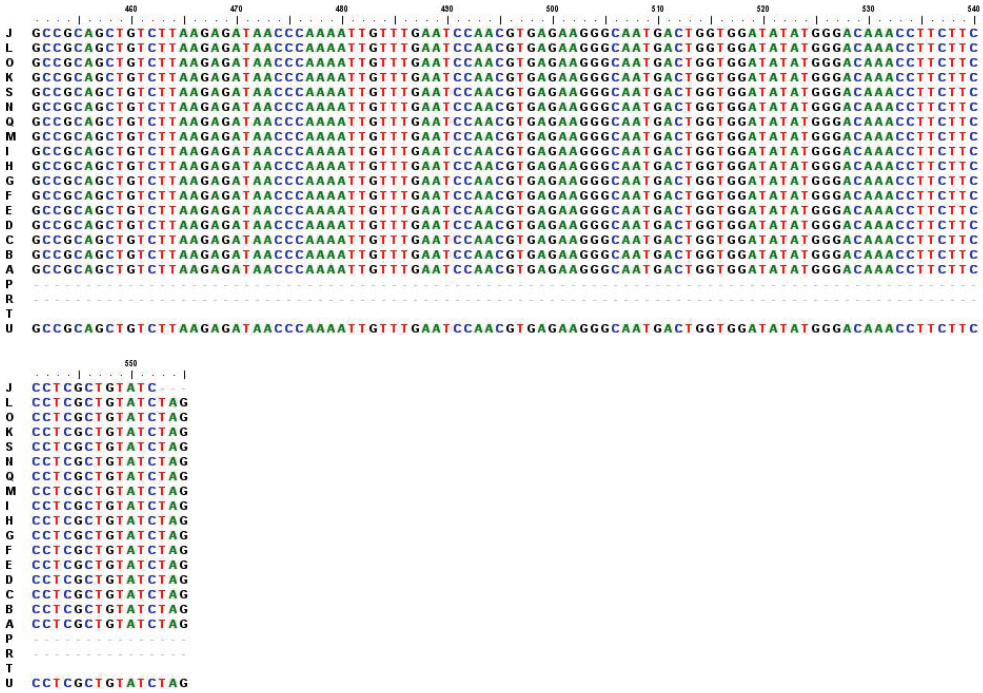

Figure A3 continued.

Figure A4. Multiple sequence alignment of predicted protein sequences from LG_VII. Letters **A**-to-**O** are the names of gene models **A:** estExt_Genewise1_LG_VII3334, **B:** estExt_Genewise1_LG_VII3336, **C:** estExt_Genewise1_LG_VII3333, **D:** estExt_Genewise1_LG_VII3332, **E:** estExt_Genewise1_LG_VII3332_2, **F:** estExt_Genewise1_LG_VII3335, **G:** grail3.0019014801, **H:** gw1.VII.3345.1, **I:** gw1.VII.3344.1, J: gw1.VII.3343.1, **K:** gw1.VII.3342.1, **L:** gw1.VII.3341.1, **M:** estExt_fgenesh1_LG_VII1000, **N:** eugene3.00071036, **O:** fgenesh1_LG_VII001011. **P:** Clustal Consensus, **Q:** Consensus protein sequence

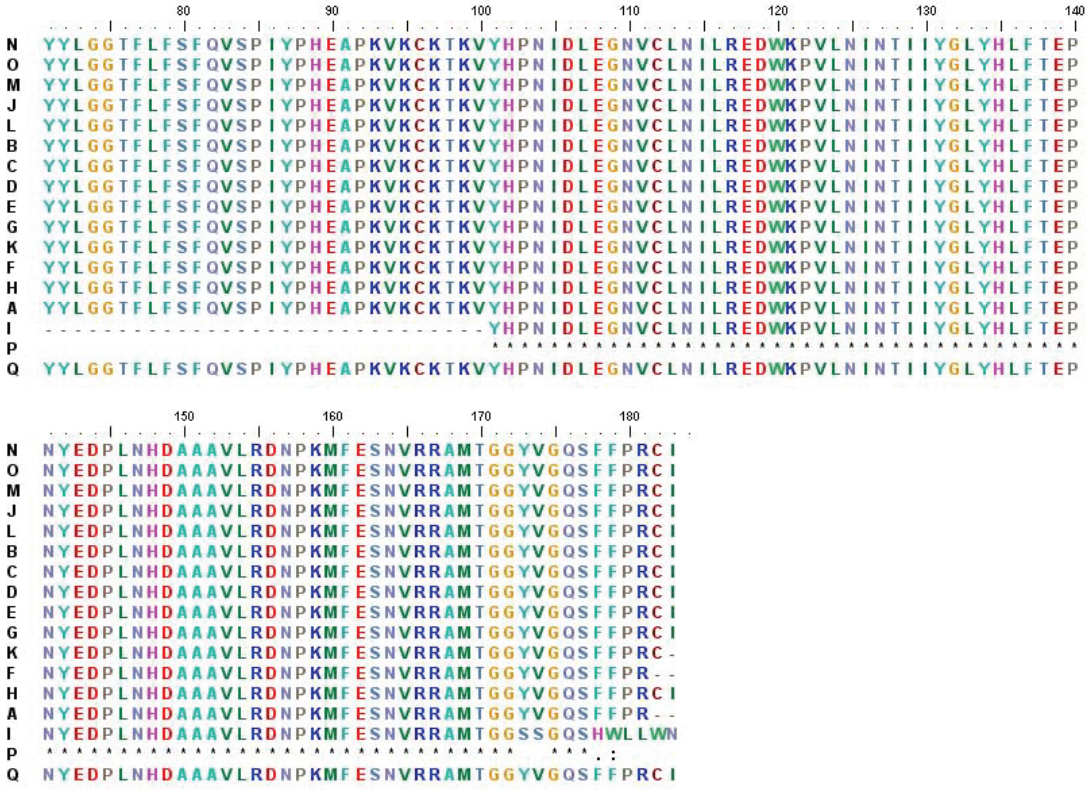

Figure A4 continued.

Figure A5. Multiple sequence alignment of predicted protein sequences from gene models from Scaffold_57 for EST 99. Letters **A**-to-**P** are the names of gene models **A:** estExt_fgenesh1_pg_v1.C_570205, **B:** estExt_fgenesh1_pm_v1.C_570101, **C:** estExt_Genewise1_v1.C_570047, **D:** estExt_Genewise1_v1.C_570229, **E:** estExt_Genewise1_v1.C_570313, **F:** estExt_Genewise1_v1.C_570348, **G:** eugene3.00570216, **H:** fgenesh1_pg.C_scaffold_57000208, **I:** fgenesh1_pm.C_scaffold_57000103, **J:** grail3.0057018501, **K:** grail3.0057018701, **L:** grail3.0057018702, **M:** gw1.57.6.1, **N:** gw1.57.41.1, **O:** gw1.57.125.1, **P:** gw1.57.307.1. **Q:** Clustal consensus, **R:** Consensus protein sequence

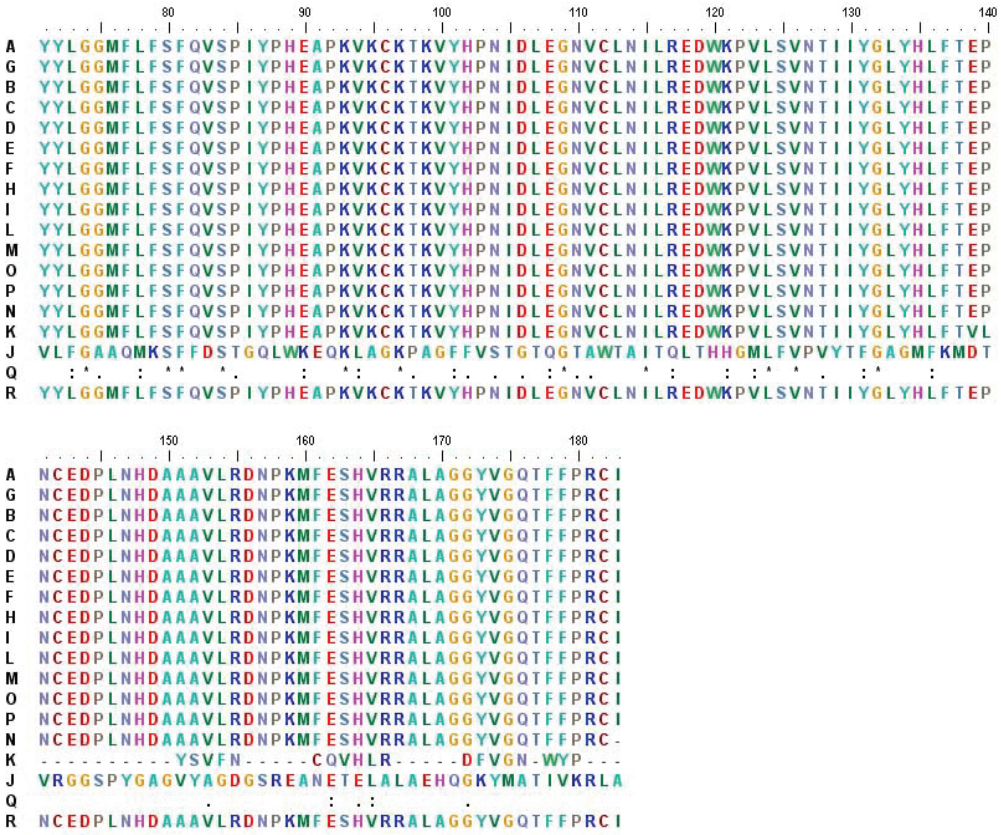

Figure A5 continued.

Figure A6. Multiple sequence alignment of predicted protein sequences from LG_IX for EST 99. Letters **A**-to-**S** are the names of gene models **A.** estExt_fgenesh1_pg_v1.C_LG_IX0520, **B.** fgenesh1_kg.C_LG_IX000028, **C.** estExt_fgenesh1_kg_v1.C_LG_IX0025, **D.** fgenesh1_pm.C_LG_IX000239, **E.** estExt_fgenesh1_pm_v1.C_LG_IX0236, **F.** fgenesh1_pg.C_LG_IX000526, **G.** fgenesh1_pg.C_LG_IX000527, **H.** estExt_fgenesh1_pg_v1.C_LG_IX0520, **I.** estExt_fgenesh1_pg_v1.C_LG_IX0521, **J.** gw1.IX.1904.1, **K.** estExt_Genewise1_v1.C_LG_IX1899, **L.** estExt_Genewise1_v1.C_LG_IX1899, **M.** estExt_Genewise1_v1.C_LG_IX1900, **N.** estExt_Genewise1_v1.C_LG_IX1901, **O.** estExt_Genewise1_v1.C_LG_IX1902, **P.** grail3.0001048201, **Q.** grail3.0001048202, **R.** grail3.0001048203, **S.** eugene3.00090545. **T.** Clustal Consensus. **U.** Consensus protein sequence

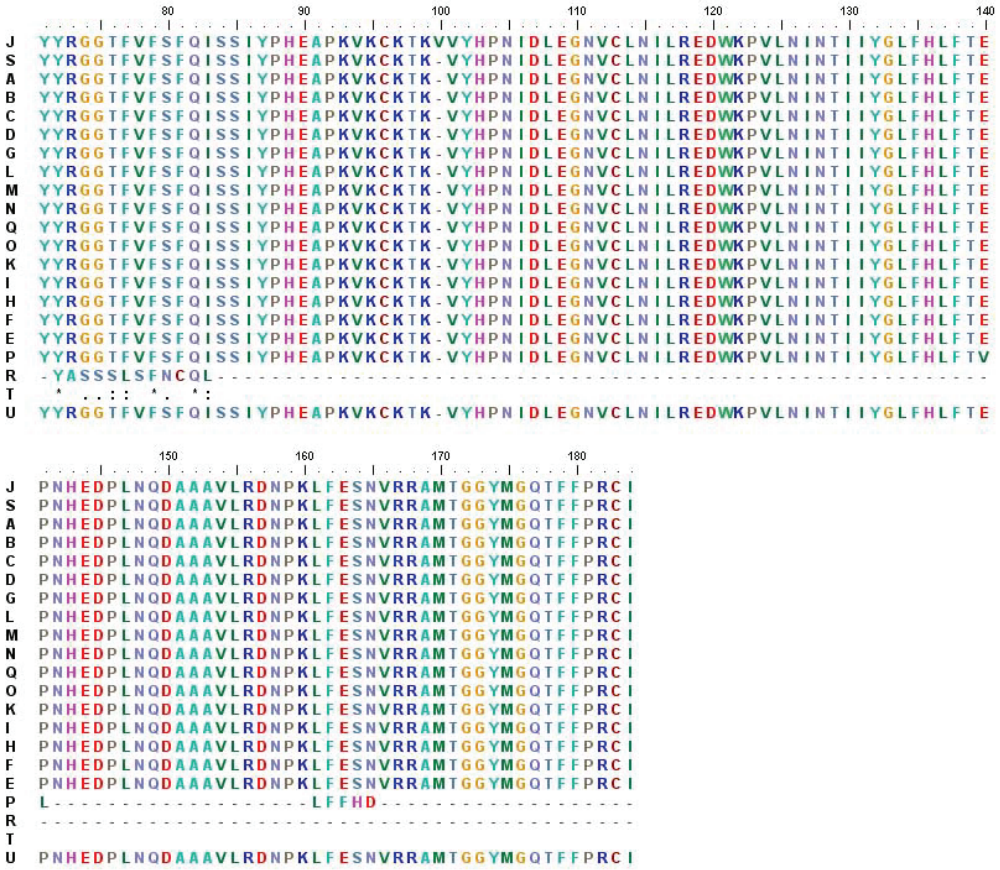

Figure A6 continued.

Table A2 shows the gene models associated with EST 181 and their locations in poplar genome. LG: Linkage Group, Sc: Scaffold

LG/ Scaffold	Gene Prediction Model Name	Gene Model ID	Location on Genome
Sc_132	Fgenesh	estExt_fgenesh1_pg_v1.C_1320039	Poptr1/scaffold_132:463454-471993
Sc_132	Fgenesh	fgenesh1_kg.C_scaffold_132000001	Poptr1/scaffold_132:464053-465696
Sc_132	Fgenesh	estExt_fgenesh1_kg_v1.C_1320001	Poptr1/scaffold_132:463454-465696
Sc_132	Fegeneh	fgenesh1_pm.C_scaffold_132000007	Poptr1/scaffold_132:463991-471113
Sc_132	Fgenesh	estExt_fgenesh1_pm_v1.C_1320006	Poptr1/scaffold_132:463454-471993
Sc_132	Fgenesh	fgenesh1_pg.C_scaffold_132000040	Poptr1/scaffold_132:463991-471113
Sc_132	Fgenesh	fgenesh1_pg.C_scaffold_132000041	Poptr1/scaffold_132:464053-465696
Sc_132	Fgenesh	estExt_fgenesh1_pg_v1.C_1320040	Poptr1/scaffold_132:463454-465696
Sc_132	Fgenesh	estExt_fgenesh1_pg_v1.C_1320039	Poptr1/scaffold_132:463454-471993
Sc_132	Genewise1	gw1.132.63.1	Poptr1/scaffold_132:463994-471101
Sc_132	Genewise1	gw1.132.64.1	Poptr1/scaffold_132:463994-471107
Sc_132	Genewise1	gw1.132.65.1	Poptr1/scaffold_132:463994-471113
Sc_132	Genewise1	gw1.132.66.1	Poptr1/scaffold_132:463994-471113
Sc_132	Genewise1	gw1.132.67.1	Poptr1/scaffold_132:463994-471113
Sc_132	Extgenewise1	estExt_Genewise1_v1.C_1320062	Poptr1/scaffold_132:463454-465190
Sc_132	Extgenewise1	estExt_Genewise1_v1.C_1320063	Poptr1/scaffold_132:463556-465209

Table A2 continued.

LG/ Scaffold	Gene Prediction Model Name	Gene Model ID	Location on Genome
Sc_132	Extgenewise1	estExt_Genewise1_v1.C_1320064	Poptr1/scaffold_132:463556-465209
Sc_132	Extgenewise1	estExt_Genewise1_v1.C_1320065	Poptr1/scaffold_132:463556-465209
Sc_132	Extgenewise1	estExt_Genewise1_v1.C_1320066	Poptr1/scaffold_132:463556-465209
Sc_132	Extgenewise1	estExt_Genewise1_v1.C_1320067	Poptr1/scaffold_132:463556-465209
Sc_132	Grail	grail3.0132002101	Poptr1/scaffold_132:463775-471993
Sc_132	Grail	grail3.0132002102	Poptr1/scaffold_132:463775-471993
Sc_132	Grail	grail3.0132002103	Poptr1/scaffold_132:463775-471993
Sc_132	Grail	grail3.0132002104	Poptr1/scaffold_132:463775-471993
Sc_132	Eugene	eugene3.01320042	Poptr1/scaffold_132:463555-471113
LG_X	extGenewise1	estExt_Genewise1_v1.C_LG_X4345	Poptr1/LG_X:4147367-4154326
LG_X	Fgenesh	fgenesh1_kg.C_LG_X000016	Poptr1/LG_X:4152103-4153750
LG_X	extFgenesh	estExt_fgenesh1_kg_v1.C_LG_X0015	Poptr1/LG_X:4149371-4154326
LG_X	Fgenesh	fgenesh1_pm.C_LG_X000093	Poptr1/LG_X:4147361-4153812
LG_X	extFgenesh	estExt_fgenesh1_pm_v1.C_LG_X0092	Poptr1/LG_X:4147361-4154326
LG_X	Fgenesh	fgenesh1_pg.C_LG_X000321	Poptr1/LG_X:4147361-4153812
LG_X	Fgenesh	fgenesh1_pg.C_LG_X000322	Poptr1/LG_X:4152103-4153750
LG_X	extFgenesh	estExt_fgenesh1_pg_v1.C_LG_X0319	Poptr1/LG_X:4147361-4154326
LG_X	extFgenesh	estExt_fgenesh1_pg_v1.C_LG_X0320	Poptr1/LG_X:4149371-4154326
LG_X	Genewise 1	gw1.X.4364.1	Poptr1/LG_X:4147361-4153809
LG_X	Genewise 1	gw1.X.4365.1	Poptr1/LG_X:4147361-4153809

Table A2 continued.

LG/ Scaffold	Gene Prediction Model Name	Gene Model ID	Location on Genome
LG_X	Genewise 1	gw1.X.4368.1	Poptr1/LG_X:4147361-4153809
LG_X	Genewise 1	gw1.X.4367.1	Poptr1/LG_X:4147367-4153809
LG_X	Genewise 1	gw1.X.4366.1	Poptr1/LG_X:4147373-4153809
LG_X	extGenewise	estExt_Genewise1_v1.C_LG_X4342	Poptr1/LG_X:4147361-4154326
LG_X	extGenewise	estExt_Genewise1_v1.C_LG_X4343	Poptr1/LG_X:4147361-4154326
LG_X	extGenewise	estExt_Genewise1_v1.C_LG_X4346	Poptr1/LG_X:4147361-4154326
LG_X	extGenewise	estExt_Genewise1_v1.C_LG_X4345	Poptr1/LG_X:4147367-4154326
LG_X	extGenewise	estExt_Genewise1_v1.C_LG_X4344	Poptr1/LG_X:4147373-4154326
LG_X	Grail	grail3.0060006901	Poptr1/LG_X:4147361-4154290
LG_X	Grail	grail3.0060006902	Poptr1/LG_X:4147361-4154290
LG_X	Eugene	eugene3.00100293	Poptr1/LG_X:4147361-4154327

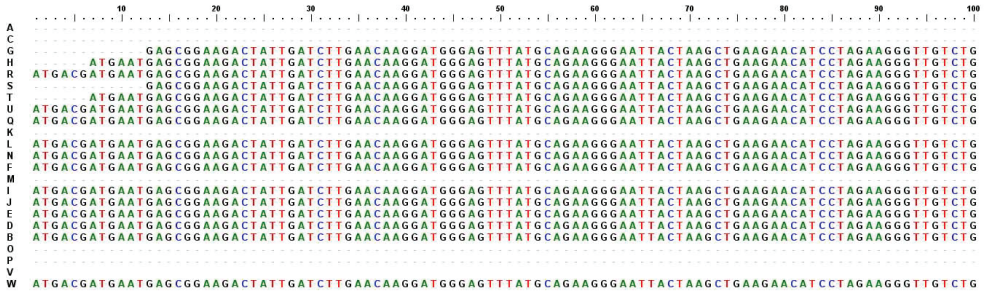

Figure A7: Multiple sequence alignment of predicted transcript sequences from LG_X for EST 181. Letters **A**-to-**U** are the names of gene models **A.** estExt_fgenesh1_kg_v1.C_LG_X0015, **B.** estExt_fgenesh1_pg_v1.C_LG_X0319, **C.** estExt_fgenesh1_pg_v1.C_LG_X0320, **D.** estExt_fgenesh1_pm_v1.C_LG_X0092, **E.** estExt_Genewise1_v1.C_LG_X4342, **F.** estExt_Genewise1_v1.C_LG_X4343, **G.** estExt_Genewise1_v1.C_LG_X4344, **H.** estExt_Genewise1_v1.C_LG_X4345, **I.** estExt_Genewise1_v1.C_LG_X4346, **J.** eugene3.00100293, **K.** fgenesh1_kg.C_LG_X000016, **L.** fgenesh1_pg.C_LG_X000321, **M.** fgenesh1_pg.C_LG_X000322, **N.** fgenesh1_pm.C_LG_X000093, **O.** grail3.0060006901, **P.** grail3.0060006902, **Q.** gw1.X.4364.1, **R.** gw1.X.4365.1, **S.** gw1.X.4366.1, **T.** gw1.X.4367.1, **U.** gw1.X.4368.1, **W.** Clustal consensus, **X.** Consensus transcript sequence

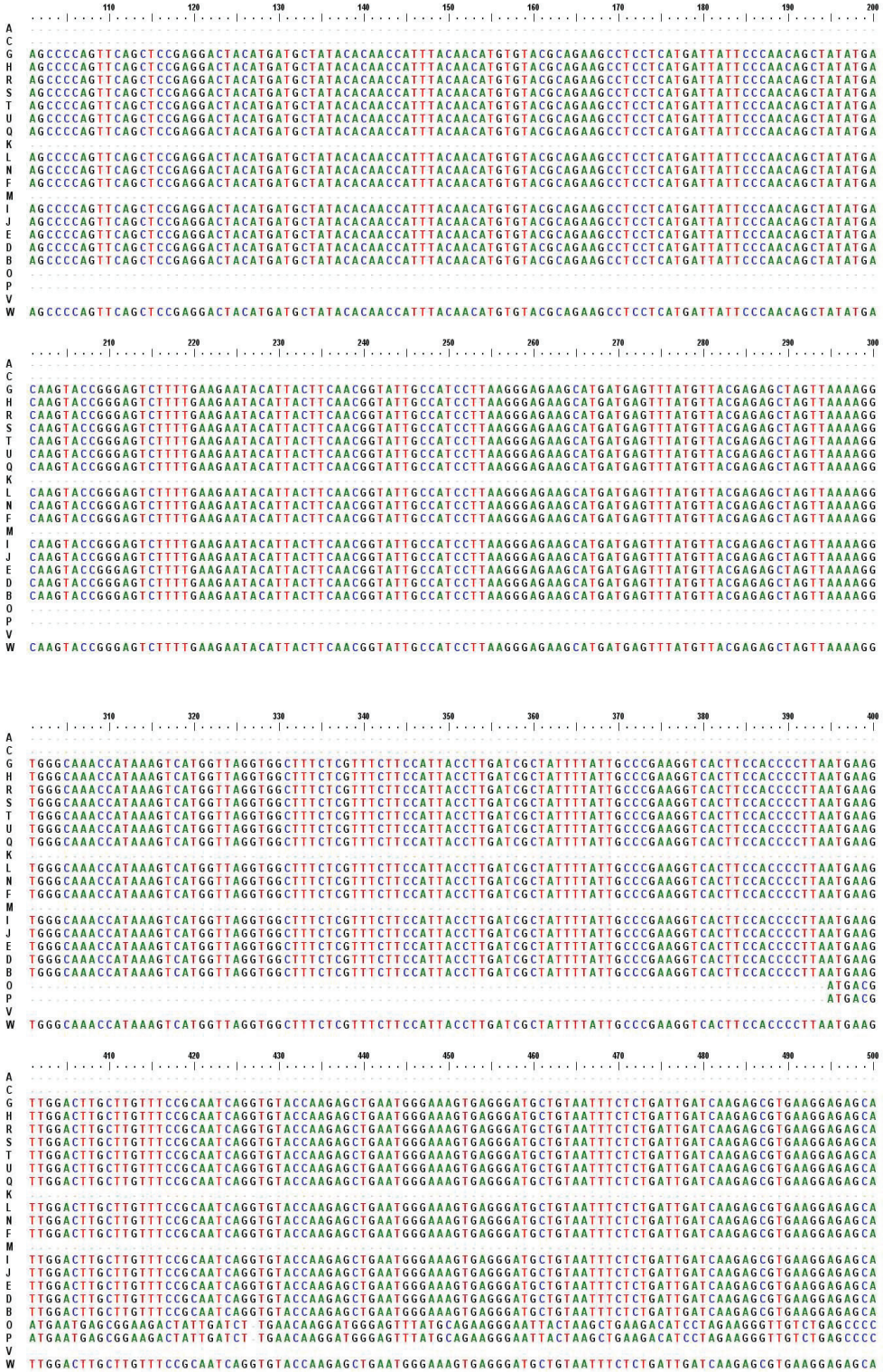

Figure A7 continued.

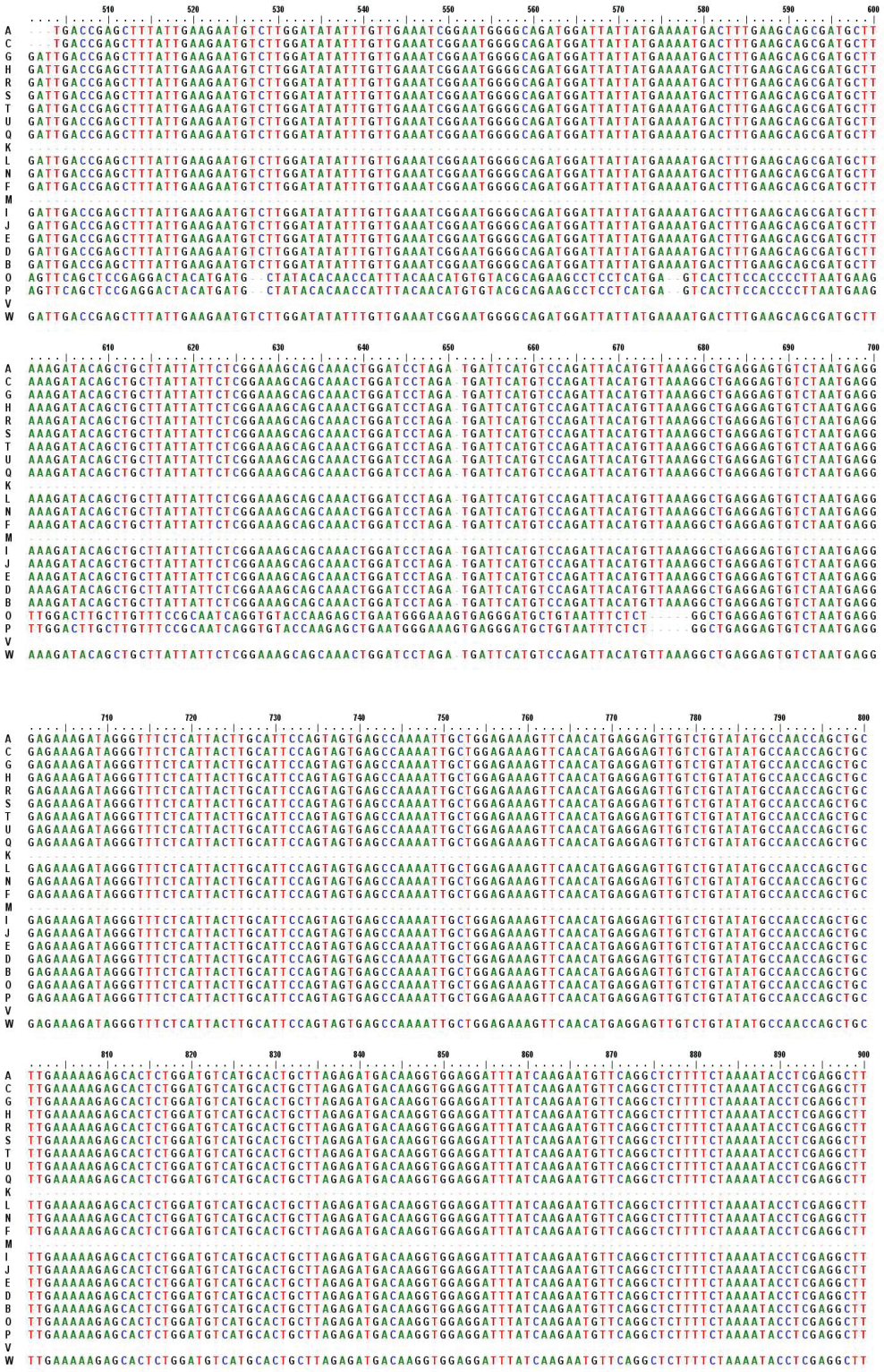

Figure A7 continued.

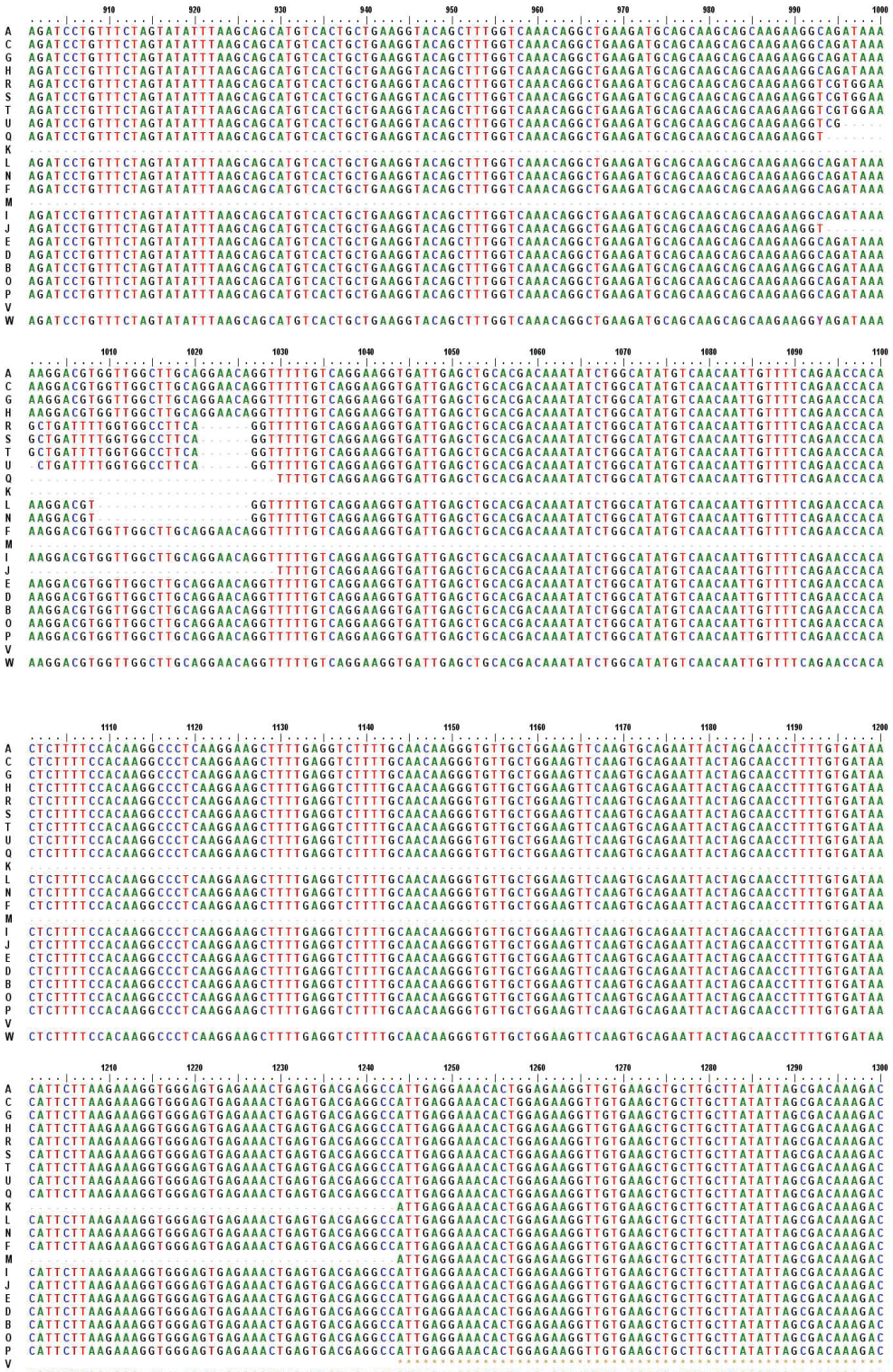

Figure A7 continued.

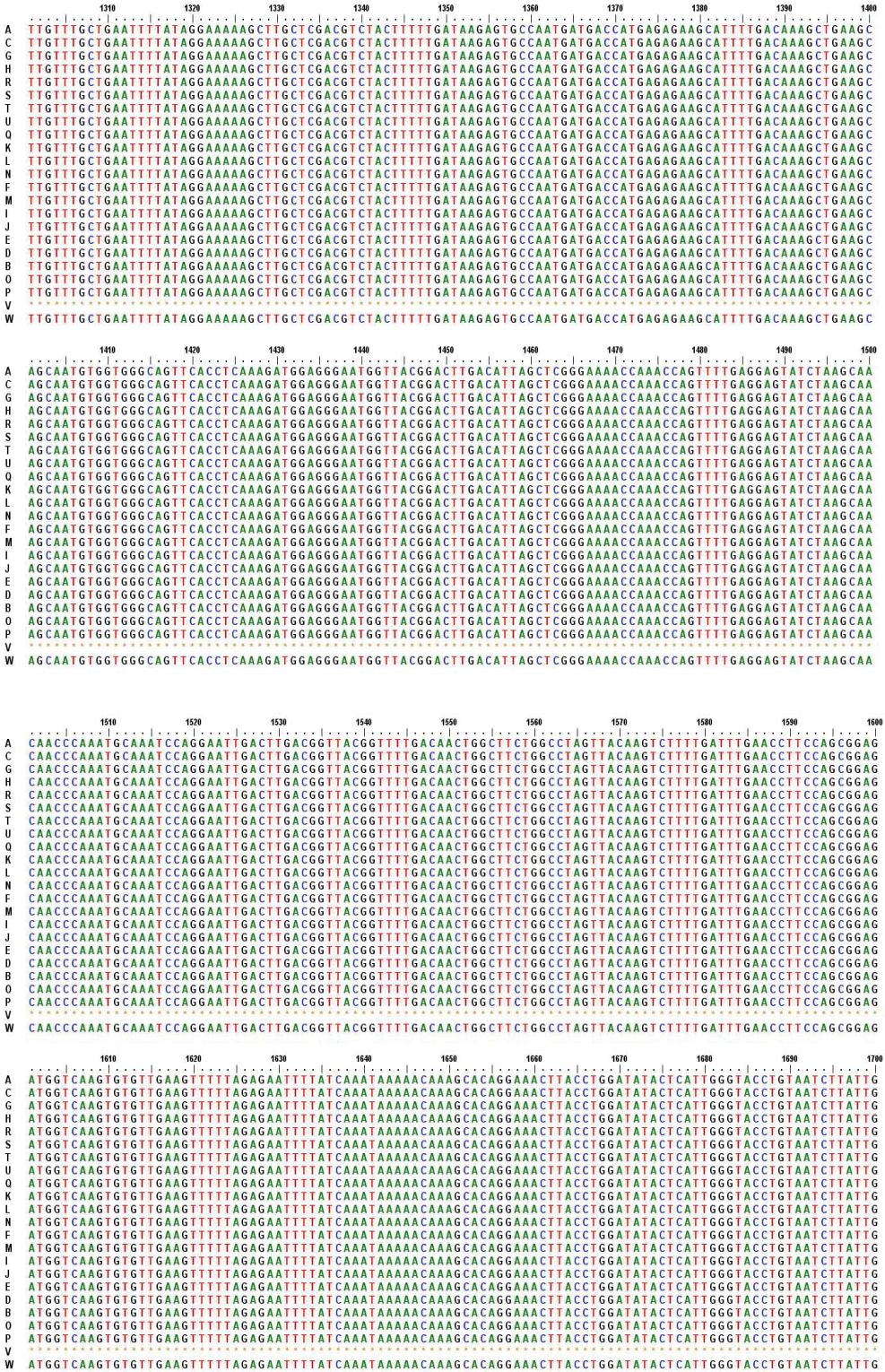

Figure A7 continued.

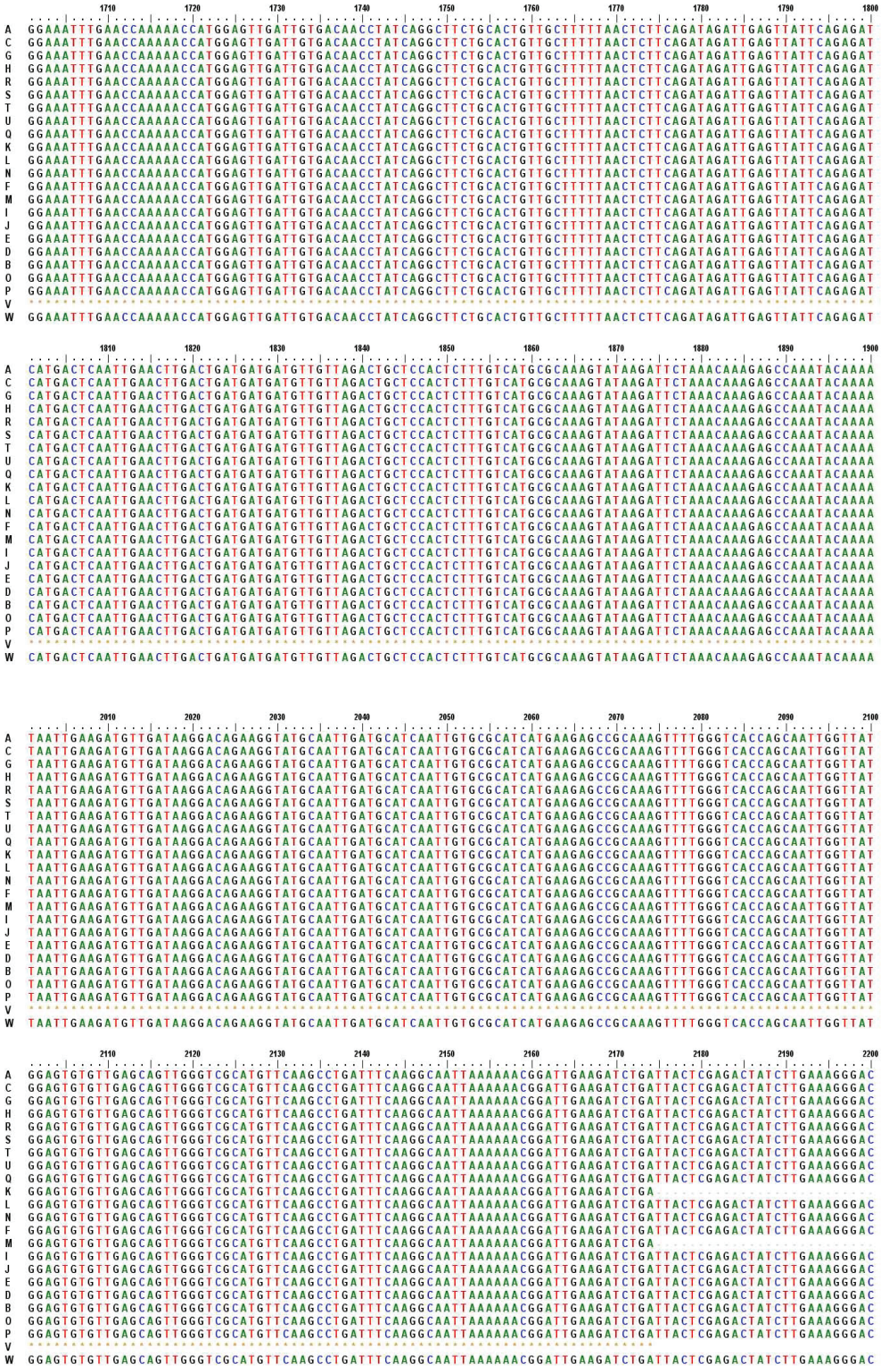

Figure A7 continued.

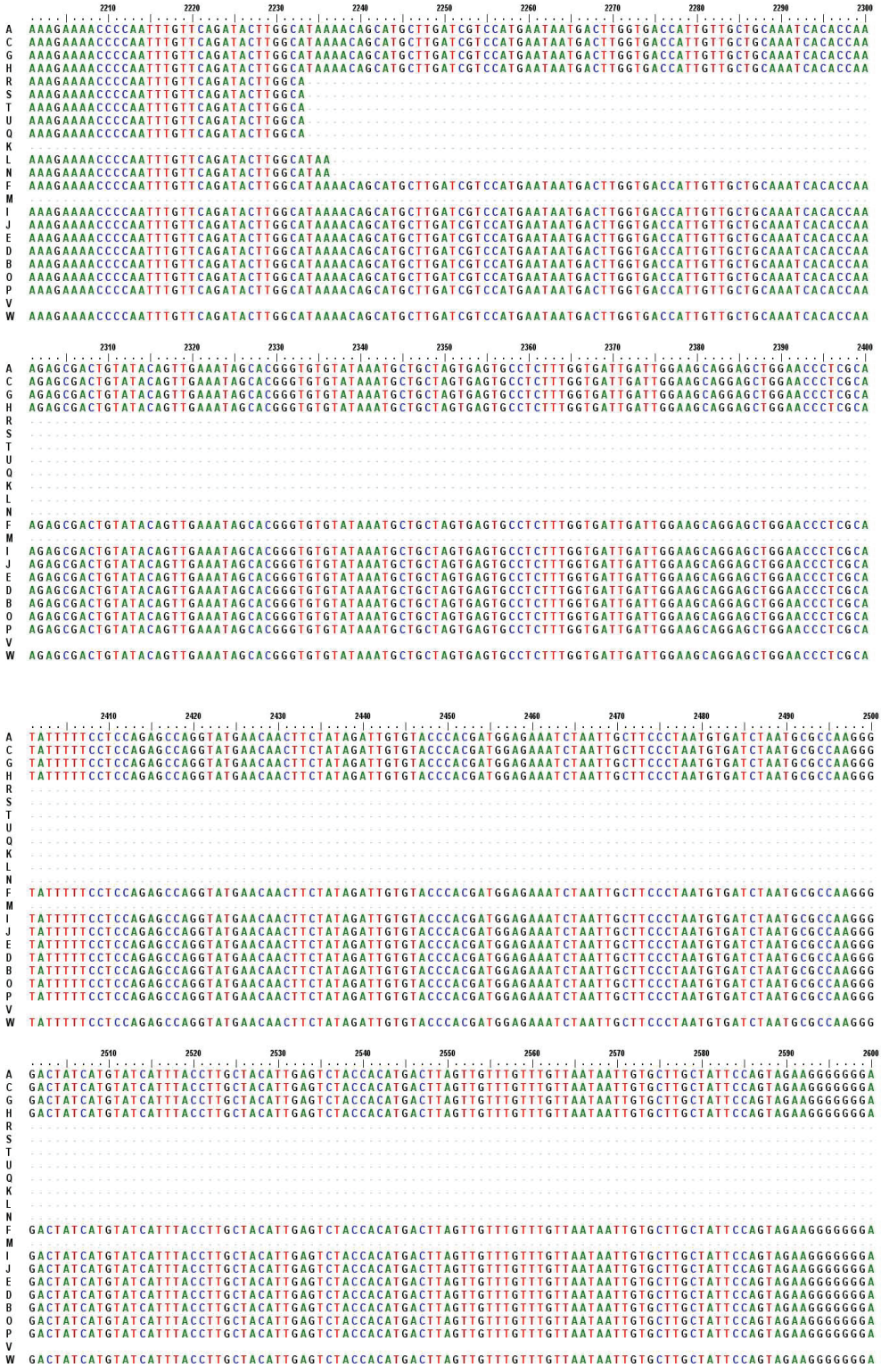

Figure A7 continued.

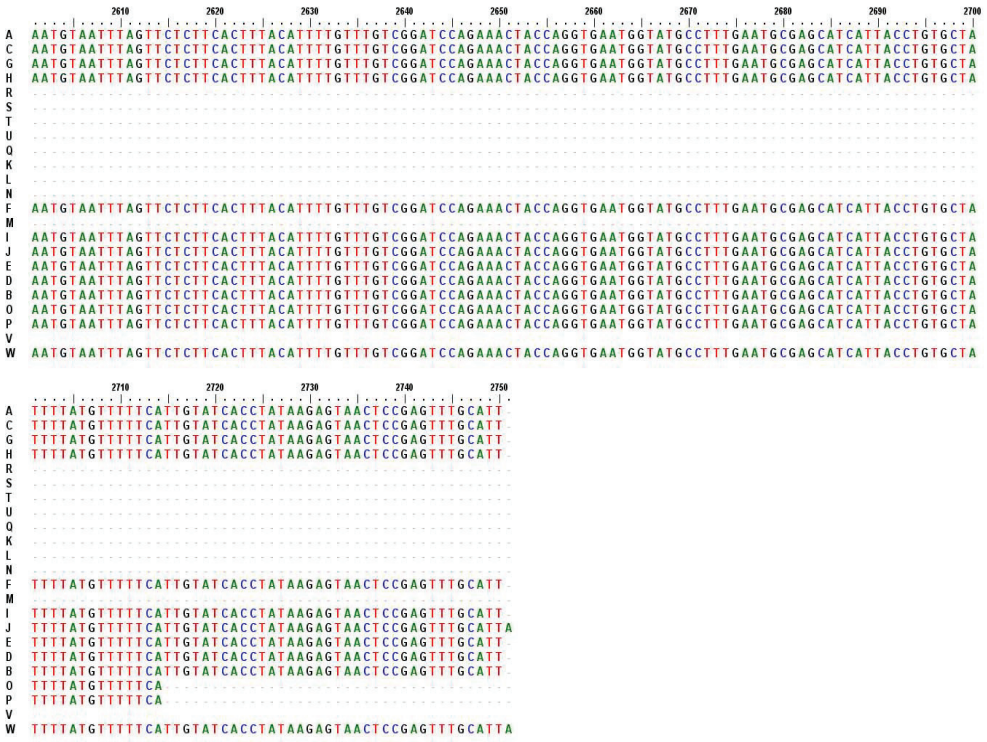

Figure A7 continued.

Figure A8: Multiple sequence alignment of predicted transcript sequences from Scaffold_132 for EST 181. Letters **A**-to-**X** are the names of gene models **A**. estExt_fgenesh1_kg_v1.C_1320001, **B.** estExt_fgenesh1_pg_v1.C_1320039, **C.** estExt_fgenesh1_pg_v1.C_1320040, **D.** estExt_fgenesh1_pm_v1.C_1320006, **E.** estExt_Genewise1_v1.C_1320062, **F.** estExt_Genewise1_v1.C_1320063, **G.** estExt_Genewise1_v1.C_1320064, **H.** estExt_Genewise1_v1.C_1320065, **I.** estExt_Genewise1_v1.C_1320066, **J.** estExt_Genewise1_v1.C_1320067, **K.** eugene3.01320042, **L.** fgenesh1_kg.C_scaffold_132000001, **M.** fgenesh1_pg.C_scaffold_132000040, **N.** fgenesh1_pg.C_scaffold_132000041, **O.** fgenesh1_pm.C_scaffold_132000007, **P.** grail3.0132002101, **Q.** grail3.0132002102, **R.** grail3.0132002103, **S.** grail3.0132002104, **T.** gw1.132.63.1, **U.** gw1.132.64.1, **V.** gw1.132.65.1, **W.** gw1.132.66.1, **X.** gw1.132.67.1. **Y.** Clustal consensus, **Z.** consensus transcript sequence

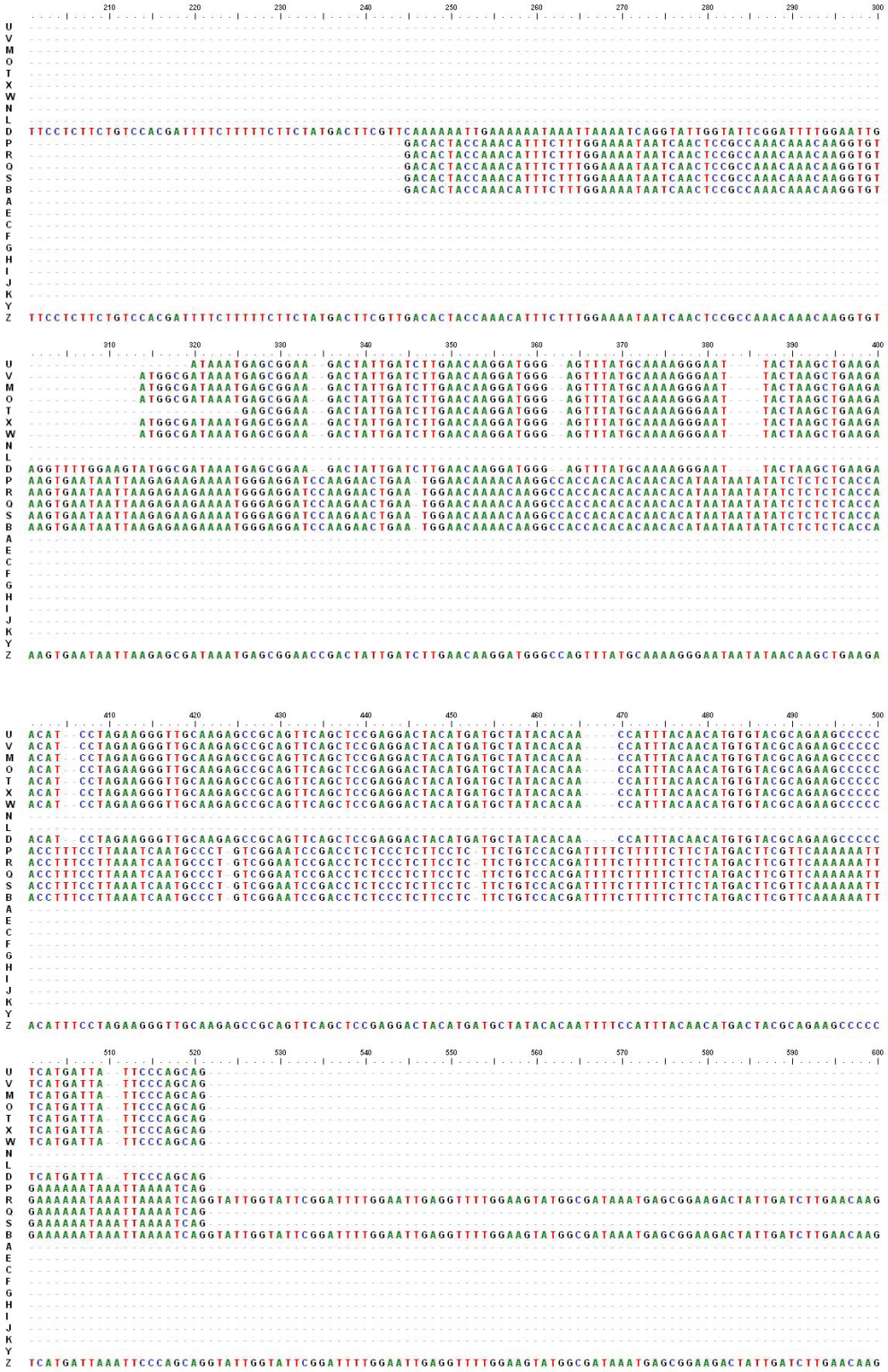

Figure A8 continued.

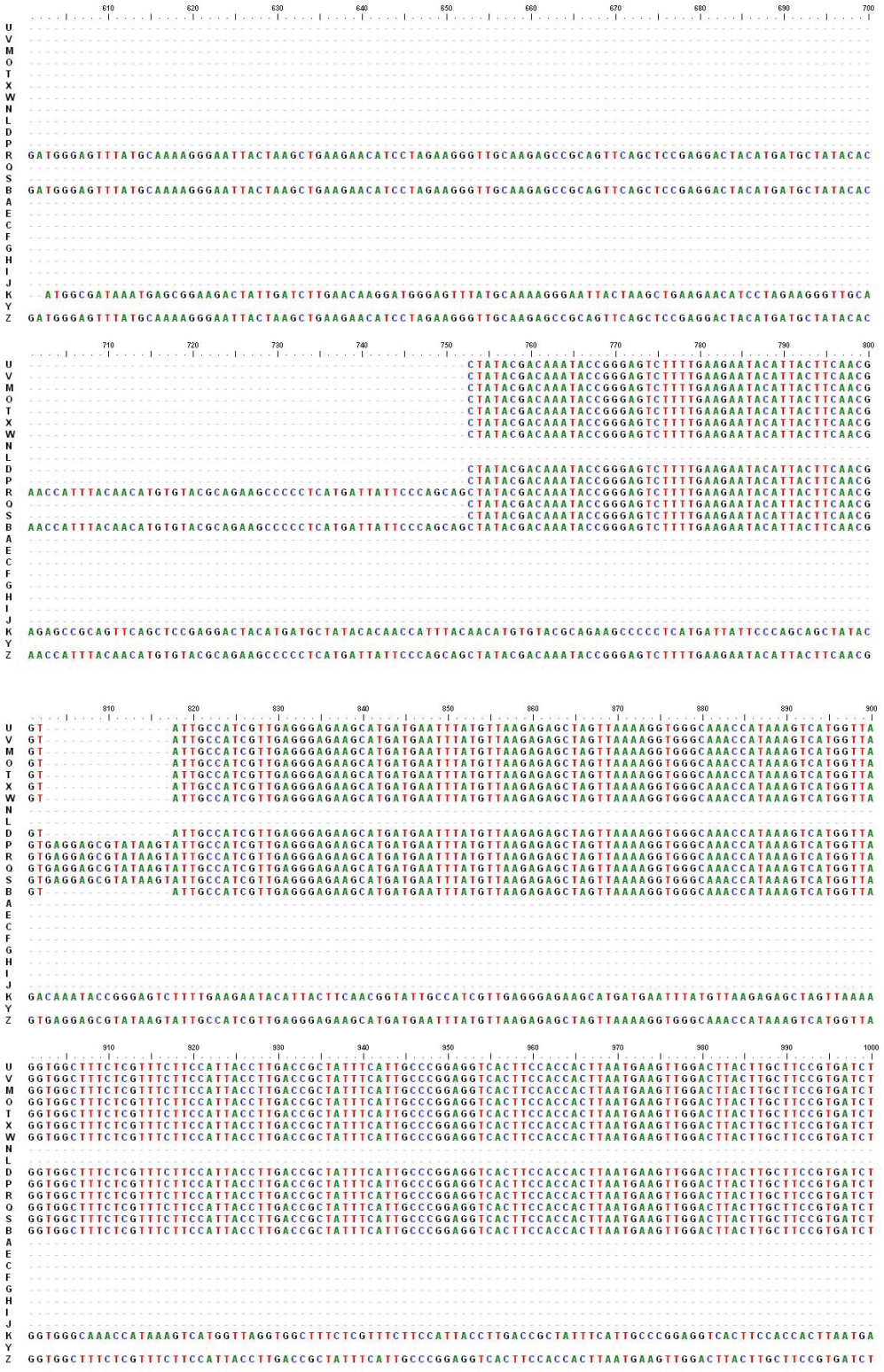

Figure A8 continued.

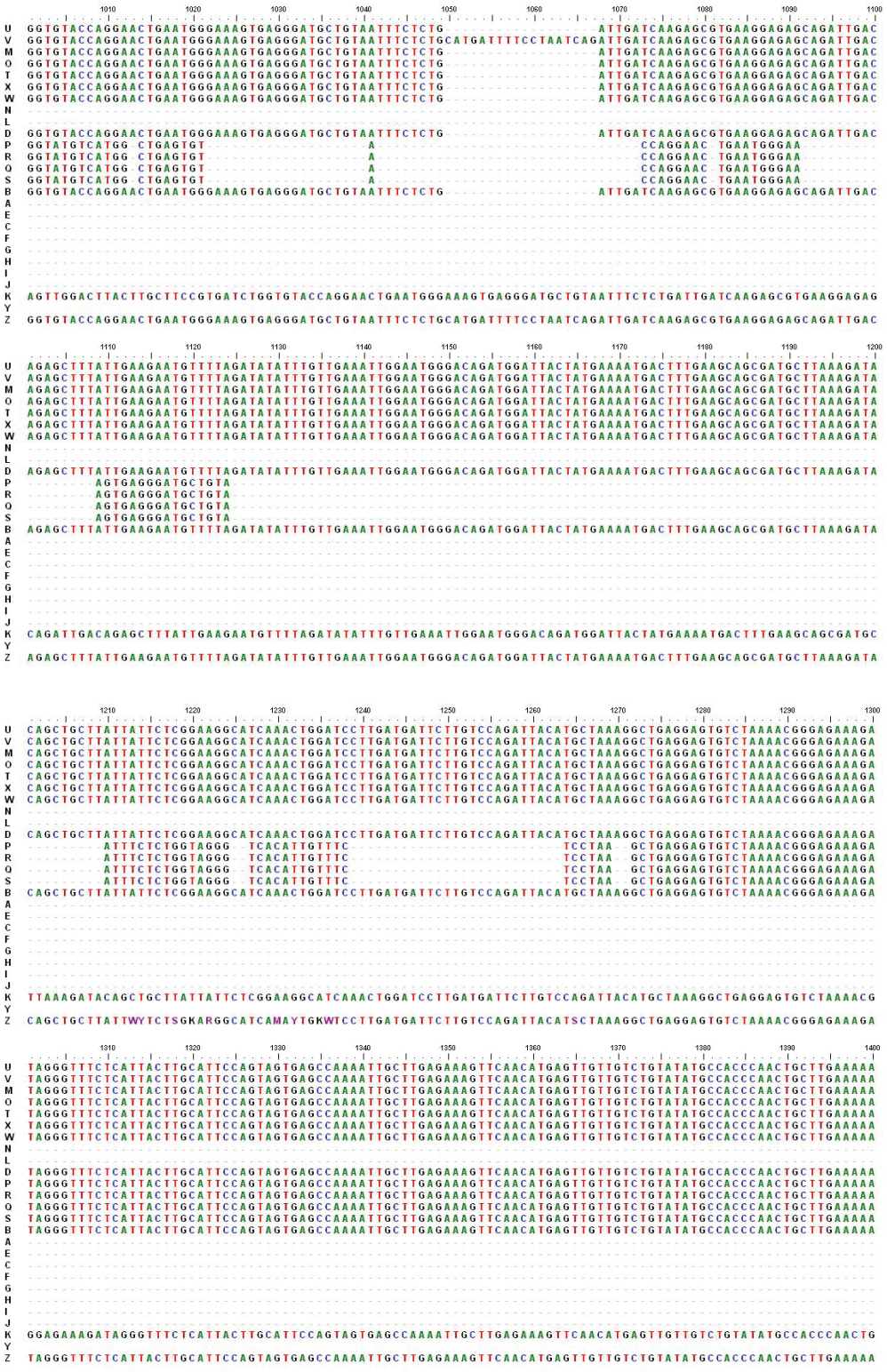

Figure A8 continued.

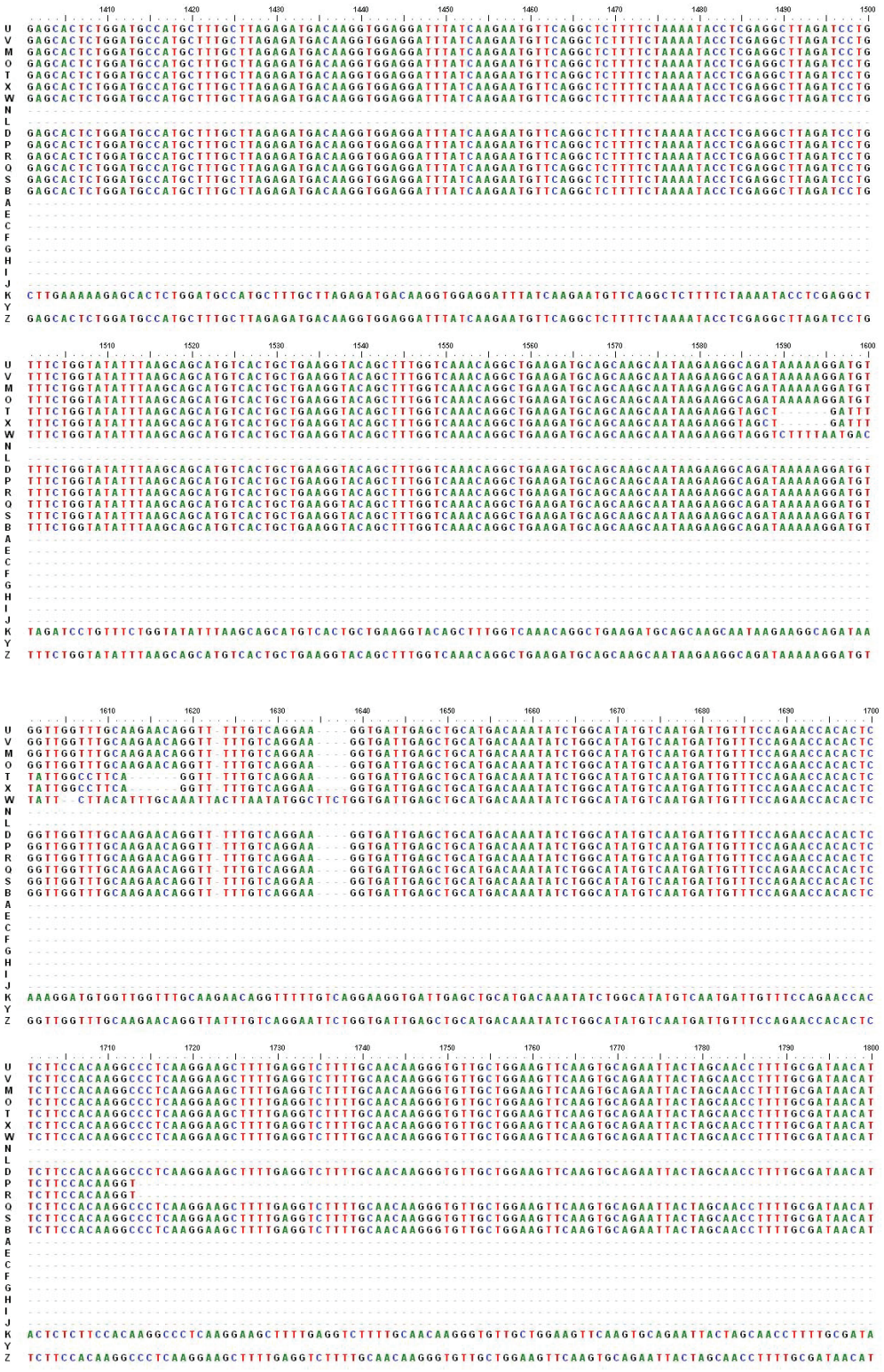

Figure A8 continued.

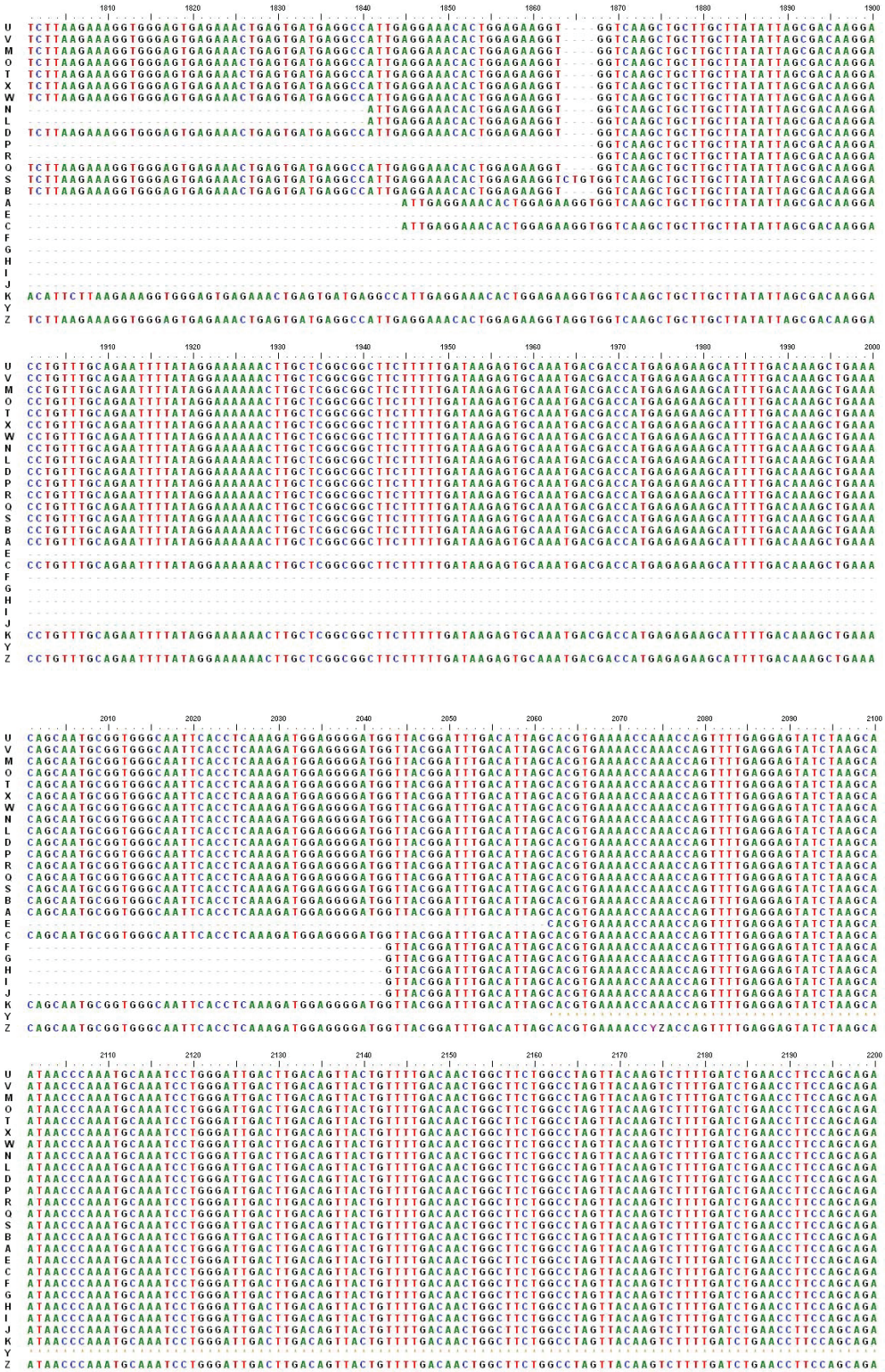

Figure A8 continued.

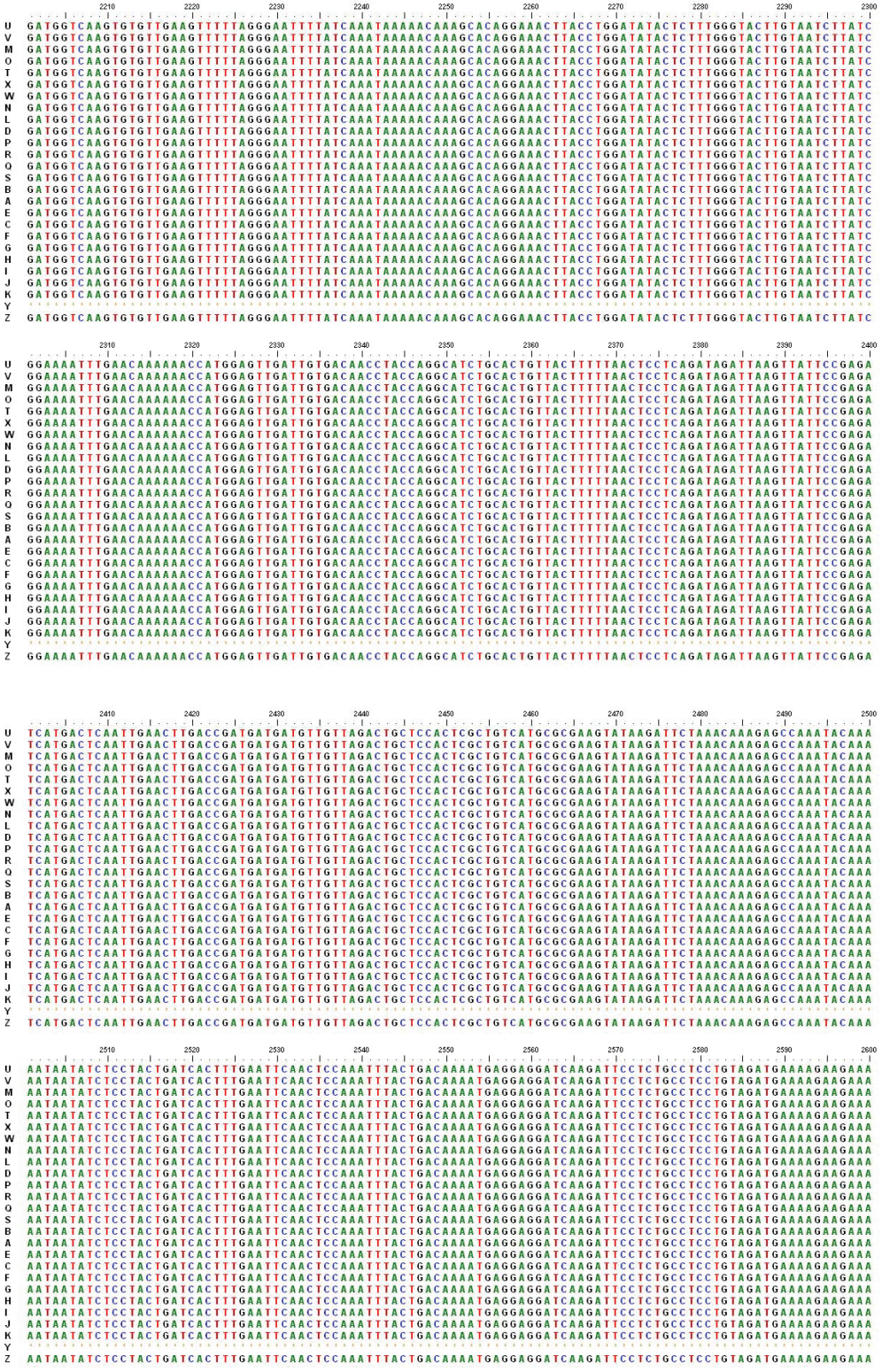

Figure A8 continued.

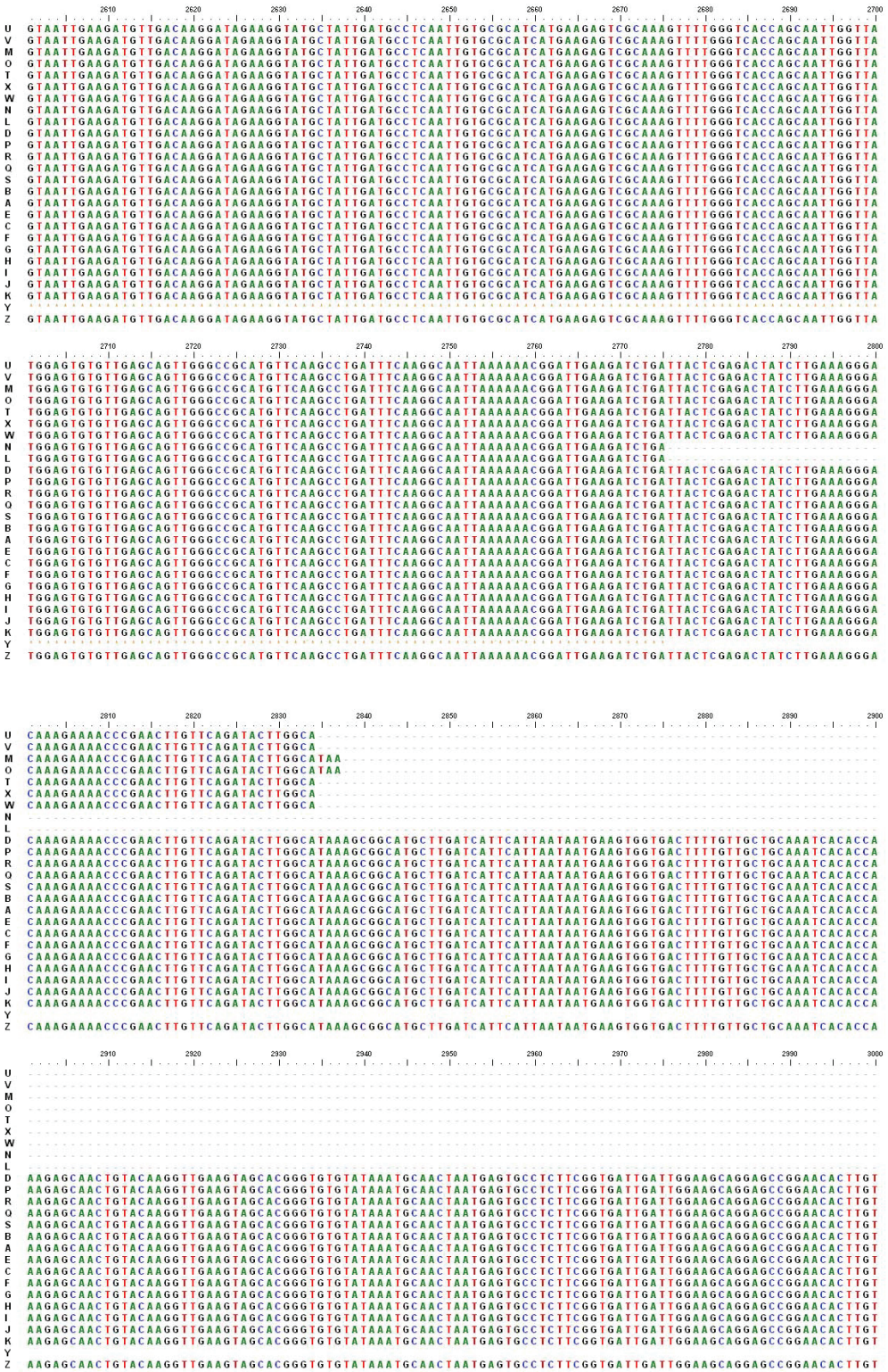

Figure A8 continued.

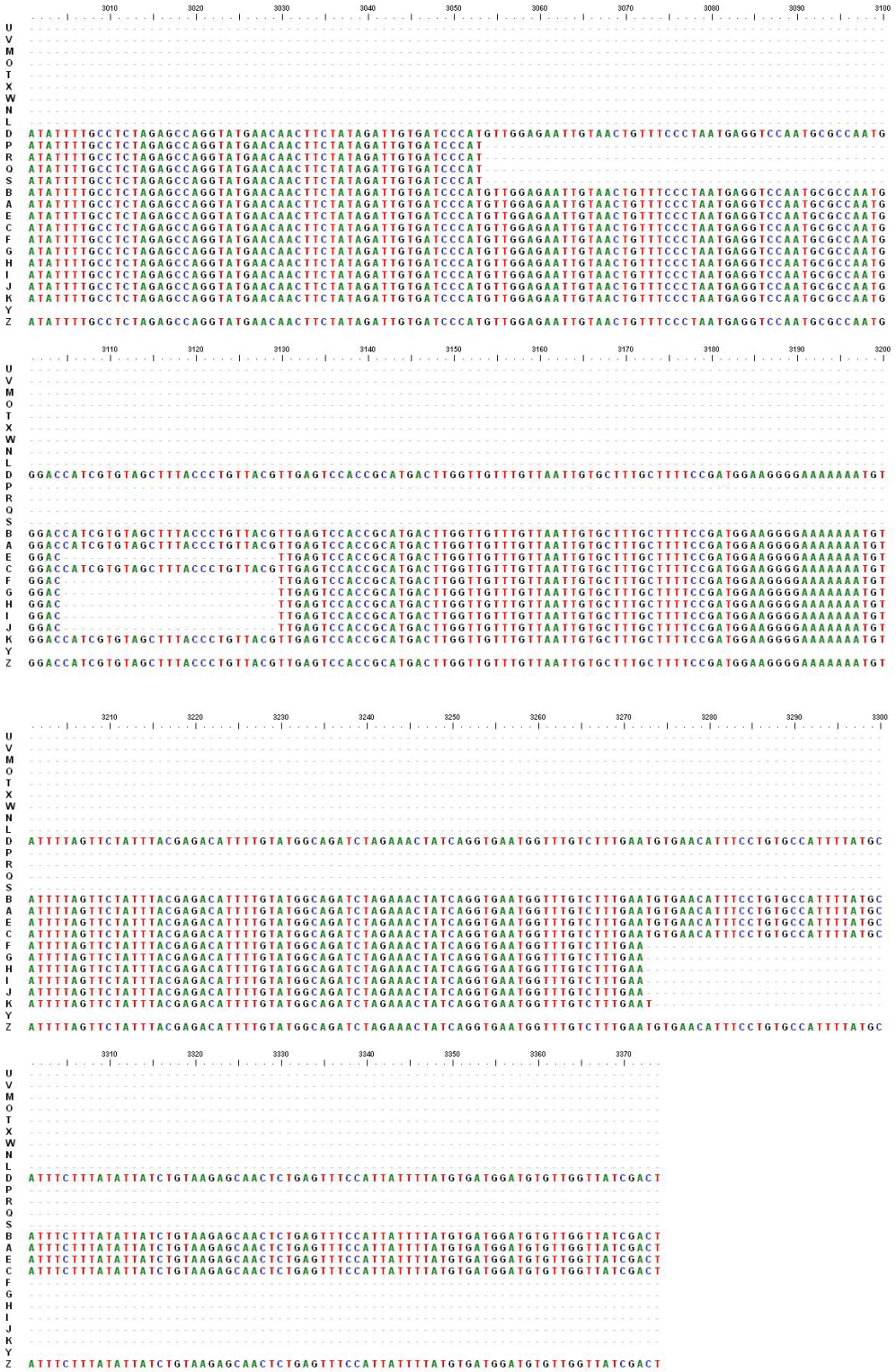

Figure A8 continued.

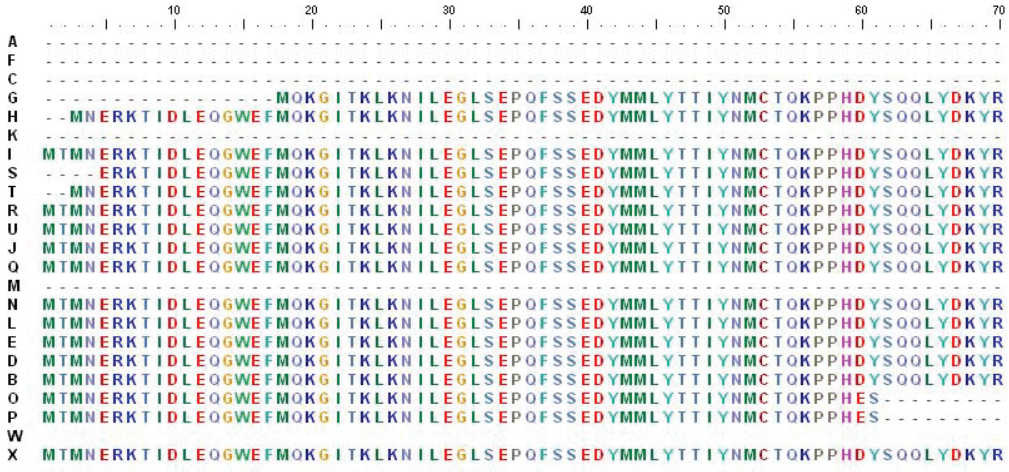

Figure A9: Multiple sequence alignment of predicted protein sequences from LG_X for EST 181. Letters **A**-to-**U** are the names of gene models **A.** estExt_fgenesh1_kg_v1.C_LG_X0015, **B.** estExt_fgenesh1_pg_v1.C_LG_X0319, **C.** estExt_fgenesh1_pg_v1.C_LG_X0320, **D.** estExt_fgenesh1_pm_v1.C_LG_X0092, **E.** estExt_Genewise1_v1.C_LG_X4342, **F.** estExt_Genewise1_v1.C_LG_X4343, **G.** estExt_Genewise1_v1.C_LG_X4344, **H.** estExt_Genewise1_v1.C_LG_X4345, **I.** estExt_Genewise1_v1.C_LG_X4346, **J.** eugene3.00100293, **K.** fgenesh1_kg.C_LG_X000016, **L.** fgenesh1_pg.C_LG_X000321, **M.** fgenesh1_pg.C_LG_X000322, **N.** fgenesh1_pm.C_LG_X000093, **O.** grail3.0060006901, **P.** grail3.0060006902, **Q.** gw1.X.4364.1, **R.** gw1.X.4365.1, **S.** gw1.X.4366.1, **T.** gw1.X.4367.1, **U.** gw1.X.4368.1, **W.** Clustal consensus, **X.** Consensus transcript sequence

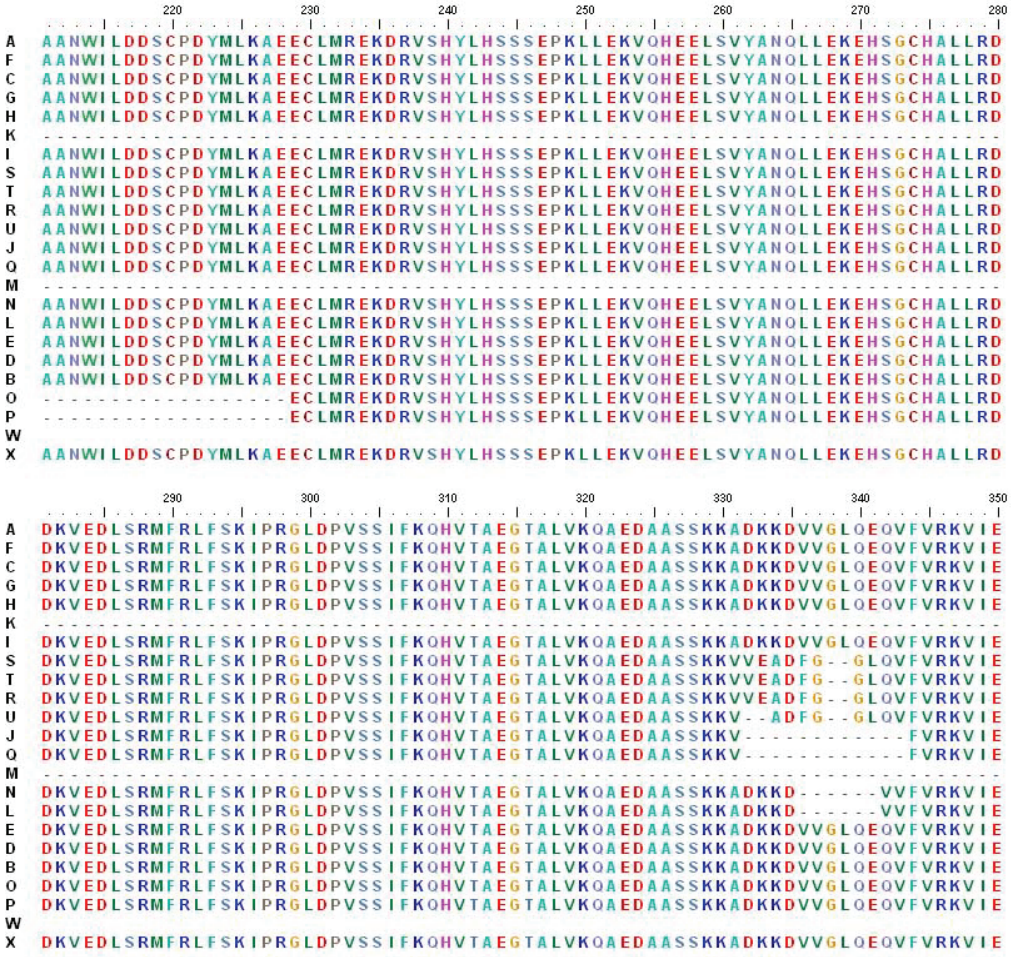

Figure A9 continued.

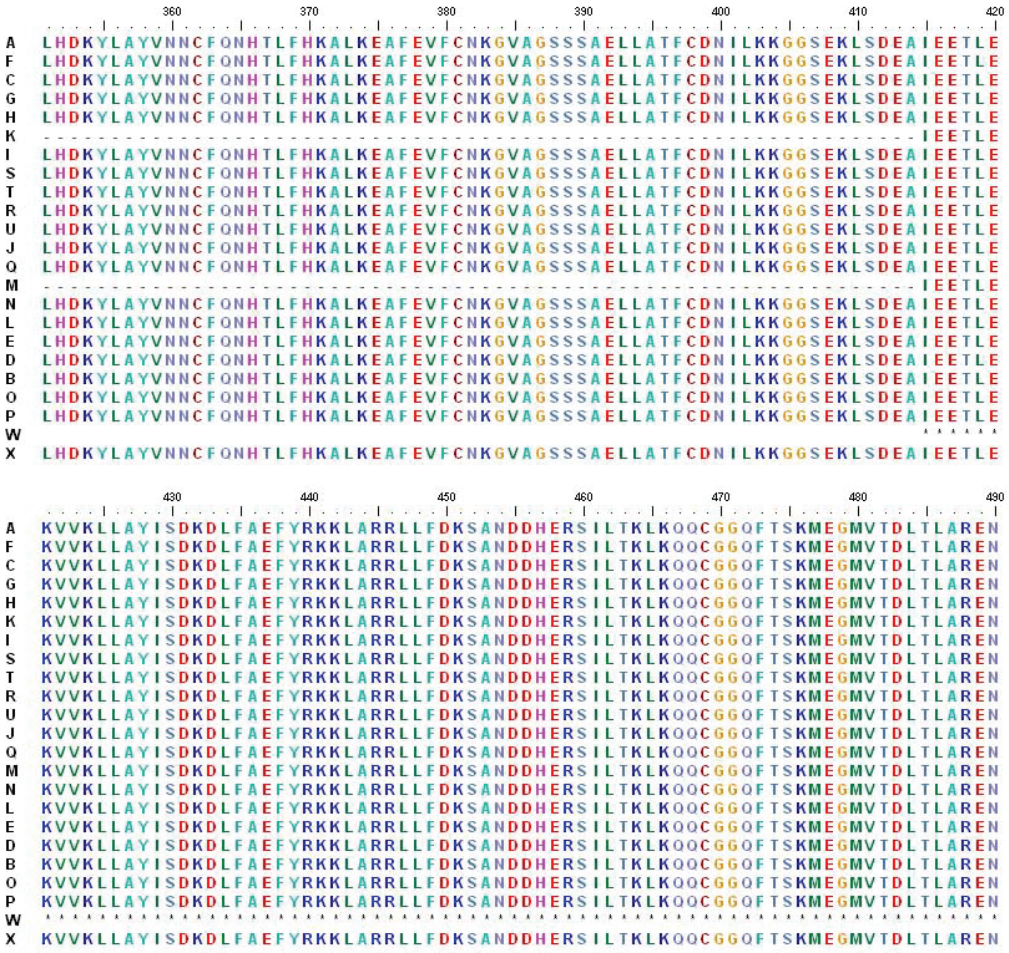

Figure A9 continued.

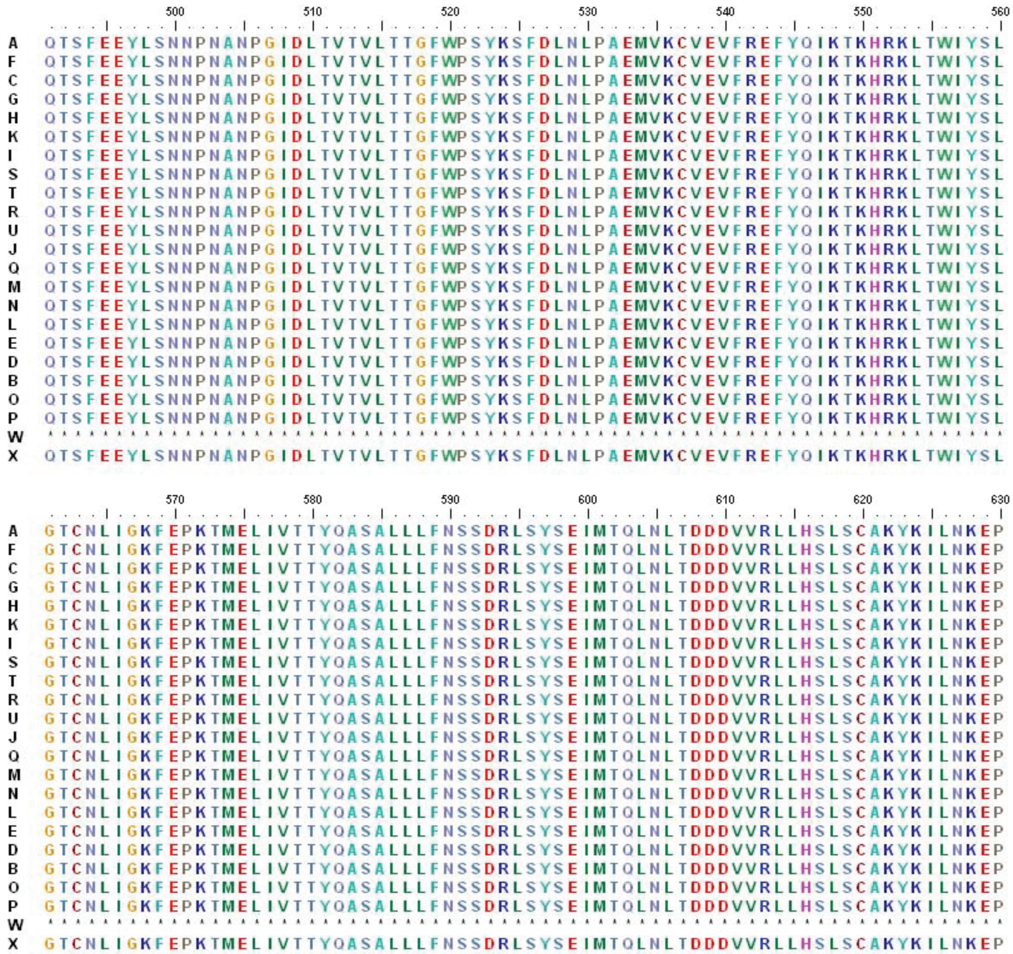

Figure A9 continued.

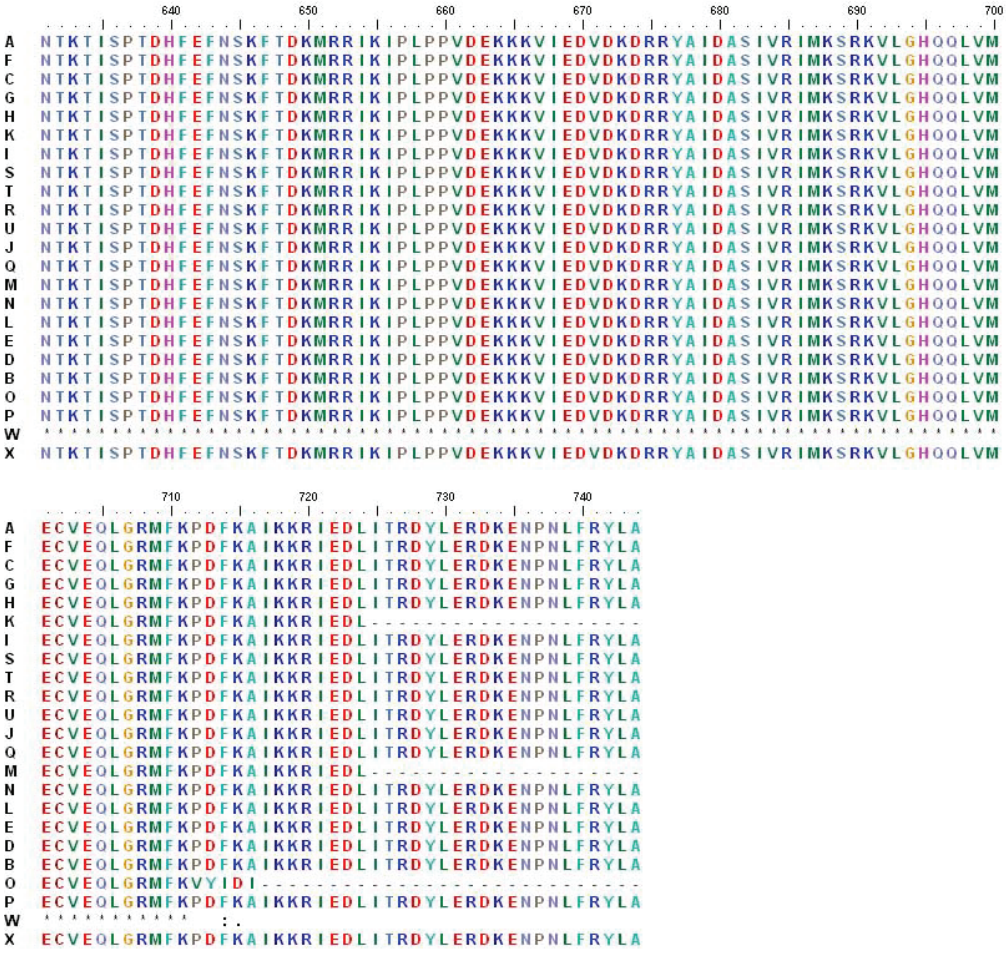

Figure A9 continued.

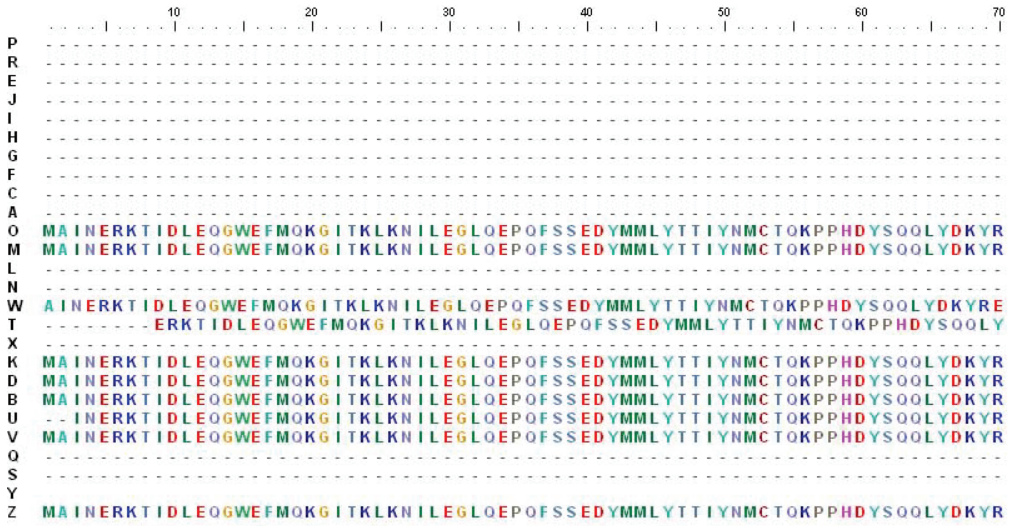

Figure A10: Multiple sequence alignment of predicted protein sequences from Scaffold_132 for EST 181. Letters **A**-to-**X** are the names of gene models **A**. estExt_fgenesh1_kg_v1.C_1320001, **B.** estExt_fgenesh1_pg_v1.C_1320039, **C.** estExt_fgenesh1_pg_v1.C_1320040, **D.** estExt_fgenesh1_pm_v1.C_1320006, **E.** estExt_Genewise1_v1.C_1320062, **F.** estExt_Genewise1_v1.C_1320063, **G.** estExt_Genewise1_v1.C_1320064, **H.** estExt_Genewise1_v1.C_1320065, **I.** estExt_Genewise1_v1.C_1320066, **J.** estExt_Genewise1_v1.C_1320067, **K.** eugene3.01320042, **L.** fgenesh1_kg.C_scaffold_132000001, **M.** fgenesh1_pg.C_scaffold_132000040, **N.** fgenesh1_pg.C_scaffold_132000041, **O.** fgenesh1_pm.C_scaffold_132000007, **P.** grail3.0132002101, **Q.** grail3.0132002102, **R.** grail3.0132002103, **S.** grail3.0132002104, **T.** gw1.132.63.1, **U.** gw1.132.64.1, **V.** gw1.132.65.1, **W.** gw1.132.66.1, **X.** gw1.132.67.1. **Y.** Clustal consensus, **Z.** consensus transcript sequence

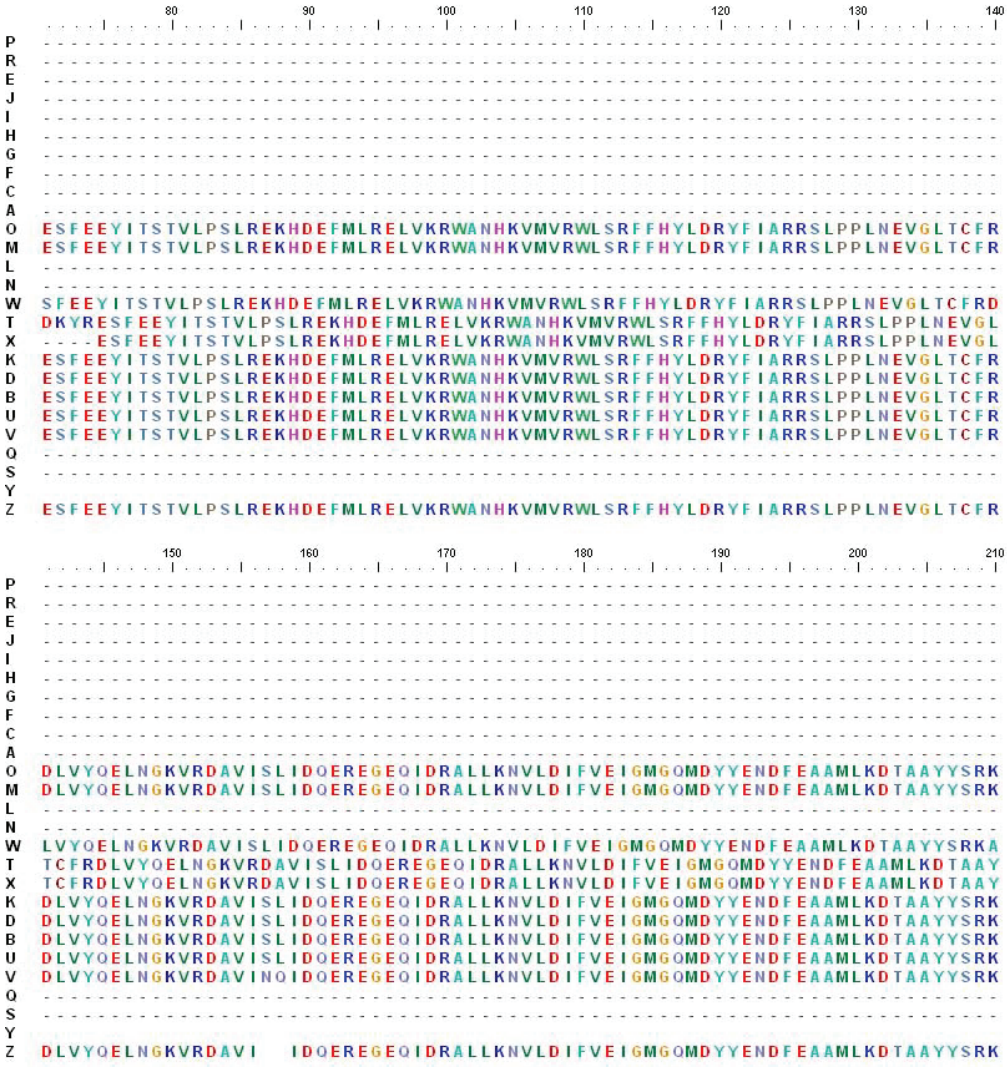

Figure A10 continued.

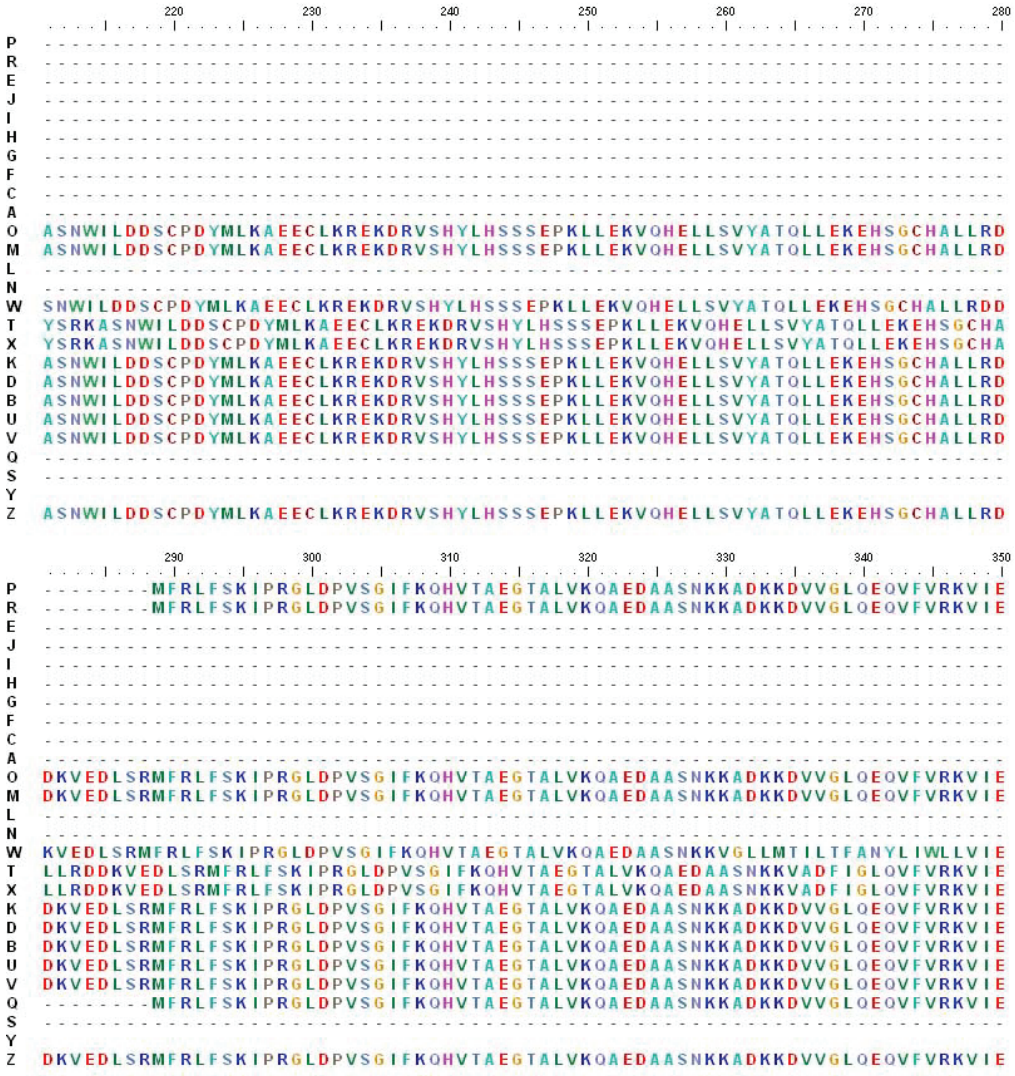

Figure A10 continued.

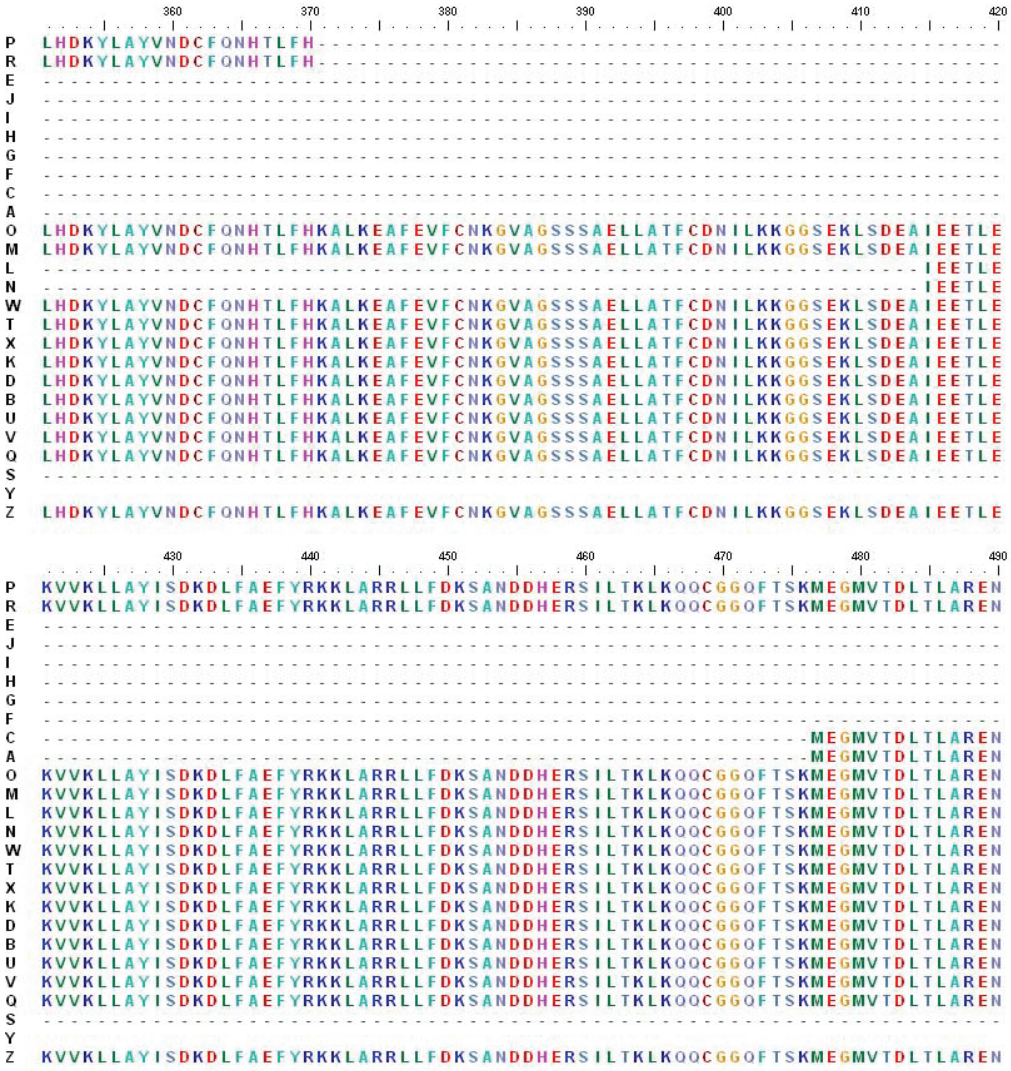

Figure A10 continued.

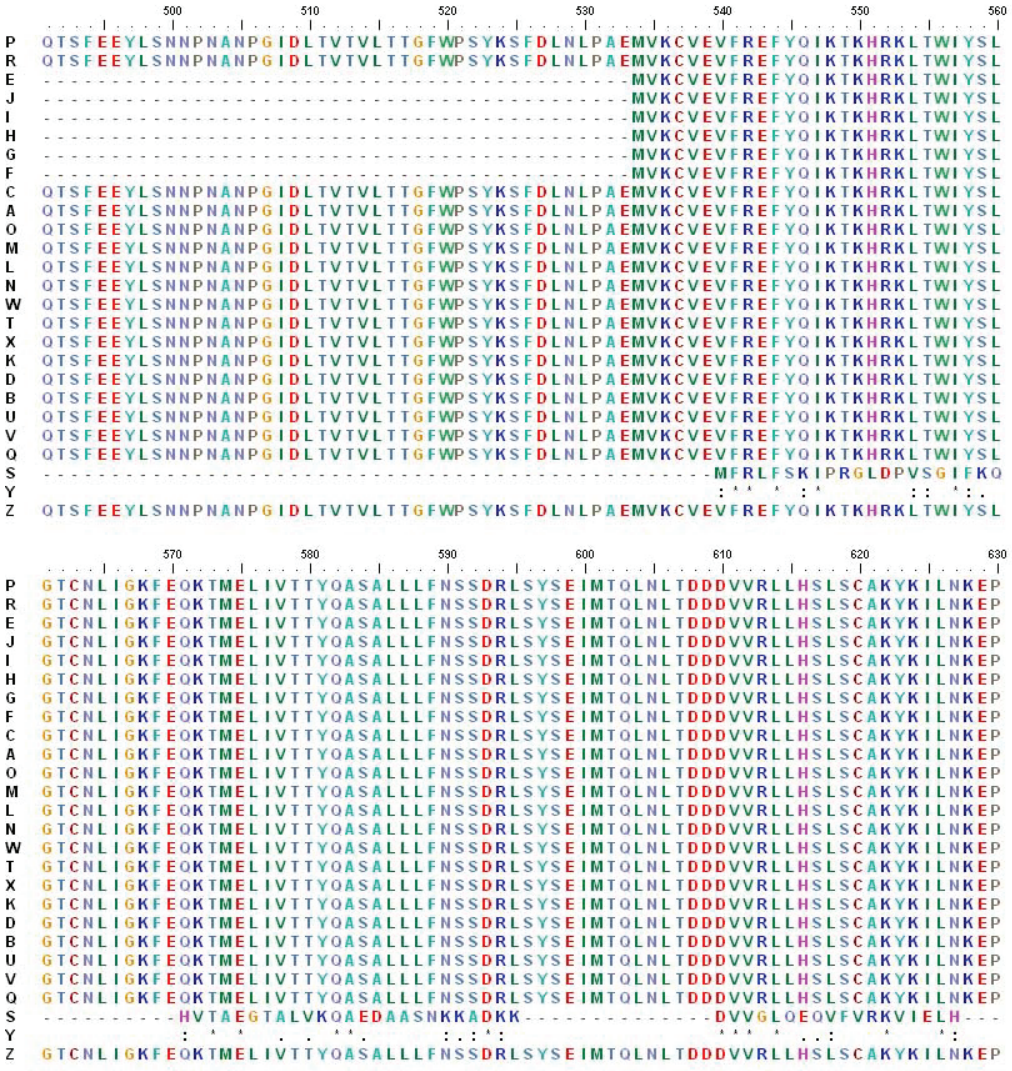

Figure A10 continued.

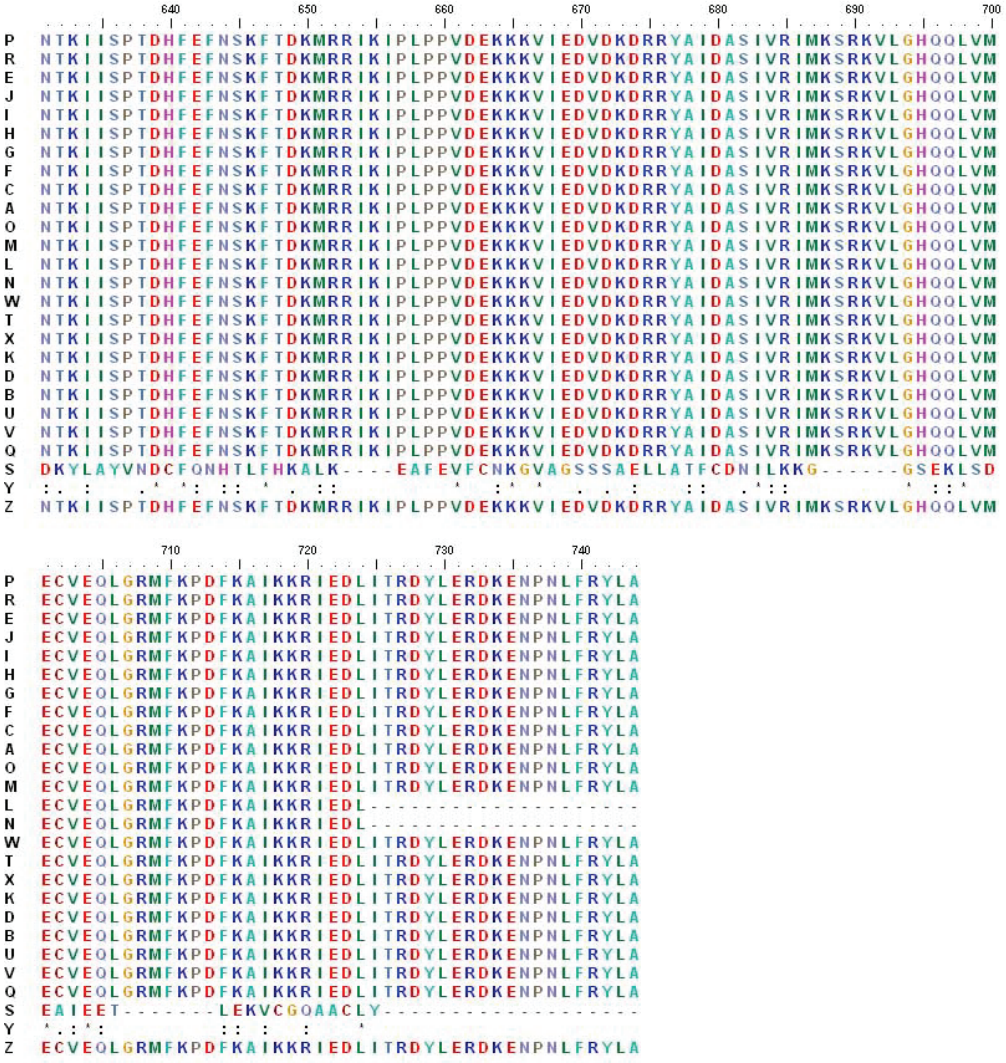

Figure A10 continued.

REFERENCES

ANDRADE M.A., GONZALES-GUZMAN M., SERRANO R., and RODROGEZ P.L. 2001. A combination of the F-box motif and kelch repeats defines a large *Arabidopsis* family of F-box proteins. Plant Mol. Biol. 46:603-614

ARORA R., ROWLAND L.J., and PANTA G.R. 1997. Chilling responsive dehydrins in blueberry: Are they associated with cold hardiness or dormancy transitions? Physiol. Plant. 101:8-16

ARORA R., WISNIEWSKI M.E., and ROWLAND L.J. 1996. Cold acclimatization and alterations in dehydrin-like and bark storage proteins in the leaves of sibling deciduous and evergreen peaches. J. Amer. Soc. Hort. Sci. 121:915-919

AZEVEDO C., SANTOS-ROSA M.J., and SHIRASU K. 2001. The U-box protein family in plants. Trends Plant Sci. 6:354-358

BACHMAIR P.W., NOVATCHKOVA M., POTUSCHAK T., and EISENHABER F. 2001. Ubiquitylation in plants: a post-genomic look at a post-translational modification. Trends Plant Sci. 6:463-470

BEWLEY J.D. 1997. Seed germination and dormancy. Plant Cell. 9:1055-1066

BOLLMARK M., CHEN H-J., MORITZ T., and ELIASSON L. 1995. Relationship between cytokinin level, bud development and apical dominance in Norway spruce, *Picea abies*. Physiol. Plant 95:563-568

BOSTICK M., LOCHHEAD S.R., HONDA A., PALMER S., and CALLIS J. 2004. Related to ubiquitin 1 and 2 are redundant and essential and regulate

vegetative growth, auxin signaling and ethylene production in *Arabidopsis*. The Plant Cell Vol.16, 2418-2432

BROWN C.L. 1971. Primary growth, in M.H. Zimmermann, and C.L. Brown, (eds). Trees: Structure and Function, Springer Verlag, New York, pp. 1-66

BYRD, P.J., STANKOVIC, T., MCCONVILLE, C.M., SMITH, A.D., COOPER, P.R., and TAYLOR, A.M. 1997. Identification and analysis of expression of human VACM-1, a cullin gene family member located on chromosome 11q22-23. Genome Res. 7: 71-75

CAPRON A., OKRESZ L., and GENSCHIK P. 2003. First glance at the plant APC/C, a highly conserved ubiquitin-protein ligase. Trends Plant Sci. 8:83-89

CARABELLI M., MORELLI G., WHITELAM G., and RUBERTI I. 1996. Twilight-zone and canopy shade induction of the *Athb-2* homeobox gene in green plants. Proc. Natl. Acad. Sci. USA 93:3530-3535

CHAU V., TOBIAS J.W., BACHMAIR A., MARRIOTT D., ECKER D.J., GONDA D.K., and VARSHAVSKY A. 1989. A multiubiquitin chain is confined to specific lysine in a targeted short-lived protein. Science. 243:1576-1583

CLACK T., MATHEWS S., and SHARROCK R.A. 1994. The pyhtochrome apoprotein in *Arabidopsis* is encoded by five genes: the sequences and expression of PHYD and PHYE/ Plant Mol. Biol. 25:413-427

CLINE M.G. 1994. The role of hormones in apical dominance. New approaches to an old problem in plant development. Physiol. Plant 90:230-237

CLINE M.G. 1996. Exogenous auxin effects on lateral bud outgrowth in decapitated shoots Ann. Bot. 78:255-266

CLOSE, T.J. 1997. Dehydrins: A commonality in the response of plants to dehydration and low temperature. Plant Physiol. 100:291-296

CRABBÉ J. and BARNOLA P. 1996. A new conceptual approach to bud dormancy in woody plants. In Plant Dormancy: Physiology, Biochemistry and Molecular Biology, G.A. Lang (ed.), CAB International, Wallingford, pp. 83-113

DAVIES P.J. 1995. Plant Hormones: physiology, biochemistry and molecular biology. Dordrecht, The Netherlands: Kluwer Academic Publishers.

del POZO J.C. and ESTELLE M. 1999a. Function of the ubiquitin proteasome pathway in auxin response. Trends Plant Sci. 4(3): 107-112

del POZO J.C. and ESTELLE M. 1999b The *Arabidopsis* cullin AtCUL1 is modified by the ubiquitin-related protein RUB1. Proc. Natl. Acad. Sci. USA 96 (26): 15342-15347

del POZO J.C., DHARMASIRI S., HELLMANN H., WALKER L., GRAY W.M., and ESTELLE M. 2002. AXR1-ECR1-dependent conjugation of RUB1 to Arabidopsis Cullin AtCUL1 is required for auxin response. The Plant Cell 14: 421-433

del POZO J.C., TIMPLE C., TAN S., CALLIS J., and ESTELLE M. 1998. The ubiquitin related protein RUB1 and auxin response in *Arabidopsis*. Natl. Acad. Sci. USA 96: 1760-1763

DELVIN P.F., HALLIDAY K.J., HARBERD N.P., and WHITELAM G.C.1996. The rosette habit of *Arabidopsis thaliana* is dependent upon phytochrome action: novel phytochromes control internode elongation and flowering time. Plant Physiol. 7: 63-78

DENG X.W., CASPAR T., and QUAIL P.H. 1991. cop1: A regulatory locus involved in light controlled development and gene expression in *Arabidopsis*. Genes Dev. 5: 1172-1182

DESHAIES R.J. 1999. SCF and Cullin/Ring H2-based ubiquitin ligases. Annu. Rev. Cell Dev. Biol. 15: 435-467

DILL A., THOMAS S.G., HU J., STEBER C.M., and SUN T.P. 2004. The *Arabidopsis* F-box protein SLEEPY1 targets gibberellin signaling repressors for gibberellin-induced degradation. Plant Cell. 16: 1392-1405

DOWNES B.P., STUPAR R.M., GINGERICH D.J., and VIERSTRA R.D. 2003. The HECT ubiquitin protein ligase (UPL) family in *Arabidopsis*: UPL3 has a specific role in trichome development. Plant J. 35: 729-742

ESSER C., ALBETI S., and HÖHFELD J. 2004. Cooperation of molecular chaperones with the ubiquitin/proteasome system. Biochimica et Biophysica Acta 1695: 171-188

FELSENSTEIN J. 2002. PHYLIP Phylogeny Inference Package version 3.6, Joseph Felsenstein

FINKELSTEIN R.R. and ROCK C.D. 2002. Abscisic acid biosynthesis and response. In CR Somerville, EM Meyerrowitz, eds, The *Arabidopsis* book. American Biology of Plant Biologists, Rockville, MD, pp. 1-52

FREWEN B.E., CHEN T.H.H., HOWE G.T., DAVIS J., ROHDE A., BOERJAN W., and BRADSHAW H.D. 2000. Quantitative trait loci and candidate gene mapping of bud set and bud flush in *Populus*. Genetics. 154: 837-845

FU X., RICHARDS D.E., FLECK B., XIE D., BURTON N., and HARBERD N.P. 2004. The *Arabidopsis* mutant sleeply1$^{gar2\text{-}1}$ protein promotes plant growth by increasing the affinity of the SCFsly1 E3 ubiquitin ligase for DELLA protein substrates. Plant Cell. 16: 1406-1418

GAGNE J.M., DOWNES B.P., SHUI S-H., DURSKI A.M., and VIERSTRA R.D. 2002. The F-box unit of SCF E3 complex is encoded by a diverse superfamily of genes in *Arabidopsis*. Proc. Natl. Acad. Sci. USA 99: 11519-11524

GAGNE J.M., SMALLE J., GINGERICH D.J., WALKER J.M., YOO S.D., YANAGISAWA S., and VIERSTRA R.D. 2004. *Arabidopsis* EIN3-binding F-box 1 and 2 form ubiquitin-protein ligases that repress ethylene action and promote growth by directing EIN3 degradation. Proc. Natl. Acad. Sci. USA 101: 6803-6808

GRAY W.M., DEL POZO J.C., WALKER L., HOBBIE L., RISSEEUW E., BANKS T., CROSBY W.L., YANG M., MA H., and ESTELLE M. 1999. Identification of an SCF ubiquitin ligase complex required for auxin response in *Arabidopsis thaliana*. Genes Dev. 13: 1678-1691

GRAY W.M., KEPINSKI S., ROUSE D., LEYSER O., and ESTELLE M. 2001. Auxin regulates SCF^{TIR1}-dependent degradation of AUX/IAA proteins. Nature. 414: 271-276

GREGORI L., POOSCH M.S., COUSINS G., and CHAU V. 1990. A uniform isopeptide-linked multiubiquitin chain is sufficient to target substrate for degradation in ubiquitin-mediated proteolysis. J. Biol. Chem. 265: 8354-8357

GROLL M., BAJOREK M., KOHLER A., MORODER L., RUBIN D.M., HUBER R., GLICKMAN M.H., and FINLEY D. 2000. A gated channel into the proteasome core particle. Nat. Struct. Biol. 7(11): 1062-1067.

GUO H. and ECKER J.R. 2003. Plant responses to ethylene gas are mediated by SCF (EBF1/EBF2)-dependent proteolysis of EIN transcription factor. Cell 115: 667-677

GUO H. and ECKER J.R. 2004. The ethylene signaling pathway: new insights. Curr. Opin. Plant Biol 7: 40-49

HAAS A.L. and ROSE I.A. 1982. The mechanism of ubiquitin activating enzyme. A kinetic and equilibrium analysis. J. Biol. Chem. 257: 10329-10337

HAAS A.L. and SIEPMANN T.J. 1997 Pathways of ubiquitin conjugation. FASEB J. 11(14): 1257-1268

HAAS A.L., WARMS J.V., HERSHKO A., and ROSE I.A. 1982. Ubiquitin activating enzyme. Mechanism and role in polyubiquitin conjugation. J. Biol. Chem. 257: 2543-2548

HALL T. License Agreement for BioEdit v7.0.4: copyright (c) 1997-2005, Tom Hall

HAPER J.W., BURTON J.L., and SOLOMON M.J. 2002. The anaphase-promoting complex: it's not just for mitosis any more. Genes Dev. 16: 2179-2206

HARTMANN-PETERSEN R., SEEGER M., and GORDON C. 2003. Transferring substrates to the 26S proteasome. Trend Biochem. Sci. 28: 26-31

HATFIELD P.M., GOSINK M.M., CARPENTER T.B., and VIERSTRA R.D. 1997. The ubiquitin activating enzymes (E1) gene family in *Arabidopsis thaliana*. Plant J. 11: 213-226

HAUSER B.A., CORDONNIER-PRATT M.M., and PRATT L.H. 1998. Temporal and photoregulated expression of five tomato phytochrome genes. Plant J. 14: 431-439

HELLMANN H., HOBBIE L., CHAPMAN A., DHARMASIRI S., DHARMASIRI N., DEL POSO C., REINHARDT D., and ESTELLE M. 2003. *Arabidopsis AXR6* encodes CUL1 implicating SCF E3 ligases in auxin regulation of embryogenesis. EMBO J. 22:3314-3325

HIGGINS, D. G., THOMPSON, J. D. and GIBSON, T. J. 1996 Using CLUSTAL for multiple sequence alignments. Methods Enzymol. 266: 383-402

HIGGINS,D.G. and SHARP,P.M. 1988 CLUSTAL: a package for performing multiple sequence alignment on a microcomputer. Gene 73: 237-244.

HOCHSTRASSER M. 1996. Ubiquitin-dependent protein degradation. Annu Rev Genet. 30: 405-39

HOCHSTRASSER M. 1998. There's the RUB: a novel ubiquitin-like modification linked to cell cycle regulation. Genes Dev. 12: 901-907

HOCHSTRASSER M. 2000. Evolution and function of ubiquitin-like protein-conjugation system. Nat. Cell Biol. 2: E153-E157

HOLM M., MA L.G., QU L.J., and DENG X.W. 2002. Two interacting bZIP proteins are direct targets of COP1-mediated control of light-dependent gene expression in Arabidopsis. Genes Dev. 16: 1247-1259

HORI T., OSAKA F., CHIBA T., MIYAMOTO C., OKABAYASHI K., SHIMBARA N., KATO S., and TANAKA K. 1999. Covalent modification of all members of human cullin family proteins by NEDD8. Oncogene 18: 6829-6834

HOWE G.T., HACKETT W.P, FURNIER G.R. and KLEVORN R.E. 1995. Photoperiodic responses of a northern and southern ecotype of black cottonwood. Phyisol. Plant. 97: 95-103

JUNTILLA O. and JENSEN E. 1988. Gibberellins and photoperiodic control of shoot elongation in *Salix*. Physiol. Plant. 74: 371-376

JUNTTILA O. 1990. Gibberellins and the regulation of shoot elongation in woody plants. N. Takahashi, B.O. Phinney, and J. MacMillan (eds), Gibberellins, Springer Verlag, Berlin, pp 199-210

KAMIYA Y. and GARCIA-MARTINEZ J. 1999. Regulation of gibberellin biosynthesis by light. Curr. Opin. Plant Biol. 2: 398-403

KIPREOS, E.T., LANDER, L.E., WING, J.P., HE, W.W., and HEDGECOCK, E.M. 1996. *cul-1* is required for cell cycle exit in *C. elegans* and identifies a novel gene family. Cell 85: 829-839

KOEPP D.M., HARPER J.W., and ELLEDGE S.J. 1999. How the cyclin became cyclin: regulated proteolysis in the cell cycle. Cell 97: 431-434

LAMMER D., MATHIAS N., LAPLAZA J.M., JIANG W., LIU Y., CALLIS J., GOEBL M., and ESTELLE M. 1998. Modification of yeast Cdc53p by ubiquitin related protein Rub1p affects function of the SCF^{cdc4} complex. Genes Dev. 12: 914-926

LANG G.A. 1987 Dormancy: A new universal terminology. HortScience. 22(5): 817-820

LARSEN P.M., and CANCEL J.S. 2004 A recessive mutation in the RUB1-conjugating enzyme, RCE1, reveals a requirement for RUB modification for

control of ethylene biosynthesis and proper induction of basic chitinase and PDF1.2 in *Arabidopsis*. The Plant J. 38: 626-638

LAVARNNE S., CHAMPAGNAT P., and BARNOLA P., 1975. Influence d'une même gamme de températures sur l'entrée et la sortie de dormance des bourgeons du frêne (*Fraxinus excelsior* L.). Physiologie Végétale 13: 215-224

LEE H.J., XIONG L.M., GONG Z.Z., ISTIHANI M., STEVENSON B., and ZHU J.K. 2001. The *Arabidopsis HOS1* gene negatively regulates cold signal transduction and encodes a RING finger protein that displays cold regulated nucleo-cytoplasmic partitioning. Genes Dev. 15: 912-924

LEPLE J.C., BRASILEIRO A.C.M., MICHEL M.F., DELMOTTE F., and JOUANIN L. 1992. Transgenic poplars: expression of chimeric genes using four different constructs. Plant Cell Reports. 11: 137-141

LIAKOPOULOS D., DOENGLES K., MATUSHEWSKI K., and JENTSCH S. 1998. A novel protein modification pathway related to the ubiquitin system. EMBO. J. 17: 2208-2214

LOEB K.R. and HAAS, A.L. 1992. The interferon-inducible 15-kDa ubiquitin homolog conjugates to intra cellular proteins. J. Biol. Chem. 267: 7806-7813

MATHEWS C.K. and VAN HOLDE K.E. 1995. Biochemistry. Second Edition. The Benjanim /Cummings Publishing Company, Inc.

MAUGET J.C. 1981. Modification des capacities de croissance des bourgeons du noyer (*Juglans regia* L.) par application d'une température de 4^{o}C à différents moments de leur période de repos apparent. Comptes-Rendus de l'Académie des Sciences, Paris III 292: 1081-1083

MAYER K.F. and HARDTKE C.S. 2002. Evaluation and classification of RING-finger domains encoded by the Arabidopsis genome. Genome Biol. 3: 1-12

MIZUSHIMA N., NODA T., YOSHIMORI T, TANAKA Y., ISHII T., GEORGE M.D., KLIONSKY D.J., OSHUMI M. and OSHUMI Y. 1998. A protein conjugation system essential for autophagy. Nature 395: 395-398

MOON J., PARRY G., and ESTELLE M. 2004. The ubiquitin-proteasome pathway and plant development. Plant Cell 16: 3181-3195

NAGY F. and SCHÄFER E. 2002. Pyhtochromes control photomorphogenesis by differentially regulated, interacting signaling pathways in higher plants. Annu. Rev. Plant Biol. 53: 329-355

NOODEN L.D. and WEBER J.A. 1978. Environmental and hormonal control of dormancy in terminal buds of plants. In Dormancy and Developmental Arrest. Experimental Analysis in Plants and Animals (Cutter M.E., ed) New York: Academic Press, pp. 221-268

OLSEN J.E., JUNTTILA O., and MORITZ T. 1997a Long-day induced bud break in *Salix pentandra* is associated with transiently elevated levels of GA1. Plant Cell Physiol. 38:536-540

OLSEN J.E., JUNTTILA O., NILSEN J., ERIKSSON M.E., MARTINUSSEN I., OLSSON O., SANDBERG G., and MORITZ T. 1997b. Ecotypic expression of oat phytochrome A in hybrid aspen changes critical daylength for growth and prevents cold acclimatization. The Plant J. 12(6): 1339-1350

OSAKA F., KAWASAKI H., AIDA N., SAEKI M., CHIBA T., KAWASHIMA S., TANAKA K., and KATO S. 1998. A new NEDD8 ligation system for Cullin4A. Genes Dev. 12: 2263-2268

OSTERLUND M.T., HADTKE C.S., WEI N., and DENG X.W. 2000. Targeted destabilization of HY5 during light regulated development of *Arabidopsis*. Nature. 405: 462-466

OWENS J.N. and MOLDER M. 1976. Bud development in Sitka spruce. I. Annual growth cycle of vegetative buds and shoots. Can. J. Bot. 54: 313-325

PAGE, R. D. M. 1996. TREEVIEW: An application to display phylogenetic trees on personal computers. Computer Applications in the Biosciences 12: 357-358

PATTON E.E., WILLEM A.R., SA D., KURAS L., THOMAS D., and CRAIG K.L. 1998. Cdc53 is a scaffold protein of multiple Cdc53/Skp1/F-box protein complex that regulates cell division and methionine biosynthesis in yeast. Genes Dev. 12: 692-705

PATTON E.E., WILLEMS A.R., and TYERS M. 1998. Combinatorial control in ubiquitin-dependent proteolysis: don't Skp the F-box hypothesis. Trends Genet. 14: 236-243

PERAZZA D., VACHON G., and HERZOG M. 1998. Gibberellins promote trichome formation by up-regulating GLABROUS1 in *Arabidopsis*. Plant Physiol. 117: 375-383

PETROSKI M.D. and DESHAIES R.J. 2005. Function and regulation of cullin-RING ubiquitin ligases. Nature Reviews 6: 9-20

PICKART C.M. 2001. Mechanisms underlying ubiquitination. Annu. Rev. Biochem. 70: 503-533

POTUSCHAK T., KECHNER E., PARMENTIER Y., YANAGISAWA S., GRAVA S., KONCZ C., and GENSCHIK P. 2003. EIN3-dependent regulation of plant ethylene hormone signaling by two Arabidopsis F box proteins: EBF1 and EBF2. Cell. 115: 679-689

POWELL L.E. and MAYBEE C. 1984. Changes in abscisic acid during chilling in buds of twenty apple cultivars. HortScience 19: 584

QUAIL P.H., BOYLAN M.T., PARKS B.M., SHORT T.W., XU Y., and WAGNER D. 1995. Phytochromes: photosensory perception and signal transduction. Science. 112: 675-680

RAO-NAIK C., DELACRUZ W., LAPLAZA J.M., TAN S., CALLIS J., and FISHER A.J. 1998. The RUB family of ubiquitin-like proteins. J. Biol. Chem. 273: 34976-34982

RISSEEUW E.P., DASKALCHUK T.E., BANKS T.W., LIU E., COTELESAGE J., HELLMANN H., ESTELLE M., SOMERS D.E., and CROSBY W.L. 2003. Protein interaction analysis of SCF ubiquitin E3 ligase subunits from *Arabidopsis*. Plant J. 34: 753-767

ROHDE A., HOWE G.T., OLSEN J.E., MORITS T., VAN MONTAGU M., and BOERJAN W., 2000. Molecular aspects of bud dormancy in trees. Molecular Biology of Woody Plants Volume1: 89-134 (eds S.M. Jain and S.C. Minocha)

RUONALA R., RINNE P.L.H., MORITZ T., TUOMINEN H., and KANGASJARVI J. 2006. Transitions in the functioning of the shoot apical meristem in birch (*Betula pendula*) involve ethylene. Plant J. 46: 628-640

SAMISH R.M. 1954. Dormancy in woody plants. Annu. Rev. Plant Physiol. 5: 183-204

SCHWARTZ S.H., QIN X., and ZEEWART J.A.D. 2003. Elucidation of the direct pathway of abscisic acid biosynthesis by mutants, genes, and enzymes. Plant Physiol. 131: 1591-1601

SCHWOB E., BOHM T., MENDENHALL M.D., and NASMYTH K. 1994. The B-type cyclin kinase inhibitor p40SIC1 controls the G1 to S transition in S. cerevisiae. Cell 79: 233-244

SEO M. and KOSHIBA T. 2002. Complex regulation of ABA biosynthesis in plants. Trends Plant Sci. 7: 41-48

SHARROCK R.A. 1994. Plant photoperception: the phytochrome system. In Development: the Molecular Genetic Approach (Russo U.E.A., Brody S., Cove D., and Ottolenghi S. eds). Berlin: Springer Verlag. pp.194-205

SHEN W.H., PARMENTIER Y., HELLMANN H., LECHNER E., DONG A., MASSON J., GRANIER F., LEPINIEC L., ESTELLE M., and GENSCHIK P. 2002. Null mutation of *AtCul1* causes arrest in early embryogenesis in *Arabidopsis.* Mol. Biol. Cell 13: 916-1928

SIMPSON M.V. 1953. The release of labeled amino acids from the proteins of rat liver slices. J. Biol. Chem. 201: 143-154

SMALLE J. and VIERSTRA R.D. 2004. The Ubiquitin 26S proteasome proteolytic pathway. Annu. Rev. Plant Biol. 55: 555-590

STONE S.L., ANDERSON E.M., MULLEN R.T., and GORING D.R. 2003. ARC1 is an E3 ubiquitin ligase and promotes the ubiquitination of proteins during the rejection of self-incompatible *Brassica* pollen. Plant Cell 15: 885-898

SUTTLE J.C. 1998. Involvement of ethylene in potato microtuber dormancy. Plant Physiol. 118: 843-848

TAYLOR I.B., BURBIDAGE A., and THOMPSON A.J. 2000. Control of abscisic acid synthesis. J. Exp. Bot. 51: 1563-1574

TUOMINEN H., SITBON F., JACOBSSON C., SANDBERG G., OLSSON O., and SUNDBERG B. 1995. Altered growth and wood characteristics in transgenic hybrid aspen expressing *Agrobacterium tumefaciens* T-DNA indoleacetic acid-biosynthetic genes, Plant Physiol. 109: 1179-1189

VARSHAVSKY A. 1997. The ubiquitin system. Trends Biochem Sci. 22(10): 383-7.

VIERSTRA R.D. 1996. Proteolysis in plants: mechanisms and functions. Plant Mol. Biol. 32: 275-30

VIERSTRA R.D. 2003. The ubiquitin/26S proteasome pathway, the complex last chapter in the life of many plant proteins. Trends Plant Sci. 8 (3): 135-142

VIERSTRA R.D. and CALLIS J. 1999. Poly peptide tags, ubiquitous modifiers for plant protein regulation. Plant Mol. Biol. 41:435-442

VINCE-PRUE D. 1984. Contrasting types of photoperiodic response in the control of dormancy. Plant, Cell and Env. 7: 507-513

VINCE-PRUE D. 1994. The duration of light and photoperiodic responses. In Photomorphogenesis in Plants (Kendrick R.E and Kronenberg G.H.M., eds). Second Edn. Dordrecht: Kluwer Academic, pp. 447-490

VOGES D., ZWICKL P., and BAUMEISTER W. 1999. The 26S proteasome: a molecular machine designed controlled proteolysis. Annu. Rev. Biochem. 68: 1015-1068

WILLEMS A.R., SCHWAB M., and TYPERS M. 2004. A hitchhiker's guide to the cullin and ubiquitin ligases: SCF and its kin. Biochimica et Biophysica Acto 1695: 133-170

XIE Q., GUO H.S., DALLMAN G., FANG S.Y., WIESSMAN A.M., and CHUA N.H. 2002. SINAT5 promotes ubiquitin-related degradation of NAC1 to attenuate auxin signals. Nature. 419: 167-170

YAN N., WANG J., LI Q., HWANG J-R., PATERSON C., and ZHANG H. 2003. *At*CHIP, a U-Box-containing E3 ubiquitin ligase, plays a critical role in temperature stress tolerance in *Arabidopsis*. Plant Physiol. 132: 1-9

ZHENG N., SCHULMAN B.A., SONG L., MILLER J.J., JEFFREY P.D., WANG P., CHU C., KOEPP D.M., ELLEDGE S.J., PAGANO M., CONAWAY R.C., CONAWAY J.W., HARPER J.W., and PAVLETICH N.P. 2002. Structure of the Cul1-Rbx1-Skp1-F boxSkp2 SCF ubiquitin ligase complex. Nature. 416(6882): 703-709.